

Universidade do Minho  
Escola de Ciências da Saúde

Susana Alexandra Rodrigues Pascoal

New aspects in coordination of vertebrate  
limb bud development

Tese de Doutoramento  
Ciências da Saúde – Ciências Biológicas e Biomédicas

Trabalho efectuado sob a orientação de:  
Doutora Isabel Palmeirim  
Professora Auxiliar da Escola de Ciências da Saúde da  
Universidade do Minho, Braga, Portugal

Outubro de 2006

## DECLARAÇÃO

Nome: Susana Alexandra Rodrigues Pascoal

Endereço electrónico: [spascoal@ecsaude.uminho.pt](mailto:spascoal@ecsaude.uminho.pt)

Telefone: +351 962858511

Número do Bilhete de Identidade: 11318373

Título tese

New aspects in coordination of vertebrate limb bud development

Novos aspectos na coordenação do desenvolvimento do membro dos vertebrados

Orientador:

Doutora Isabel Palmeirim

Ano de conclusão: 2006

Designação do Ramo e Área de Conhecimento do Doutoramento:

Ciências da Saúde – Ciências Biológicas e Biomédicas

É AUTORIZADA A REPRODUÇÃO INTEGRAL DESTA TESE/TRABALHO  
APENAS PARA EFEITOS DE INVESTIGAÇÃO, MEDIANTE DECLARAÇÃO  
ESCRITA DO INTERESSADO, QUE A TAL SE COMPROMETE

Universidade do Minho, 30/10/2006

Assinatura: \_\_\_\_\_

---

## *AGRADECIMENTOS / ACKNOWLEDGEMENTS*

I want to express all my gratefulness, my feelings, my admiration and also my deep respect to all of you that during these years help me along this journey. To all thank you very much.

Quero expressar a minha gratidão, os meus sentimentos, a minha admiração e o meu mais profundo respeito por todos os que me ajudaram nesta fase da minha vida. Para todos um muito obrigado.

A ti Isabel, tenho que te agradecer estes quatro anos da minha vida, pela oportunidade de trabalhar num projecto fantástico e num ambiente divertido e acolhedor. Por sentir que és mais que uma orientadora, sentir que és a minha mamã científica com quem eu aprendi muito, e mais que isso uma grande amiga em quem sei que posso confiar e desabafar quando mais preciso. Muito obrigado por tudo, principalmente por seres uma pessoa fantástica que eu admiro muito e que nunca esquecerei.

À Professora Doutora Cecília Leão, Directora do Instituto de Ciências da Vida e da Saúde da Universidade do Minho, agradeço a oportunidade e confiança em mim depositada ao aceitar-me como aluna de doutoramento desta instituição, assim como a sua enorme simpatia e o seu constante estímulo à investigação. Muito obrigado pela prontidão que sempre demonstrou em ajudar-me.

Agradeço o financiamento dos trabalhos descritos nesta tese de doutoramento à Fundação para a Ciência e a Tecnologia (FCT), através de fundos Nacionais e do FSE através do programa POCTI 2010. Agradeço à FCT por me ter concedido a bolsa de doutoramento com a referência SFRH/BD/8657/2002 e pelo projecto POCTI/BCI/42040/2001 que me permitiu desenvolver os estudos realizados nesta tese. Agradeço também à Rede Europeia de Excelência, “Cells into Organs” ([www.cellsintoorgans.net](http://www.cellsintoorgans.net)) EU/FP6 o financiamento dispensado.

## *Agradecimentos/Acknowledgements*

---

Ao Instituto de Ciências da Vida e da Saúde da Escola de Ciências da Saúde na Universidade do Minho agradeço as excelentes condições de trabalho e o facto de me ter proporcionado o acesso a uma cultura científica e uma massa crítica excepcionais.

A todo o grupo (aos que estão e aos que estiveram) do laboratório ID8 em Braga onde “vivi” literalmente estes quatro anos da minha vida. Muito obrigada meninas por todo o apoio, amizade e por toda a paciência que tiveram comigo ao longo deste tempo. Muito obrigado Raquel Andrade e Fernanda Bajanca por todo o apoio e pelos comentários entusiastas e construtivos que fizeram ao lerem esta tese, foi muito importante para mim. A ti Raquel a minha primeira coleguinha de laboratório em Braga, obrigado por estes quatro anos de companheirismo e de entusiastas discussões científicas que muito me ajudaram. Fernanda um muito obrigado por teres estado presente quando mais precisei. Mónica Ferreira, um obrigado muito especial por tomares conta de nós e por seres uma pessoa muito querida e sempre pronta a ajudar. Rute Moura, Marta Santos, Sílvia Gonzaga e Cristina Silva adorei ser vossa “vizinha” de laboratório, obrigado pelo apoio e amizade.

À Goreti Pinto, à Magda Carlos e ao Gil Castro um obrigado muito especial pela sua amizade e pelo apoio que me deram ao longo destes anos.

À Sofia Rodrigues e à Leonor Saúde obrigado por todo o apoio e incentivo que me deram durante a escrita da tese. Leonor muito obrigado por todo o carinho e por seres uma amiga muito especial.

Ao Super-Grupo de Biologia do Desenvolvimento pelas ótimas discussões científicas que muito me ajudaram ao longo do meu trabalho de doutoramento.

Ao Fernando Rodrigues pelo seu interesse no meu trabalho e pelas ótimas discussões científicas a que isso proporcionou. Obrigado pelo entusiasmo e apoio que me transmitiste.

À Paula Ludovico e ao Gustavo Rocha – Obrigado amigos, pela companhia, amizade, carinho, força e incentivo que me deram ao longo destes anos. E por toda a paciência

## *Agradecimentos/Acknowledgements*

---

que tiveram em me aturar nos momentos mais complicados desta jornada. Sem vocês tudo teria sido mais difícil. Gosto muito de vocês, muito obrigado.

E por fim, aos meus pais e avós que tanto sofreram com a minha ausência para que eu pudesse chegar até aqui, é a eles que dedico esta tese. OBRIGADO.



---

## ABSTRACT

Limb development requires precise orchestration of cell proliferation and differentiation in both time and space. Chick limb skeletal elements are laid down as cartilaginous primordia with the same initial size and grow differentially in a proximal-distal (P-D) sequence giving rise to seven skeletal compartments. Two models seek to explain cell fate specification along the P-D limb axis. Although fundamentally different, both models imply the existence of a limb bud distal zone where cells reside until they reach the time to differentiate - progress zone model -, or to expand - early specification model. However, how these cells measure time remains unknown.

In 1997, the identification of the somitogenesis molecular clock brought new insight into how embryonic cells measure time. Another interesting discovery made in the somitogenesis system is the observation of a maturation wavefront. When this maturation wavefront is experimentally shifted anteriorly by placing an Fibroblast Growth Factor (FGF)8-coated bead in the mid-presomitic mesoderm (PSM), smaller somites are formed.

In the work developed during the course of this PhD thesis, we analysed the expression of the somitogenesis molecular clock components *hairy1* and *hairy2* during chick forelimb development. We provide the first evidence for a molecular clock operating during limb outgrowth and patterning by showing that the expression of the somitogenesis clock component *hairy2* cycles in limb chondrogenic precursor cells with a 6 hour periodicity. We determined the time period required to form an autopod skeletal limb element and propose that the forelimb second phalanx takes 12 hours to be formed, suggesting that an autopod limb skeletal element is formed by cells with “n” and “n+1” *hairy2* expression cycles.

In analogy to the somitogenesis maturation wavefront, we also hypothesise the existence of a wavefront that could be travelling in limb bud distal mesenchyme. Since FGF8 protein and *fgf8* mRNA expressed in the Apical Ectodermal Ridge (AER) is activating *MAPK phosphatase 3 (mkp3)* expression in the distal limb mesenchyme, we have characterized the expression pattern of this gene and found that *mkp3* presents a graded distribution of its transcripts in distal limb bud mesenchyme. We also analysed the expression pattern of intronic *mkp3* probe and propose that *mkp3* in limb distal mesenchyme acts in a similar way to *fgf8* in the PSM. Furthermore, similarly to what

## ***Abstract***

---

occurs during somitogenesis, shorter limb elements are obtained when *mkp3* expression under influence of FGF8 is extended proximally. We also demonstrate that AER-derived FGF8 signalling positively regulates *hairy2* expression in the distal limb mesenchyme.

The work performed in this thesis proposes that somitogenesis and limb bud are two parallel systems. Both have a zone where cells are maintained in an undifferentiated state (PSM and distal limb mesenchyme). In both these zones a molecular clock is operating regulating the periodicity of structure formation. We also suggest that these zones are maintained undifferentiated by the FGF/ Wingless int (WNT) signalling pathways that control the size of the elements formed. Recently, Mitogen Activated Protein Kinase/ Extracellular signal-Regulated Kinase (MAPK/ERK) pathway has been implicated in this process. We moreover propose that retinoic acid (RA) and FGF have mutually inhibitory roles in limb bud development, similarly to what occurs during somitogenesis, playing a function in allocating a certain number of cells to the initiation of the chondrogenic differentiation program, resulting in the regulation of element size.

Until now, all studies regarding cyclic gene expression during development have focused exclusively on somitogenesis. However, time control is absolutely required during all embryonic development and may even be considered the fourth developmental dimension. The studies performed in this thesis suggest that temporal control exerted by cyclic gene expression can be a widespread mechanism providing cellular temporal information during vertebrate embryonic development, not being an exclusive propriety of PSM cells, as previously thought.



---

## RESUMO

O desenvolvimento dos membros dos vertebrados envolve uma regulação temporal e espacial estrita, quer da proliferação, quer da diferenciação celulares. As células precursoras dos elementos esqueléticos que formam o membro são dispostas sequencialmente ao longo do eixo proximal-distal (P-D). Na asa da galinha, estes elementos esqueléticos são formados com o mesmo tamanho inicial, crescendo depois diferencialmente e dando origem a sete compartimentos esqueléticos. Existem dois modelos que tentam explicar a especificação dos destinos celulares ao longo do eixo P-D do membro dos vertebrados. Embora essencialmente diferentes, ambos postulam a existência de uma zona distal no membro onde as células residem até chegar o tempo de diferenciarem – modelo da zona de progresso - , ou de expandirem – modelo da especificação precoce. Contudo, continua ainda por determinar a forma como estas células adquirem a noção de tempo.

Em 1997, a identificação de um relógio molecular ligado ao processo da somitogénese proporcionou novos conhecimentos na forma de como é que as células adquirem a noção de tempo. Outra descoberta interessante realizada no processo da somitogénese foi a observação de uma “wavefront” de maturação. Quando esta “wavefront” de maturação é deslocada anteriormente através da introdução de esferas embebidas em proteína *Fibroblast Growth Factor* (FGF)8 na região mediana da mesoderme presomítica (MPS), formam-se sómitos mais pequenos.

Os estudos realizados durante o curso desta tese de doutoramento, permitiram-nos mostrar pela primeira vez a existência de um relógio molecular que actua durante o desenvolvimento do membro superior do embrião de galinha. Experiências realizadas nesse sentido permitiram-nos estudar o padrão de expressão dos componentes do relógio molecular da somitogénese, *hairy1* e *hairy2* durante o desenvolvimento do membro superior da galinha e observar que um dos componentes do relógio, o gene *hairy2* apresenta ciclos de expressão com uma periodicidade de 6 horas nas células precursoras condrogénicas do membro. Foram realizados estudos para determinar o período de tempo necessário para a formação de um elemento esquelético do membro, e propomos que cada falange é formada em 12 horas, sugerindo que um elemento esquelético do membro é formado por células com “n” e “n+1” ciclos de expressão do gene *hairy2*.

## Resumo

---

Em analogia com a “wavefront” descrita no modelo da somitogênese, sugerimos que um processo semelhante possa estar a ocorrer no mesênquima distal do membro dos vertebrados. Devido à expressão da proteína de FGF8 e do RNAm de *fgf8* na *Apical Ectodermal Ridge* (AER) activar a expressão de *MAPK phosphatase 3* (*mkp3*) no mesênquima distal do membro, fomos caracterizar o padrão de expressão deste gene e observámos que existe um gradiente de expressão de *mkp3* no mesênquima distal do membro. Analisamos também o padrão de expressão obtido com uma sonda intrónica de *mkp3*, e sugerimos que *mkp3* no mesênquima distal do membro actua de uma maneira semelhante à de *fgf8* na MPS. De modo idêntico ao modelo proposto para a somitogênese, demonstramos também que quando a expressão de *mkp3* sob a influência de FGF8 é estendida proximalmente, os elementos esqueléticos do membro que se estão a formar nessa altura são menores. Por último, demonstramos que a sinalização de FGF8 proveniente da AER regula positivamente a expressão de *hairy2* no mesênquima distal do membro.

O trabalho realizado nesta tese sugere a existência de um paralelismo entre o processo da somitogênese e do membro. Ambos apresentam uma zona onde as células são mantidas num estado indiferenciado (MPS e o mesênquima distal do membro) onde está presente o relógio molecular responsável por regular a periodicidade da formação das estruturas. Em ambos os casos, estas zonas são mantidas num estado indiferenciado pelas vias de sinalização FGF/ *Wingless int* (WNT) que controlam o tamanho dos elementos formados. Recentemente, a via do *Mitogen Activated Protein Kinase/ Extracellular signal-Regulated Kinase* (MAPK/ERK) também foi implicada neste processo. Outro paralelismo interessante entre estes dois sistemas é o facto do ácido retinóico (AR) e da via de sinalização FGF inibirem-se mutuamente dando origem a que um certo número de células se distribuam para a iniciação do programa de diferenciação condrogénico, resultando na regulação do tamanho dos elementos.

Até ao presente momento, todos os estudos relativos à expressão cíclica de genes ao longo do desenvolvimento embrionário, têm-se focado exclusivamente na somitogênese. Porém, o controlo temporal é absolutamente necessário durante todo o desenvolvimento embrionário, podendo mesmo ser considerado uma quarta dimensão do desenvolvimento. Os estudos realizados nesta tese de doutoramento sugerem que o controlo temporal exercido pela expressão cíclica de genes pode ser um mecanismo geral para atribuição de informação temporal celular durante o desenvolvimento

---

embrionário dos vertebrados, e não uma propriedade exclusiva das células da MPS como acreditado até agora.



---

## TABLE OF CONTENTS

ABSTRACT.....	VII
RESUMO.....	IX
ABREVIATIONS.....	XXI
AIMS.....	27
THESIS PLANNING.....	33
<b>CHAPTER I – INTRODUCTION.....</b>	<b>35</b>
1. VERTEBRATE LIMB DEVELOPMENT.....	37
1.1 BUILDING THE LIMB BUD: THE INITIATION PROGRAM.....	38
1.2 SPECIFICATION AND DETERMINATION OF LIMB BUD IDENTITY.....	41
1.3 PATTERNING THE VERTEBRATE LIMBS.....	42
1.3.1 PROXIMAL-DISTAL (D-V) AXIS.....	42
1.3.1.1 APICAL ECTODERMAL RIDGE.....	43
1.3.1.2 MODELS PROPOSED FOR P-D PATTERNING.....	44
1.3.1.3 OPOSSING RA AND FGF SIGNALS CONTROL P-D VERTEBRATE LIMB.....	45
1.3.2 ANTERIOR-POSTERIOR (A-P) AXIS.....	46
1.3.2.1 ZONE OF POLARIZING ACTIVITY.....	47
1.3.2.2 MODELS FOR A-P POSITIONAL VALUE SPECIFICATION IN CHICK AND MOUSE LIMB BUDS.....	48
1.3.2.3 A-P PATTERNING OF LIMB PROXIMAL STRUCTURES IS SHH INDEPENDENT.....	48
1.3.2.4 PATTERNING THE DIGITS.....	49
1.3.3 DORSAL-VENTRAL (D-V) AXIS.....	50
1.3.4 COORDINATION OF THE LIMB SIGNALLING CENTRES.....	52
1.4 HOX GENES COLLINEARITY DURING LIMB DEVELOPMENT.....	53
1.5 THE ROLE OF MITOGEN ACTIVATED PROTEIN KINASE/EXTRACELLULAR SIGNAL REGULATED KINASE (MAPK/ERK) SIGNALLING IN LIMB DEVELOPMENT.....	56
1.6 THE ROLE OF NOTCH SIGNALLING PATHWAY IN LIMB BUD ELEMENT FORMATION.....	57
2. THE SOMITOGENESIS MOLECULAR CLOCK.....	58
2.1 THE EMERGENCE OF THE SEGMENTATION CLOCK ERA.....	59
2.2 THE CLOCK SINCE ITS DISCOVERY UNTIL NOWADAYS.....	61
2.3 THE ROLE OF NOTCH SIGNALLING PATHWAY IN SOMITE FORMATION.....	63

## ***Table of Contents***

---

2.4 THE WAVEFRONT – THE PARTNER OF THE CLOCK.....	63
2.5 HOX GENES AND SEGMENTATION CLOCK.....	64
2.6 THE MOLECULAR CLOCK IN TWO DIMENSIONS.....	66
2.7 COULD THE MOLECULAR CLOCK BE OPERATING IN OTHER BIOLOGICAL SYSTEMS?.....	68
<b>CHAPTER II - MATERIALS AND METHODS.....</b>	<b>69</b>
1. MATERIAL AND METHODS.....	71
1.1 EGGS AND EMBRYOS.....	71
1.2 RNA PROBES.....	71
1.2.1 ANTISENSE RNA PROBES SYNTHESIS.....	71
1.2.1.1 GENERATION OF COMPETENT BACTERIA.....	71
1.2.1.2 BACTERIA TRANSFORMATION.....	72
1.2.1.3 PLASMID AMPLIFICATION.....	72
1.2.1.4 PLASMID ISOLATION.....	72
1.2.1.5 PLASMID LINEARIZATION.....	72
1.2.1.6 AGAROSE GEL ELECTROPHORESIS.....	72
1.2.1.7 IN VITRO FITC OR DIG-LABELLED ANTISENSE RNA PROBE TRANSCRIPTON.....	73
1.2.2 CLONING OF INTRONIC MKP3 PROBE.....	73
1.3 RNA EXTRACTION AND REVERSE TRANSCRIPTION.....	75
1.4 QUANTITATIVE REAL-TIME RT-PCR.....	75
1.4.1 STATISTICAL ANALYSIS.....	75
1.5 IN SITU HYBRIDIZATION.....	75
1.5.1 WHOLE-MOUNT.....	75
1.5.1.1 WHOLE-MOUNT IN SITU HYBRIDIZATION PROTOCOL.....	76
1.5.2 TISSUE SECTIONS.....	77
1.5.2.1 ON SECTIONS IN SITU HYBRIDIZATION PROTOCOL.....	77
1.6 IN OVO EMBRYONIC MANIPULATIONS.....	78
1.6.1 DETERMINATION OF THE FORMATION TIME OF THE FORELIMB SECOND PHALANX.....	78
1.6.2 DETERMINATION OF THE HAIRY2 EXPRESSION CYCLE TIME PERIOD.....	79
1.6.3 AER REMOVAL.....	79
1.6.4 BEAD IMPLANTS.....	79
1.7 ALCIAN BLUE STAINING.....	80
1.8 TUNEL ASSAY.....	81

1.9 IMMUNOHISTOCHEMISTRY (IHC).....	81
1.10 IMAGING.....	82
1.11 CELL LINES.....	82
1.11.1 CHICKEN FIBROBLASTS PREPARATION.....	82
1.11.1.1 PROTOCOL TO DILUTE THE CELLS.....	83
1.11.1.2 PROTOCOL FOR CELL FREEZE.....	83
1.12 VIRUS STOCK PREPARATION.....	83
1.13 BUFFERS AND SOLUTIONS.....	84
<b>CHAPTER III – RESULTS.....</b>	<b>89</b>
1. STUDY OF THE EXPRESSION PATTERNS OF THE SOMITOGENESE MOLECULAR CLOCK COMPONENTS HAIRY1 AND HAIRY2 DURING FORELIMB DEVELOPMENT.....	91
1.1 HAIRY1 IS EXPRESSED DURING LIMB BUD DEVELOPMENT.....	91
1.2 HAIRY2 IS EXPRESSED DURING FORELIMB DEVELOPMENT.....	92
2. A MOLECULAR CLOCK OPERATES DURING PROXIMAL-DISTAL LIMB OUTGROWTH IN THE CHICK EMBRYO.....	94
2.1 HAIRY2 IS DYNAMICALLY EXPRESSED ALONG THE LIMB PROXIMAL- DISTAL AXIS.....	94
2.2 THE FORMATION TIME OF A FORELIMB DIGIT CARTILAGINOUS ELEMENT IS 12 HOURS.....	96
2.3 CYCLIC HAIRY2 EXPRESSION HAS A 6 HOUR PERIODICITY IN THE DISTAL FORELIMB BUD.....	97
3. IS A WAVEFRONT TRAVELING ALONG THE DISTAL LIMB MESENCHYME?.....	99
3.1 MKP3 AND FGF8 – FUNCTIONAL PARTNERS IN THE DISTAL LIMB MESENCHYME.....	99
3.2 A PROXIMAL SHIFT IN FGF8 ACTIVITY CAUSES A SIZE REDUCTION OF LIMB SKELETAL ELEMENTS.....	102
3.3 FGF8 REGULATES HAIRY2 GENE EXPRESSION IN DISTAL LIMB MESENCHYME.....	104
<b>CHAPTER IV – GENERAL DISCUSSION.....</b>	<b>107</b>
1. HAIRY2 IS CYCLICALLY EXPRESSED IN LIMB BUD CARTILAGINOUS PROGENITOR CELLS WITH AN OSCILLATION PERIOD THAT CORRELATES WITH THE FORMATION TIME OF AN AUTOPOD LIMB ELEMENT.....	109
2. CYCLIC HAIRY2 EXPRESSION AND THE ACQUISITION OF TEMPORAL INFORMATION.....	111
3. NOTCH SIGNALLING PATHWAY AND PROXIMAL-DISTAL LIMB OUTGROWTH..	112

*Table of Contents*

---

4. <i>COULD A WAVEFRONT BE TRAVELING DURING LIMB BUD DEVELOPMENT?.</i>	113
5. <i>FGF8 ACTIVITY AND THE REGULATION OF LIMB ELEMENT SIZE.....</i>	115
6. <i>COMPENDIUM PARALELISMS.....</i>	116
<i>CHAPTER V – CONCLUSIONS AND FUTURE PERSPECTIVES.....</i>	119
<i>CHAPTER VI – PUBLISHED OR UNDER REVISION PAPERS IN THE SCOPE OF THE THESIS WORK.....</i>	125
<i>CHAPTER VII – REFERENCES.....</i>	195



---

## LIST OF FIGURES

<b>FIGURE1-</b> REPRESENTATION OF A CHICK EMBRYO, A CHICK WING AND THE MAIN SIGNALLING CENTRES THAT CONTROL LIMB BUD FORMATION.....	38
<b>FIGURE2-</b> ILLUSTRATION OF AN INTEGRATIVE MODEL SHOWING THE MAIN SIGNALS INVOLVED DURING LIMB BUD INITIATION.....	41
<b>FIGURE3-</b> MODELS PROPOSED FOR A-P PATTERNING.....	45
<b>FIGURE4-</b> ILLUSTRATION OF THE OPPOSING SIGNALS BETWEEN FGF AND RA/MEIS GENES.....	46
<b>FIGURE5-</b> SCHEMATIC REPRESENTATION OF THE MODELS PROPOSED FOR A-P POSITIONAL VALUES SPECIFICATION IN CHICK WING AND MOUSE FORELIMB.....	48
<b>FIGURE6-</b> REPRESENTATION OF THE SIGNALS REQUIRED FOR D-V PATTERNING.....	51
<b>FIGURE7-</b> SIGNALLING PATHWAYS IN VERTEBRATE LIMB DEVELOPMENT.....	53
<b>FIGURE8-</b> MODEL OF COLLINEAR REGULATIONS DURING LIMB BUD DEVELOPMENT.....	55
<b>FIGURE9-</b> ILLUSTRATION OF THE EXPRESSION PATTERNS OF THE FGF8/ERK ACTIVITY AND MKP3/AKT ACTIVITY.....	57
<b>FIGURE10-</b> SCHEMATIC REPRESENTATION OF THE DYNAMIC AND CYCLIC NATURE OF HAIRY1 EXPRESSION.....	61
<b>FIGURE11-</b> ILLUSTRATION OF HAIRY1 DYNAMIC EXPRESSION OBSERVED ALONG THE TIME FORMATION OF ONE SOMITE-PAIR.....	67

## ***Table of Contents***

---

<b><i>FIGURE12- REPRESENTATION OF THE pCRII-MKP3 INTRON VECTOR CIRCULAR MAP.....</i></b>	<b><i>74</i></b>
<b><i>FIGURE13- HAIRY1 EXPRESSION PATTERN DURING FORELIMB DEVELOPMENT.....</i></b>	<b><i>92</i></b>
<b><i>FIGURE14- HAIRY2 EXPRESSION PATTERN DURING FORELIMB DEVELOPMENT.....</i></b>	<b><i>93</i></b>
<b><i>FIGURE15- DYNAMIC HAIRY2 EXPRESSION IN THE DISTAL LIMB MESENCHYME.....</i></b>	<b><i>95</i></b>
<b><i>FIGURE16- ESTIMATING THE FORMATION TIME OF AN AUTOPOD LIMB ELEMENT.....</i></b>	<b><i>97</i></b>
<b><i>FIGURE17- PERIODICITY OF HAIRY2 CYCLIC EXPRESSION ALONG LIMB P-D AXIS.....</i></b>	<b><i>98</i></b>
<b><i>FIGURE18- FGF8 mRNA AND FGF8 PROTEIN DETECTION IN THE CHICK LIMB BUD.....</i></b>	<b><i>99</i></b>
<b><i>FIGURE19- CHARACTERIZATION OF THE MKP3 mRNA GRADIENT IN THE CHICK LIMB BUD.....</i></b>	<b><i>100</i></b>
<b><i>FIGURE20- EXPRESSION PATTERNS OBTAINED USING MKP3 EXONIC VERSUS MKP3 INTRONIC PROBES.....</i></b>	<b><i>101</i></b>
<b><i>FIGURE21- PROXIMAL EXTENSION OF THE MKP3 DOMAIN RESULTS IN A SHORTENING OF SKELETAL ELEMENTS IN THE FORELIMB.....</i></b>	<b><i>103</i></b>
<b><i>FIGURE22- MKP3 EXPRESSION PATTERN UNDER INFLUENCE OF THE FGF INHIBITOR SU5402.....</i></b>	<b><i>104</i></b>
<b><i>FIGURE23- THE EFFECT OF FGF8 ON HAIRY2 EXPRESSION.....</i></b>	<b><i>105</i></b>
<b><i>FIGURE24- COMPARATIVE MODEL OF MOLECULAR CLOCK GENE EXPRESSION</i></b>	

*CYCLES UNDERLYING THE FORMATION OF TRUNK AND LIMB SKELETAL SEGMENTS..... 111*

*FIGURE25- MODEL PROPOSED FOR MKP3 EXPRESSION PATTERN IN THE CHICK LIMB BUD..... 114*

*FIGURE26- PARALLELISMS BETWEEN SOMITOGENESIS AND LIMB BUD DEVELOPMENT DURING STRUCTURES FORMATION..... 117*



---

## ABBREVIATIONS

<b>AER</b>	<b>Apical Ectodermal Ridge</b>
<b>A-P</b>	<b>Anterior-Posterior</b>
<b>BMP</b>	<b>Bone Morphogenic Protein</b>
<b>BMPR1a</b>	<b>Bone Morphogenic Protein Receptor 1a</b>
<b>BX-C</b>	<b>Bithorax homeotic gene complex</b>
<b>cDNA</b>	<b>complementary Deoxyribonucleic acid</b>
<b>DAPT</b>	<b>Difluorophenacetyl Alanyl Phenylglycine T-butyl ester</b>
<b>dp-ERK</b>	<b>di-phosphorylated forms of ERK</b>
<b>D-V</b>	<b>Dorsal-Ventral</b>
<i>E. coli</i>	<i>Escherichia coli</i>
<b>EDTA</b>	<b>Ethylen diamin tetra acid</b>
<b>EGTA</b>	<b>Ethylene Glycol Tetraacetic Acid</b>
<b>EN1</b>	<b>Engrailed1</b>
<b>ERK</b>	<b>Extracellular signal-Regulated Kinase</b>
<b>EtOH</b>	<b>Ethanol</b>
<b>FGF</b>	<b>Fibroblast Growth Factor</b>
<b>g</b>	<b>Gravity acceleration</b>
<b>GCR</b>	<b>Global Control Region</b>
<b>gr</b>	<b>Grames</b>
<b>HES</b>	<b>Hairy and Enhancer of Split</b>
<b>HH</b>	<b>Hamburguer and Hamilton</b>
<b>HOX</b>	<b>Homeobox</b>
<b>IHC</b>	<b>Immunohistochemistry</b>
<b>IM</b>	<b>Intermediate Mesoderm</b>
<b>INT-BCIP</b>	<b>Iodophenyl Nitrophenyl Tetrazolium – Bromo Chloro Indolyl Phosphate</b>
<b>LB</b>	<b>Luria Broth</b>
<b>Lfng</b>	<b>Lunatic fringe</b>
<b>LiCl</b>	<b>Lithium Chloride</b>
<b>LPM</b>	<b>Lateral Plate Mesoderm</b>
<b>M</b>	<b>Molar</b>

## *Abbreviations*

---

<b>MAPK</b>	<b>Mitogen Activated Protein Kinase</b>
<b>mg</b>	<b>Milligram</b>
<b>MKP3</b>	<b>MAPK phosphatase 3</b>
<b>ml</b>	<b>millilitre</b>
<b>mM</b>	<b>milliMolar</b>
<b>mRNA</b>	<b>messenger Ribonucleic Acid</b>
<b>µg</b>	<b>micrograme</b>
<b>µl</b>	<b>microliter</b>
<b>µm</b>	<b>micrometers</b>
<b>NBT-BCIP</b>	<b>Nitro Blue Tetrazolium – Bromo Chloro Indolyl Phosphate</b>
<b>OD</b>	<b>Optical Density</b>
<b>PBS</b>	<b>Phosphate-buffered saline solution</b>
<b>PBT</b>	<b>Phosphate-buffered saline solution with Tween</b>
<b>PCR</b>	<b>Polymerase Chain Reaction</b>
<b>P-D</b>	<b>Proximal-Distal</b>
<b>PFA</b>	<b>Paraformaldehyde</b>
<b>pH</b>	<b>Power Hidrogen</b>
<b>PI(3)K</b>	<b>Phosphotidylinositol 3-kinase</b>
<b>PK</b>	<b>Proteinase K</b>
<b>PL-PSM</b>	<b>Prospective Lateral Presomitic Mesoderm</b>
<b>PM-PSM</b>	<b>Prospective Medial Presomitic Mesoderm</b>
<b>PSM</b>	<b>Presomitic Mesoderm</b>
<b>PZ</b>	<b>Progress Zone</b>
<b>RA</b>	<b>Retinoic Acid</b>
<b>Raldh2</b>	<b>Retinaldehyde dehydrogenase 2</b>
<b>RNA</b>	<b>Ribonucleic Acid</b>
<b>RT</b>	<b>Room Temperature</b>
<b>RT-PCR</b>	<b>Real Time Polymerase Chain Reaction</b>
<b>Shh</b>	<b>Sonic hedgehog</b>
<b>siRNA</b>	<b>Small interference ribonucleic acid</b>
<b>SSC</b>	<b>Standard Saline Citrate</b>
<b>TAE</b>	<b>Tris.acetate EDTA buffer</b>
<b>Tbx</b>	<b>T-box</b>
<b>TE</b>	<b>Tris-HCl EDTA buffer</b>

<b>TUNEL</b>	<b>T</b> dt-mediated dUTP <b>n</b> ick <b>e</b> nd <b>l</b> abelling
<b>U/V</b>	<b>U</b> ltra <b>V</b> iolet
<b>V</b>	<b>V</b> elocity
<b>V/V</b>	<b>V</b> olume/ <b>V</b> olume
<b>WNT</b>	<b>W</b> ingless <b>w</b> int
<b>W/V</b>	<b>W</b> eight/ <b>V</b> olume
<b>ZPA</b>	<b>Z</b> one of <b>P</b> olarizing <b>A</b> ctivity





---

*Aims*



Throughout the Animal Kingdom, the time of embryonic development is maintained and strictly controlled. Each step of the process is successful only when it occurs at the right time and place. This raises the question: How is time controlled during embryonic development? Time control is particularly crucial during embryo segmentation processes, where the number of generated segments, as well as the time of formation of each segment, is extraordinarily constant and specific for each species.

The first molecular evidence for the existence of a molecular clock controlling developmental timing was found in the somitogenesis process and until now all the studies regarding embryonic cyclic gene expression have focused exclusively on this process. Nevertheless, it was recently shown that periodic expression of one of the components of the somitogenesis molecular clock can be triggered in a variety of cultured cell lines. This led us to postulate that a molecular clock could play a role in the temporal control of other embryonic structure formation.

The limb bud is a segmented structure that requires precise orchestration of cell proliferation and differentiation in both space and time. During development, the chick limb skeletal elements are laid down as cartilaginous primordia in a proximal-distal (P-D) sequence. Two models were proposed to explain limb patterning along the P-D axis: both models imply the existence of a limb bud distal zone where cells reside until they reach the time to differentiate (progress zone model) or expand (progenitor expansion model). However, nothing is known about how cells measure this time. This led us to postulate that the somitogenesis molecular clock could be operating during limb bud development.

***GENERAL AIM:***

The work developed throughout this thesis aimed at answering the following question: Is the Clock and Wavefront model proposed for somitogenesis also applicable to limb bud outgrowth and patterning?

***SPECIFIC AIMS:***

To attain our goal, we pursued the following specific aims:

**1. To study the expression patterns of the somitogenesis molecular clock components *hairyl* and *hairyl2* during forelimb development**

Our first approach to reach the principal aim of this thesis was to observe if the somitogenesis molecular clock components *hairyl* and *hairyl2* were expressed during limb bud development. To address this question we performed *in situ hybridization* experiments to characterize the expression patterns of *hairyl* and *hairyl2* genes along embryonic limb bud development stages.

**2. To establish that a molecular clock operates during proximal-distal limb outgrowth in the chick embryo**

To further address the study of *hairyl2* expression pattern during limb bud development we carried out a detailed analysis of forelimbs of different embryos at the same stage of development, where the undifferentiated chondrogenic precursors cells are been laid down to form the limb bud elements. This experiment allowed us to observe if *hairyl2* presented a dynamic expression pattern during limb bud development, in a similar way to what happens in the PSM.

In the PSM, *hairyl2* expression occurs with a cycle of 1.5 hours, corresponding to the formation time of one somite (Jouve et al, 2000). If *hairyl2* has similar cyclic expression in undifferentiated chondrogenic precursors of the forelimb bud, we would expect the period of this gene's expression cycle to be related to the time of limb skeletal element formation. However, the formation time of the limb skeletal elements has not yet been determined. Our first step towards identifying the period of *hairyl2* expression cycles was to determine the formation time of a limb skeletal element. If our analogy to somitogenesis is correct, then dynamic *hairyl2* expression in undifferentiated chondrogenic precursor cells should present a cycle time-period correlating with digit formation time. Our final step was to determine the time period of *hairyl2* expression cycles.

**3. To determine if a wavefront is travelling along the distal limb mesenchyme.**

To further extend the hypothesised parallelism between P-D limb patterning and somitogenesis, our last set of experiments was to determine if a similar mechanism to the PSM wavefront could be acting during forelimb development. To address this question, we characterized the graded distribution of *mkp3* transcripts in limb bud mesenchyme and looked for the expression patterns of both exonic and intronic *mkp3*

probes in the developing limb bud. During somitogenesis, somite size is determined by the number of cells that escape *fgf8* influence every 1.5 hours. Thus, somite size can be altered by manipulating FGF8 availability (Dubrulle et al, 2001). Similarly, we placed FGF8-soaked beads in embryos' right wings, at the proximal end of the expression domain of the FGF8 downstream effector *mkp3* and observed how this influenced the size of the limb elements formed.

It has been suggested that *fgf8* expressed by the tail bud maintains posterior PSM cells in an undifferentiated state (Dubrulle et al., 2001). Whether this "undifferentiated state" involves maintenance of cyclic gene expression remains to be determined. Therefore, our last experiment was an attempt to observe if FGF8 activity is involved in *hairy2* expression regulation in the distal limb mesenchyme.



---

## *Thesis Planning*





The present PhD thesis is organized into seven different chapters. In Chapter I a general introduction to the theme of the thesis is presented, including a literature review focusing limb bud development and the somitogenesis molecular clock and wavefront. Chapter II provides a brief description of the materials and methods used to perform the different experiments concerning the thesis work. In Chapter III, a compendium of the most relevant results obtained during the PhD work is presented, addressing the questions raised in the specific aims. The general discussion of the thesis is offered in Chapter IV, followed by the conclusions and future perspectives in Chapter V. Chapter VI includes all published and submitted papers produced by this work. In the last chapter of this PhD thesis (Chapter VII), the list of references is presented.



---

# ***CHAPTER I***

## ***Introduction***

- 1. Vertebrate limb bud formation*
- 2. The somitogenesis molecular clock*



## **1. VERTEBRATE LIMB BUD FORMATION**

All land vertebrates develop four limb buds, each pair always opposite to each other with respect to the midline. These form at specific positions along the body axis of an embryo. Limb bud development starts with a contribution from the lateral plate mesoderm (LPM) and somitic mesoderm (Figure 1A; Chevallier *et al.*, 1977; Christ *et al.*, 1977). LPM cells proliferate under the epidermal tissue at specific regions of the embryo flank, forming buds at presumptive limb levels (Searls and Janners, 1971). Later on, cells from the lateral edges of the nearby somites migrate into the limb. Skeletogenic precursors originate from LPM cells, while all the muscles that form the adult limb have their origin in the cells that migrate from the somites.

The limb skeleton is formed by a distinct number of bones with a characteristic size and shape, arranged in a specific pattern (Figure 1B). Three orthogonal axes describe the anatomy of the limb: proximal-distal (P-D), from the shoulder to the fingertips; anterior-posterior (A-P), from the thumb to little finger; and the dorsal-ventral (D-V), from the back of the hand to the palm (Figure 1C). Patterning of each limb axis is controlled by key signalling centres within the limb bud (Figure 1C). The determination of the P-D patterning is controlled by cells of the apical ectodermal ridge (AER), a specialised ectodermal structure that runs along the length of the limb bud distal tip and that expresses proteins belonging to the fibroblast growth factor (FGF) family of secreted proteins (Figure 1C; reviewed by Martin, 1998). The A-P axis is regulated by cells in a posterior domain of the limb bud called the zone of polarizing activity (ZPA), which express the secreted protein sonic hedgehog (SHH) (Figure 1C; reviewed by Tickle, 2003). D-V patterning of the limb is controlled, at least in part, by signalling molecules arising from the dorsal ectoderm to the underlying mesoderm, possibly *Wnt7a* (reviewed by Chen and Johnson, 1999). For the limb bud to develop correctly, cell proliferation, cell death and movement, as well as the assignment and interpretation of positional information, must be coordinated along all three axes.

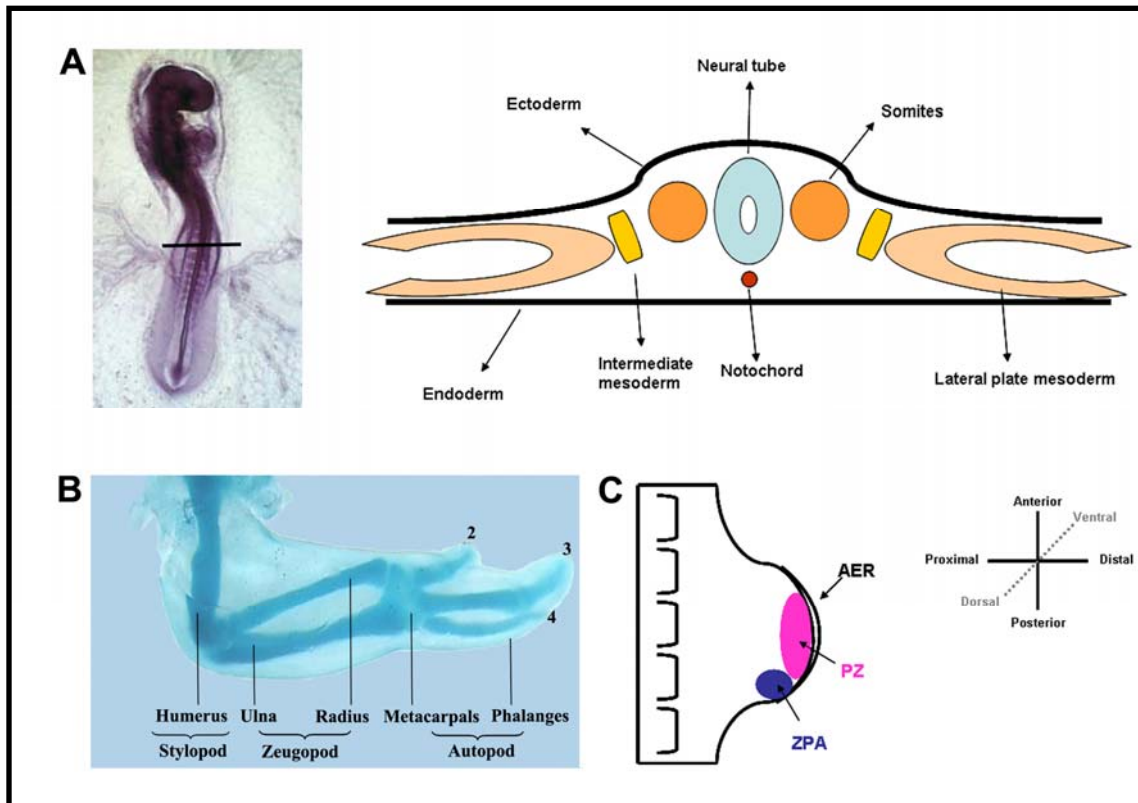


**Figure 1** – Representation of a chick embryo, a chick wing and the main signaling centers that control limb bud formation. (A) Dorsal picture of a chick embryo with 48 hours of incubation and illustration of a transversal section at level of the presumptive wing region (somites 15-20; bracket). (B) Dorsal view of a chick wing with 7 days of incubation showing all the skeletal elements that formed the chick forelimb (humerus, ulna, radius, metacarpals and phalanges). (C) Illustration of the main signaling centers responsible for limb bud outgrowth and representation of the three axes that describe the anatomy of the limb bud.

### 1.1 Building the limb bud: the initiation program

The expression of specific *Hox* genes along the anterior-posterior axis of the embryo body defines the levels where limb buds will form (reviewed by Christ *et al.*, 1998). In fish (in which the pectoral and pelvic fins correspond to the anterior and posterior limbs, respectively), amphibians, birds, and mammals, the forelimb buds are found at the most anterior expression region of *Hoxc-6*, the position of the first thoracic vertebra (Oliver *et al.*, 1988; Molven *et al.*, 1990; Burke *et al.*, 1995).

In chick, previous studies showed that the intermediate mesoderm (IM) is required for limb bud initiation (Stephens and McNulty, 1981, Strecker and Stephens, 1983, Geduspan and Solursh, 1992), since when a foil barrier was placed between the

LPM and IM limbs did not form. Likewise, removal of the IM results in loss of adjacent limb tissue. These experiments indicate that the IM produces a factor that maintains the proliferation of the flank at presumptive limb regions. Chick *fgf8* expression pattern, as well as its morphogenetic capacity, makes it an excellent candidate for playing a role in this process (Crossley *et al.*, 1996, Vogel *et al.*, 1996). *Fgf8* expression is transiently localized to the IM at limb bud levels just prior to limb bud outgrowth. When a bead embedded in FGF8 or other FGF family members was placed in the flank of an embryo, at any A-P position, a new ectopic limb was formed from the LPM (Cohn *et al.*, 1995; Crossley *et al.*, 1996; Vogel *et al.*, 1996). These experiments demonstrate FGF's capacity to induce an entire program of limb bud initiation and subsequent patterning. However, recent studies made by Boulet and collaborators in mice show that when *fgf8* is inactivated, in the IM, both position and timing of forelimb bud initiation are unaffected and limb bud development proceeds normally. Moreover, inactivation of both *fgf4* and *fgf8* leads to the complete absence of forelimbs in newborns. These results indicate that *fgf8* is not the only limb bud induction player in the IM but other members of the FGF family, or as yet unidentified signals from the IM or axial regions, may be working together to initiate the process of limb bud formation (Boulet *et al.*, 2004).

The molecular mode of action described for FGF8 implies feedback loops with FGF10. *fgf8* expressed in the IM is capable of inducing *fgf10* expression in the LPM of the presumptive limb areas. FGF10 operates on the overlying surface ectoderm to induce expression of *fgf8* in this tissue. This induction occurs in parallel with the appearance of the AER, and expression of the *fgf8* in the AER is required for the maintenance of *fgf10* in the nascent limb mesenchyme and the localization of the *shh* to the posterior margin of the limb bud. The SHH protein produced in the posterior part of the LPM directly or indirectly induces expression of *fgf4* in the posterior part of the overlying ectoderm. Interaction between FGF10, FGF8, SHH and FGF4 maintain the outgrowth of the established limb bud (Crossley *et al.*, 1996; Ohuchi *et al.*, 1997; reviewed by Martin, 1998).

Simultaneously, another discovery was made; retinoic acid (RA) appears to be critical for the initiation of limb bud outgrowth, since blocking RA synthesis prevents limb bud initiation (Stratford *et al.*, 1996). Bryant and Gardiner (1992) suggested that a gradient of RA along the anterior-posterior axis might activate certain homeotic genes in particular cells and thereby specify them to become included in the limb field. This is the case of *Hoxb8*, rapidly induced by exogenous application of RA in the absence of

## ***Introduction***

---

protein synthesis, while down-regulation of its expression occurs in the presence of retinoid receptor antagonists. In addition, *Hoxb8* domains and polarizing activity are coextensive in the LPM. Since retinoid receptor antagonists applied to presumptive wing region block the formation of the ZPA, this suggests that retinoids are required for the establishment of the ZPA and that retinoids act, at least in part, through *Hoxb8*, a gene associated with ZPA formation (Charité *et al.*, 1994; Lu *et al.*, 1997).

Studies performed by Kawakami and collaborators (2001) provide novel insights in the model established for limb bud initiation, proposing an expanded model with the addition of WNT signalling pathway members. This new model consists of: (a) Previous to limb initiation (stage HH12), *fgf8* is expressed in the IM adjacent to the presumptive forelimb area. *fgf10* is expressed at the same level in the LPM and diffusely in the caudal portion of the LPM, where it co-localizes with *wnt8c*. *wnt8c* may be regulating *fgf10* in this area, as suggested by ectopic induction of *fgf10* by *wnt8c* expressing cells implanted in the embryo flank. (b) During limb induction (stage HH14), both *fgf8* and *wnt2b* are expressed in the IM. *wnt2b* is also expressed in the LPM of the presumptive forelimb area. WNT2B signals through  $\beta$ -catenin to induce and/or maintain *fgf10* specifically in the prospective forelimb. (c) In a later stage of limb bud initiation (stage HH16), *wnt2b* and *fgf10* expression is confined to the presumptive forelimb bud field in the LPM. Here, FGF10 signals to the surface ectoderm (SE) to induce *wnt3a*, resulting in activation of *fgf8*. In the chick, *wnt3a* expression persists in the AER throughout limb development where it maintains *fgf8* expression and AER function (Kengaku *et al.*, 1998). To complete the loop, FGF8 signals back to the mesenchyme of the nascent limb, where it contributes to maintain expression of *fgf10* and to initiate and/or maintain *shh* expression (Kawakami *et al.*, 2001).

An illustrative picture that represents all the interactions involved during limb bud initiation can be observed in Figure 2.



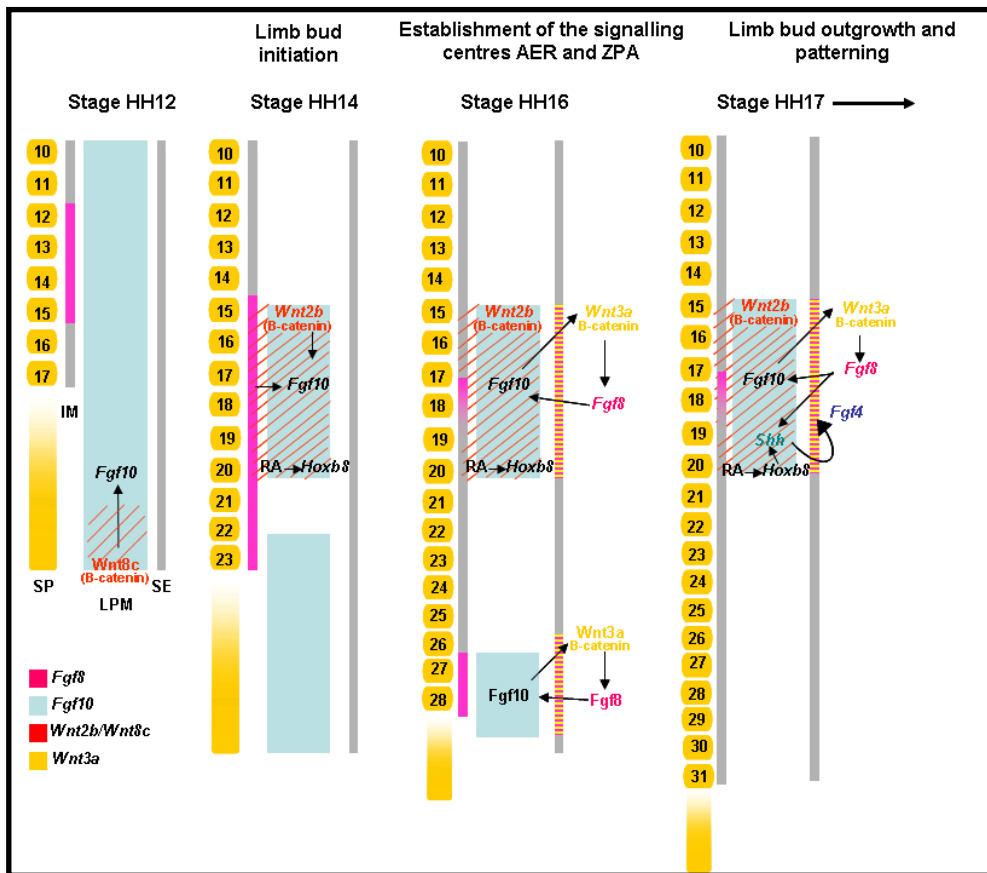


**Figure 2** – Illustration of an integrative model showing the main signals involved during limb bud initiation.

## 1.2 Specification and determination of limb bud identity

Classical experiments on limb identity (Saunders *et al.*, 1957; Saunders *et al.*, 1959; Stephens *et al.*, 1989) and recent studies on the function of T-box transcription factors (*Tbx5* and *Tbx4*) (Gibson-Brown *et al.*, 1998; Isaac *et al.*, 1998; Logan *et al.*, 1998; Ohuchi *et al.*, 1998; Rodriguez-Esteban *et al.*, 1999; Takeuchi *et al.*, 1999) have provided many insights into how two characteristic structures (forelimb and hindlimb) are committed from the lateral plate mesoderm in each particular position along the main body axis.

It has been postulated that *Tbx5* and *Tbx4*, and a paired-like homeodomain factor *Pitx1*, play important roles in type-specific limb initiation. *Tbx5* expression starts in the presumptive forelimb region and its expression is maintained in the forelimb bud during limb development, whereas the expression of *Tbx4* and *Pitx1* is totally hindlimb bud-specific (Gibson-Brown *et al.*, 1998; Isaac *et al.*, 1998; Logan *et al.*, 1998; Ohuchi *et al.*, 1998; Saito *et al.*, 2002). Moreover, using chick manipulation systems, it has been

## ***Introduction***

---

demonstrated that wings with leg-like characters and legs with wing-like characters were obtained when *Tbx4* and *Tbx5* were introduced into the presumptive hindlimb and forelimb regions, respectively (Rodriguez-Esteban *et al.*, 1999; Takeuchi *et al.*, 1999). *Tbx5*, *Tbx4* and *Pitx1* gain-of-function and loss-of-function studies suggest that these molecules are involved in the limb initiation process, associating with several members of the FGF and WNT families (Minguillon *et al.*, 2005; Agarwal *et al.*, 2003; Takeuchi *et al.*, 2003; Rallis *et al.*, 2003; Garrity *et al.*, 2002; Ahn *et al.*, 2002; Ng *et al.*, 2002; Marcil *et al.*, 2003). *Pitx1* is thought to be the upstream regulator of *Tbx4* (Logan and Tabin, 1999; Szeto *et al.*, 1999), and both *Pitx1* and *Tbx4* are necessary for hindlimb outgrowth. Chick studies on *Tbx5*, *Tbx4*, or *Pitx1* have suggested that these genes function as selector genes for limb identity (Takeuchi *et al.*, 1999; Rodriguez-Esteban *et al.*, 1999; Logan and Tabin, 1999), while a recent study using genetic methods in the mouse (Minguillon *et al.*, 2005) has suggested that *Tbx5* and *Tbx4* do not determine limb-specific identities, but that *Pitx1* plays a role in the specification of hindlimb-type identity. Further, Minguillon and co-workers (2005) proposed a role for *Tbx5* and *Tbx4* in initiation of limb outgrowth. Overall, it is thought that *Tbx5* and *Tbx4* are accurate markers of forelimb and hindlimb identity, but these authors suggest that they do not themselves play a significant role in specification of limb-type identity (Minguillon *et al.*, 2005). Until now, little is known about the upstream mechanism for limb initiation/outgrowth in each limb region. Minguillon and collaborators (2005) also proposed a model in which limb specific identity and ultimately limb-specific morphology is specified by different combinatorial codes of factors in the LPM at anterior versus posterior positions. These factors may include a particular combination of HOX proteins and *Pitx1*. Recent work reported by Saito and colleagues (2006) suggests that the paraxial mesoderm, which has level-specific characteristics along the anterior-posterior axis, is the source of the environmental signal responsible for limb bud initiation (Saito *et al.*, 2006).

### **1.3 Patterning the vertebrate limbs**

#### **1.3.1 Proximal-Distal (P-D) axis**

P-D limb development depends on a stripe of specialized epithelium at the junction between the dorsal and ventral ectoderm at the distal tip of the limb bud, the apical ectodermal ridge (AER) (Figure 1C). The AER is responsible for P-D limb

outgrowth and its activity keeps the subjacent mesoderm in an undifferentiated state (Saunders, 1948; Summerbell *et al.*, 1973). During development, the chick limb skeletal elements are laid down as cartilaginous primordia in a P-D sequence. These elements, believed to be all initially the same size, grow differentially, giving rise to seven skeletal compartments: humerus, radius/ulna, two carpal elements and three elements in the third digit (Figure 1B; Wolpert *et al.*, 1975).

#### *1.3.1.1 Apical Ectodermal Ridge*

Microsurgical removal of the AER in chick embryos halts limb bud outgrowth and the laying down of the structures along the P-D axis. When the AER is removed from early developing chick limb buds almost all limb structures are lost, whereas if its removal occurs at progressively latter stages, progressively more distal structures are lost, with the proximal structures being unaffected (Saunders, 1948; Summerbell, 1974). Thus, the AER is essential for P-D growth and patterning. Experiments in which an older AER was placed onto a young limb bud, or vice versa, showed that the signal from the AER is permissive, rather than instructive; in both cases, the skeleton was patterned normally, indicating that it is the limb bud mesenchyme and not the AER that contains the information for P-D patterning (Rubin and Saunders, 1972).

The key signals that mediate AER function are the FGFs. *fgf8* is expressed very early throughout the AER, whereas *fgf4*, *fgf9* and *fgf17* are restricted to the posterior and distal part and *fgf2* is expressed throughout the limb ectoderm in chick, including the AER. The first indications of the molecular nature of the AER signal were published in the 1990s, when it was shown that substituting the AER for FGF-soaked beads (FGF2, FGF4 or FGF8) could rescue P-D development of the chick limb after ridge removal (Fallon *et al.*, 1994; Niswander *et al.*, 1993; Mahmood *et al.*, 1995). More recently, *fgf4* conditional knockouts were shown to present normal limbs (Sun *et al.*, 2000; Moon *et al.*, 2000), while in *fgf8* conditional knockouts there are skeletal defects, with anterior and proximal structures being most severely affected (Lewandoski *et al.*, 2000; Moon and Capecchi, 2000). Inactivation of both *fgf4* and *fgf8* in the AER of mouse limb buds produced more severe phenotypes than inactivating *fgf8* alone (Sun *et al.*, 2002). These studies suggest that other FGFs or other molecules expressed in the ridge, alone or in combination, can to some extent, rescue limb development.

### *1.3.1.2 Models proposed for P-D patterning*

One paradigm to explain cell fate specification along the P-D limb axis is the Progress Zone (PZ) model proposed by Summerbell, Lewis and Wolpert in the 1970s (Figure 3A; Summerbell *et al.*, 1973). According to this model, there is a mesenchymal region at the tip of the limb bud beneath the AER (the PZ) where the positional value of a cell changes with time. AER signals (FGFs) maintain PZ cells in an undifferentiated state and their positional value only becomes fixed when they leave this area (Summerbell *et al.*, 1973). Thus, cells convert the time spent in the PZ into positional information: cells leaving the PZ early give rise to humerus and those leaving last form digits. This model was based on experiments showing that AER removal at progressive stages of limb development results in progressively more distal truncations (Saunders, 1948; Summerbell, 1974). AER removal results in loss of the PZ due to the lack of a signal from the ridge and also some cell death occurs, resulting in truncation of the limb when the experiment is done in early stages. By contrast if cells in the PZ are killed by X-irradiation or cytotoxic drugs at an early stage, the distal structures develop and proximal ones are lost, indicating recovery of the PZ in the presence of AER. This is the finest support for the PZ model, since the remaining cells spend more time in the PZ to repopulate, then when they leave the zone they will form the more distal structures (Wolpert *et al.*, 1979). Another study that supports this model is based on experiments in which the distal tips of limbs from two different staged embryos were exchanged; the older tip generated only distal structures, whereas the younger tip generated all P-D structures. These experiments put in evidence that cells undergo progressive changes in specification from a proximal to distal fate as they remain under the influence of the AER, as a measure of time spent in the PZ. So, according to the PZ model, P-D fate is specified progressively.

An alternative model proposes that cell populations giving rise to different P-D limb structures are already specified within the distal mesenchyme of early limb buds (Figure 3B; Dudley *et al.*, 2002; Sun *et al.*, 2002). Specified limb cell populations expand sequentially in time, such that cells of proximal structures start proliferating first and cells of distal structures last. This model suggests that cell death and reduction in proliferation that occur in the distal mesenchyme after AER removal are sufficient to explain the resulting truncation phenotype. Furthermore, labelling experiments show that the descendants of cells located at a certain distance of the AER are usually found

exclusively in one limb segment corresponding to the initial position of the marked cells.

Thus, both models imply the existence of a limb bud distal zone where cells reside until they reach the time to differentiate (progress zone model) or expand (early specification model). However, nothing is known about how cells measure this time.

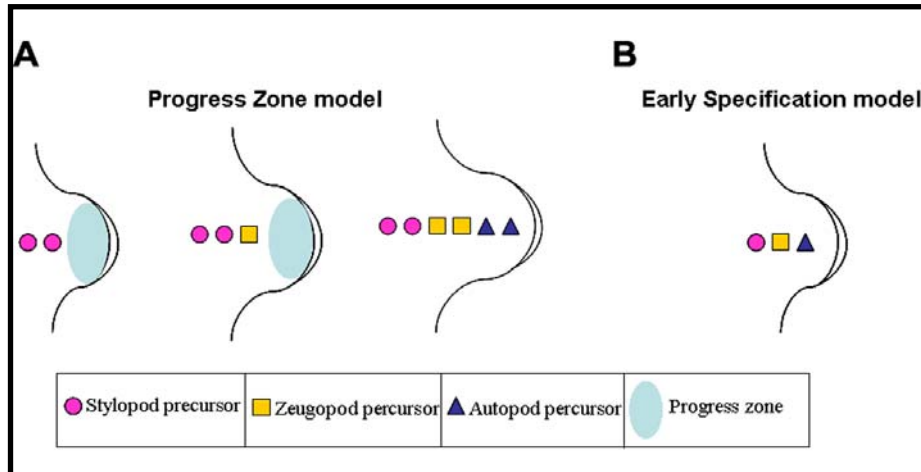


**Figure 3** – Models proposed for P-D patterning. (A) Illustration of the Progress Zone model, where P-D fate is specified progressively. (B) Schematic representation of the Early Specification model, where cells are already specified at early stages of limb bud development.

### 1.3.1.3 Opposing RA and FGF signals control P-D vertebrate limb

Two closely related homeobox genes, *meis1* and *meis2* are expressed in the lateral plate mesoderm and later in the proximal limb region, up to the humerus-radius/ulna boundary (Cecconi *et al.*, 1997; Moskow *et al.*, 1995; Nakamura *et al.*, 1996; Oulad-Abdelghani *et al.*, 1997). These genes have recently been identified as determinants of proximal limb compartments, since overexpression of either *meis1* or *meis2* leads to inhibition or truncation of the distal compartments. In addition, ectopic distal *meis1* expression inhibits the progressive distalization of PZ cells, resulting in limbs with proximally shifted identities along the P-D axis (Capdevila *et al.*, 1999; Mercader *et al.*, 1999).

Since regulation of Meis activity along the P-D limb axis is essential for the proper distalization of limb cells, the mechanisms involved must play a central role in P-D limb specification. Although combinations of distal diffusible factors such as bone morphogenetic protein (BMP) plus a FGF, or BMP plus a WNT, have been shown to

## Introduction

---

inhibit *meis* expression and to distalize proximal limb cells (Capdevila *et al.*, 1999), the mechanism that promotes Meis activity in the proximal limb remains unknown.

Mercader and collaborators (2000) have explored this mechanism and found that RA is an activator of *meis* genes. Along the P-D limb axis, RA has been shown to proximalize regenerating urodele limbs, leading to tandem P-D duplication of limb structures (Maden, 1982). Additionally, grafts of chick limb tissue exposed to RA develop structures with a more proximal identity than expected (Tamura *et al.*, 1997). RA activates *meis* genes ectopically in the distal limb, promoting proximalization of limb cells and it is required endogenously to maintain the proximal *meis* domain in the limb. After limb-bud appearance, RA synthesis and signalling is restricted to the proximal limb by FGF activity. The model proposed by Mercader and collaborators supports that FGF activity promotes limb distalization through inhibition of the proximalizing RA signal required to maintain the Meis activity, providing a molecular basis for the role of RA in specifying proximal limb fates in different vertebrates, and suggests a mechanism by which FGF promotes limb distalization (Figure 4; Mercader *et al.*, 2000).

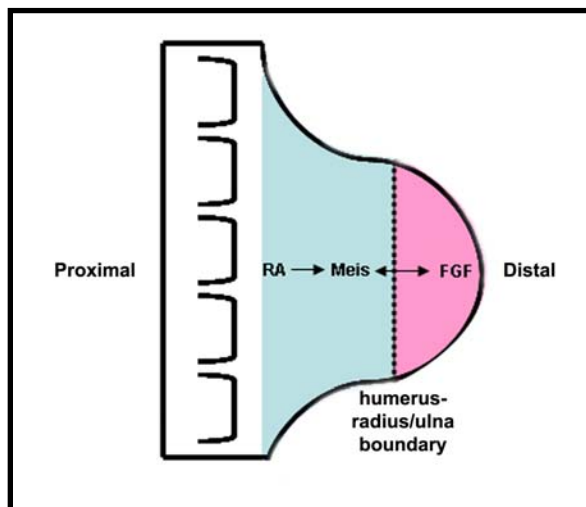


**Figure 4** – Illustration of the opposing FGF and RA / Meis signals.

### 1.3.2 Anterior-Posterior (A-P) axis

The limb bud A-P axis is regulated by cells residing in the limb bud posterior domain, the so-called zone of polarizing activity (ZPA), which is responsible for digit patterning (Figure 1C). Normal chick forelimb digit pattern is digit2-digit3-digit4 (2-3-4) (Figure 1B) different from the mouse forelimb that has five digits with the pattern digit1-digit2-digit3-digit4-digit5 (1-2-3-4-5).

### *1.3.2.1 Zone of Polarizing Activity*

In 1968, Saunders and Gasseling discovered that the posterior region of the limb mesenchyme, a region now called ZPA, can re-pattern the A-P axis when grafted at the anterior of the developing limb buds: it causes anterior cells to form additional digits in a mirror image duplication of the normal digits, being the additional digits derived from the host embryo and not from the transplanted cells (Tickle *et al.*, 1976). In 1969, Lewis Wolpert proposed that the ZPA cells produce a morphogen, a small diffusible molecule that forms a gradient across the limb bud, and that the polarity and fate of digit precursor cells would be determined by their response to specific morphogen thresholds. The anterior and posterior digits would form at low and high concentrations, respectively (Wolpert, 1969). Wolpert's model provided a straightforward explanation for most experimental manipulations of the polarizing region in chick limb buds and the theoretical basis to search for this morphogen signal. Extensive series of experiments showed that polarizing region signalling is dose dependent and acts in a long range fashion, as predicted by the model (Tickle *et al.*, 1975). The first defined chemical capable of mimicking signalling by the polarizing region, was discovered in chick. Tickle and colleagues (1982) achieved a new breakthrough by establishing that the implantation of a bead soaked in RA into a chick limb bud mimicked transplants of polarizing region cells.

The constant search for the morphogen proposed by Wolpert, led Clifford Tabin and colleagues (Riddle *et al.*, 1993) to identify *shh*, a homologue of the *Drosophila hedgehog* gene, as the signal expressed by the polarizing region in vertebrate limb buds. Insertion of *shh*-expressing cells or recombinant SHH protein to the anterior of chick limb bud caused mirror-image digit duplications (Riddle *et al.*, 1993). On the contrary, genetic removal of *shh* in mice resulted in a pleiotropic phenotype (Chiang *et al.*, 1996), including complete disruption of distal limb development (at best, just digit1 developed) (Chiang *et al.*, 2001; Kraus *et al.*, 2001). A similar phenotype is observed in the chick mutant *oligozeugodactyly (ozd)*, which lacks *shh* function in the limb (Ros *et al.*, 2003). Furthermore, posterior mesenchyme from knockout *shh* limbs lacks polarizing activity (Chiang *et al.*, 2001). Together, these studies indicate that *shh* is the key signal from the ZPA driving limb A-P patterning.

## Introduction

### 1.3.2.2 Models for A-P positional value specification in chick and mouse limb buds

Two models have been proposed to explain limb A-P patterning. The first is the morphogen-gradient model, in which SHH concentration specifies the A-P positional values. Positional values are progressively specified as the SHH gradient becomes established in chick early limb, these values are then remembered. The digit primordia develop approximately 24 hours after the positional values are fixed (Figure 5A; Yang *et al.*, 1997).

Fate maps performed in mouse embryo limbs revealed that the length of time that cells are exposed to the highest concentrations of SHH might contribute to digit patterning (Harfe *et al.*, 2004; Ahn and Joyner, 2004). This led to a new detailed model explaining the specification of positional value for each mouse digit, which integrates both concentration and the length of exposure to SHH (Harfe *et al.*, 2004). Specification of digit1 is probably SHH independent because the single digit that develops in the limbs of knockout *shh* mice most closely resembles digit1 (Chiang *et al.*, 2001). Low concentrations of SHH specify the positional value that leads to the formation of digit2, whereas cells are specified to form digit3, digit4 and digit5 according to the length of time of exposure to SHH (Figure 5B).

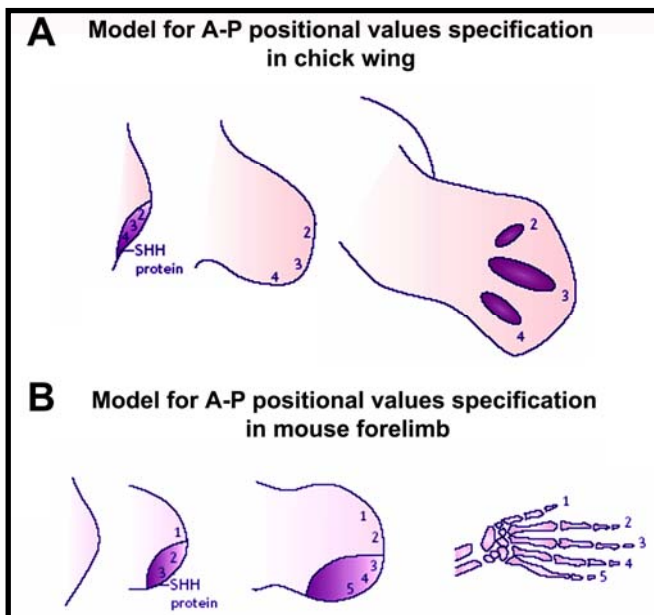


**Figure 5** – Schematic representation of the models proposed for A-P positional values specification in chick wing (A) and mouse forelimb (B). Adapted from Tickle, 2006.

### 1.3.2.3 A-P patterning of limb proximal structures is *shh* independent

A *shh*-independent network seems to pattern the humerus until the elbow/knee joint, since the *shh* knockout embryo has four limbs with recognizable humerus/femur bones that have anterior–posterior polarity. Distal to the elbow/knee joints, skeletal



elements representing the radius/ulna or tibia/fibula form but lack identifiable anterior–posterior polarity. Therefore, *shh* specifically becomes necessary for normal limb development at or just distal to the elbow/knee joints during mouse limb development. The forelimb autopod is represented by a single distal cartilage element, while the hindlimb autopod is invariably composed of a single digit with well-formed interphalangeal joints and a dorsal nail bed at the terminal phalanx (Chiang *et al.*, 2001). A similar phenotype is observed in *gli3* knockout mutants and in the double knockout for *gli3* and *shh* (te Welscher *et al.*, 2002b; Litingtung *et al.*, 2002).

The GLI proteins, largely conserved during evolution, are transcriptional effectors of the SHH signalling (Hooper and Scott, 2005). Another important gene for *shh* expression localization in early fin/limb buds, is the transcription factor *dHand* (Charité *et al.*, 2000; Fernandez-Teran *et al.*, 2000; Yelon *et al.*, 2000). The early molecular A-P network includes all these elements. *gli3*, expressed in the anterior limb mesenchyme is a negative regulator of both *shh* and *dHand* expression. In turn, *dHand*, expressed in the posterior mesenchyme, is a negative regulator of *gli3* expression (te Welscher *et al.*, 2002a; te Welscher *et al.*, 2002b). Together with the FGF signals from the AER, *dHand* is required to activate *shh* expression (Figure 7A; Sun *et al.*, 2002; Charité *et al.*, 2000). This *shh* signalling-related network is not required for humerus or radius/ulna patterning and growth; instead it regulates digit number and identity.

#### 1.3.2.4 Patterning the digits

Digits are an evolutionary acquisition of the tetrapod limb and present specific morphologies according to their position along the A-P axis. In the chick limbs, separate condensations of chondrogenic cells that will form each of the three wing digits or four leg digits emerge between stages HH27 and HH28 (Hamilton–Hamburger stages; 5–6 days of development) in a posterior to anterior sequence (Hinchliffe, 1977). Digital rays start off as continuous rods of cartilage that elongate and periodically segment to form interphalangeal joints and thus generate a precise number of phalanges. Digit development is finally completed by formation of a terminal phalange that carries ectodermal derivatives such as nails or claws. When SHH beads are implanted in interdigital spaces between digit primordia at stages prior to segmentation, several effects can be produced in a dose- and stage-dependent manner. These include digit truncations, soft tissue fusions and fusions between the tips of adjacent digits and, more remarkably, formation of elongated digits with an extra phalange (Dahn and Fallon,

## ***Introduction***

---

2000; Sanz-Esquerro and Tickle, 2000; Sanz-Ezquerro and Tickle, 2003). Bone morphogenetic protein (BMP) signalling was implicated in this latter effect (Dahn and Fallon, 2000). In 2003, Sanz-Esquerro and Tickle demonstrated that FGFs are also involved and proposed a mechanism for controlling phalange number. They proposed that a signalling feedback loop involving Hedgehogs, BMPs and BMP antagonists might operate at the tip of each digit and regulate FGF signalling. When beads soaked in SHH are added, FGF signalling is prolonged and an additional phalanx is produced - a more 'posterior' toe phenotype - while when beads soaked in FGF inhibitors are added, FGF signalling is halted and the toe lacks a phalanx - a more 'anterior' phenotype. In both cases, the tip of the toe forms normally, suggesting that there is a specific mechanism for 'finishing' off the digit and making the tip that comes into play when FGF signalling ceases. This means that the process that generates digit tips is independent of that which generates more proximal phalanges.

The separation of individual digits is mediated by cell death of the soft tissue webs between the digits (Hurlé and Ganan, 1986; Saunders and Fallon, 1966). While this interdigital mesenchyme normally disappears, it has been shown that it still has the potential to form digits. In fact, when the ectoderm of the interdigital region in chick embryo legs is injured, this can lead to the formation of a rudimentary digit with 1–2 phalanges and a tip (Hurlé and Ganan, 1986). One class of molecules that has been revealed to be implicated in the regulation of interdigital cell death is BMP (Zou and Niswander, 1996). Interdigital cell death is a particularly well known example of programmed cell death occurring during normal embryonic development; cell death also occurs in earlier limb bud stages at both anterior and posterior margins of the limb buds (anterior and posterior necrotic zones) and more centrally (the opaque patch). The posterior necrotic zone overlaps with the polarizing region and experimental manipulations show that cell death acts as a buffering mechanism to regulate the number of cells that express *shh* in the limb bud (Sanz-Ezquerro and Tickle, 2000).

### 1.3.3 Dorsal-Ventral (D-V) axis

D-V asymmetry is a characteristic feature of adult vertebrate limb anatomy. In most species, the skin that covers the dorsal and ventral limbs is uniquely specialized, as exemplified by ventral footpads in mice and by the dorsal nails and increased density of hair follicles in mammals, as well as by the number and arrangement of feathers and

scales in the chick. Likewise, internal limb tissues such as the skeleton, muscles, tendons and nerves are differentially arranged in the dorsal versus the ventral limb.

D-V patterning is regulated by the covering ectoderm, since when limb ectoderm is rotated 180° relative to the mesenchyme, the mesenchymal structures (skeleton, muscle and tendons) become inverted such that they correspond to the polarity of the ectoderm (MacCabe *et al.*, 1974). The transcription factor *Lmx1b* has been shown to be important in D-V patterning; it is expressed in the dorsal limb mesenchyme and is required for cells to adopt a dorsal character (Chen *et al.*, 1998). Although the early regulator of *Lmx1b* expression is unknown, *Lmx1b* is induced by *wnt7a* which is expressed in the dorsal limb ectoderm, as the limb bud forms. In the absence of *wnt7a*, the dorsal pattern of the distal structures is not established and the limbs appear bi-ventral (Parr and McMahon, 1995). Expression of *wnt7a* is restricted to the dorsal ectoderm because it is repressed in ventral ectoderm by the transcription factor *Engrailed1* (*En1*). In *En1* knockout limbs, *wnt7a* is misexpressed in the ventral ectoderm and the distal structures develop with bi-dorsal character (Loomis *et al.*, 1996). *En1* itself is induced in the ventral ectoderm by BMP signalling through the type I receptor, *Bmpr1a*. Loss of BMP signalling also leads to *wnt7a* misexpression and bi-dorsal limbs (Chen and Johnson, 1999; Ahn *et al.*, 2001; Pizette *et al.*, 2001). The signals required for D-V patterning are represented in Figure 6.

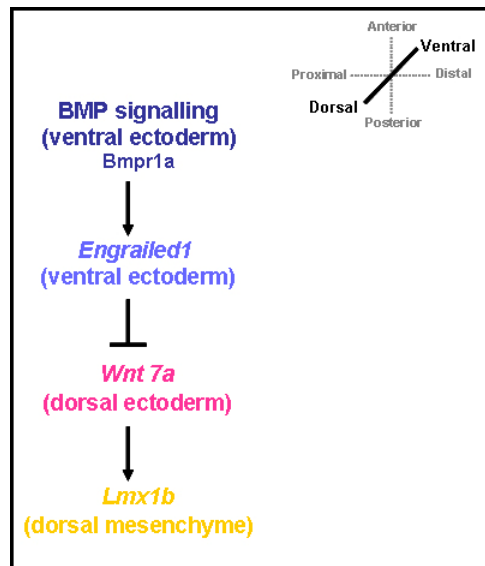


**Figure 6** – Representation of the signals required for D-V patterning.

### 1.3.4 Coordination of the limb signalling centres

Limb patterning and growth in three dimensions is coordinated through interactions between the limb organizing centres and the molecules that they produce (AER-FGFs, ZPA-SHH, dorsal ectoderm-WNT7A) (Niswander, 2002).

ZPA vs AER signalling: AER removal results in the rapid downregulation of *shh*, which can be rescued by an FGF-soaked bead (Laufer *et al.*, 1994; Niswander *et al.*, 1994). More direct evidence for the role of FGF in the induction of *shh* expression is provided by the *fgf4/8* double-knockout mice: in the absence of these AER signals, *shh* expression is not induced (Sun *et al.*, 2002). SHH, in turn, maintains *fgf4* expression in the AER by acting through the Formin protein (encoded by the gene disrupted in the *limb deformity* mouse mutant) to maintain the expression of *Gremlin*, a BMP antagonist (Figure 7A). *Gremlin* inhibits BMP-mediated *fgf4* inhibition, allowing *fgf4* expression in the AER (Figure 7A; Zuniga *et al.*, 1999; Pizette and Niswander, 1999; te Welscher *et al.*, 2002).

ZPA vs Dorsal ectoderm signalling: The removal of the dorsal ectoderm or the loss of *wnt7a* by gene targeting causes a reduction or loss of *shh* expression (Parr and McMahon, 1995; Yang and Niswander, 1995). So, the dorsal ectoderm is also required to maintain *shh* expression, in conjunction with the AER (Figure 7B). Interactions between FGFs, SHH and WNT7A might serve to coordinate signalling from the AER, ZPA and dorsal ectoderm (Figure 7B).

AER and D–V axis formation are already linked during early limb development. Studies of BMP gain- and loss-of-function in chick (Pizette *et al.*, 2001), as well as conditional inactivation of *Bmpr1a* in mouse (Ahn *et al.*, 2001), have shown that in the absence of BMP signalling, the AER is not formed and *fgf8* expression is not induced. Furthermore, the limbs become bi-dorsal due to the loss of *En1* and misexpression of *wnt7a*. Thus, BMP signalling acts upstream of both AER formation and D–V patterning. Moreover, BMP-mediated regulation of these two processes is independent of one another: it is the *En1/Wnt7a/Lmx1b* pathway that affects D–V patterning (Ahn *et al.*, 2001; Pizette *et al.*, 2001), while the regulation of AER formation may involve *Msx* transcription factors (Pizette *et al.*, 2001). The interactions between these signals are illustrated in Figure 7C.

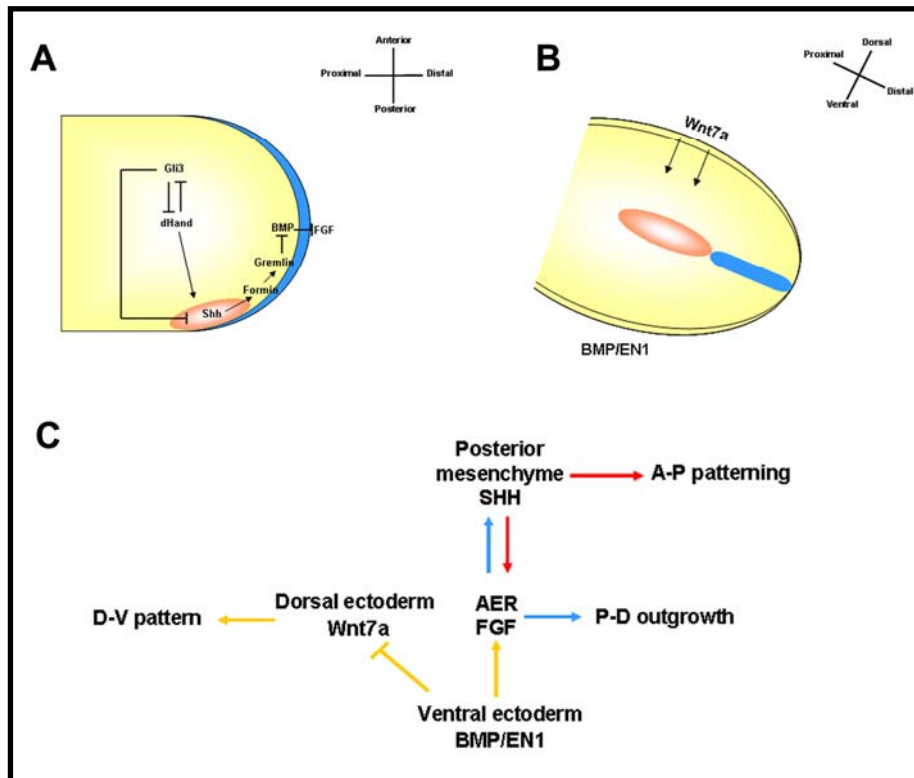


**Figure 7** - Signalling pathways in vertebrate limb development. (A) Illustration of the molecular interactions that coordinate limb growth and patterning along the P-D axis (under the control of FGFs), and A-P axis (under the control of SHH). (B) Schematic representation of the limb bud D-V axis that is under the control of BMPs and EN1 from the ventral ectoderm and Wnt7a from the dorsal ectoderm. (C) Schematic representation of the main signals required during vertebrate limb development.

#### 1.4 *Hox* genes collinearity during limb development

Mammalian genomes contain 39 *Hox* genes, organized in four clusters: *HoxA*, *HoxB*, *HoxC* and *HoxD* (McGinnis and Krumlauf, 1992). These series of contiguous genes encode transcription factors necessary for proper development to proceed. Coordinated *Hox* gene expression in both time and space, is partly dictated by their order along the chromosome, so that genes are activated sequentially from the 3'- end of the gene cluster toward its 5'- extremity. Genes activated early on during embryonic development will establish an anterior expression boundary in a variety of trunk derivatives, whereas subsequent gene activations will generate progressively more posterior boundaries, following molecular mechanisms that are only beginning to be understood (Kmita and Duboule, 2003). This phenomenon is referred to as collinearity, originally described by Edward B. Lewis from genetic studies with the fruit fly *Bithorax*

## Introduction

---

homeotic gene complex (BX-C) (Lewis, 1978), being later extended to the establishment of the vertebrate A-P body axis (Gaunt *et al.*, 1988). In the course of vertebrate evolution, this collinear regulation was appointed several times along with the emergence of structures developing from secondary axes, such as external genital organs and limbs (Tarchini and Duboule, 2006).

In mammals, both *HoxA* and *HoxD* gene clusters play a main growth-promoting function during early limb development, as shown by the effect of their partial, full or combined inactivation leading to severe truncations (Davis *et al.*, 1995; Kmita *et al.*, 2005). In contrast, neither *HoxB* nor *HoxC* complexes appear to have an analogous role, based on observation of their expression patterns and in the minor effects of their deletions *in vivo* (Suemori and Noguchi, 2000; Medina-Martinez *et al.*, 2000). *Hoxa* gene expression patterns suggest a function in the definition of proximal-to-distal domains while the *Hoxd* genes display asymmetric patterns along the A-P axis, indicating an additional role in the establishment of this critical skeletal polarity. This was confirmed by experiments in which a uniform expression of *Hoxd* genes led to limbs with bilateral symmetry (Zakany *et al.*, 2004).

*Hoxd* genes are activated in limb buds following multiple collinear strategies. In the early limb, genes are activated according to a time sequence, starting with the most 3'-located members, such as *Hoxd1* and *Hoxd3*. *Hoxd1* through *Hoxd9* are expressed throughout the entire emerging bud, in a slightly uniform expression. From *Hoxd10* onward, however, the expression domains become progressively restricted to more posterior limb cells, until *Hoxd12* and *Hoxd13* positive cells, as a set of nested patterns (Dollé *et al.*, 1989; Nelson *et al.*, 1996). Consequently, two collinear processes can be observed in the early limb bud, occurring in both time and space, the first one supposedly controlling the latter. The restriction of the most 5'-located *Hox* gene expression in the posterior part of the developing limb is vital to activate and/or maintain expression of the *shh* gene at the posterior margin, as shown by both gain- and loss-of-function experiments (Charité *et al.*, 1994; Knezevic *et al.*, 1997; Zakany *et al.*, 2004; Kmita *et al.*, 2005). In turn, *shh* will modulate the second wave of *Hoxd* gene expression in the presumptive digit domain, probably by antagonizing the repressive effect of the *gli3* gene product (Litington *et al.*, 2002; te Welscher *et al.*, 2002). *Hox* gene expression in digits will be restricted to five genes located at the centromeric 5'-end of the cluster, with a 5' to 3' progressive collinear diminishing of the transcriptional

efficiency. The posterior location of the *shh* signal induces an A-P asymmetry in the expression of *Hoxd* genes in emerging digits, which will be translated into the skeletal A-P polarity observed in our hands and feet. Accordingly, *Hoxd* gene expression in developing limbs appears in two waves, before and after *shh* signalling (Zakany *et al.*, 2004).

Recently, Tarchini and Duboule (2006) analyzed a set of mouse strains containing systematic deletions and duplications in the *HoxD* cluster, showing that two waves of transcriptional activation, controlled by different mechanisms, generate the observed developmental expression patterns. The first wave is time-dependent, involves the action of opposite regulatory modules, and is essential for the growth and polarity of the limb up to the forearm. The second phase involves a different regulation and is required for the morphogenesis of digits (Tarchini and Duboule, 2006). The model proposed by these authors is based on two distinct waves of expression illustrated in Figure 8.

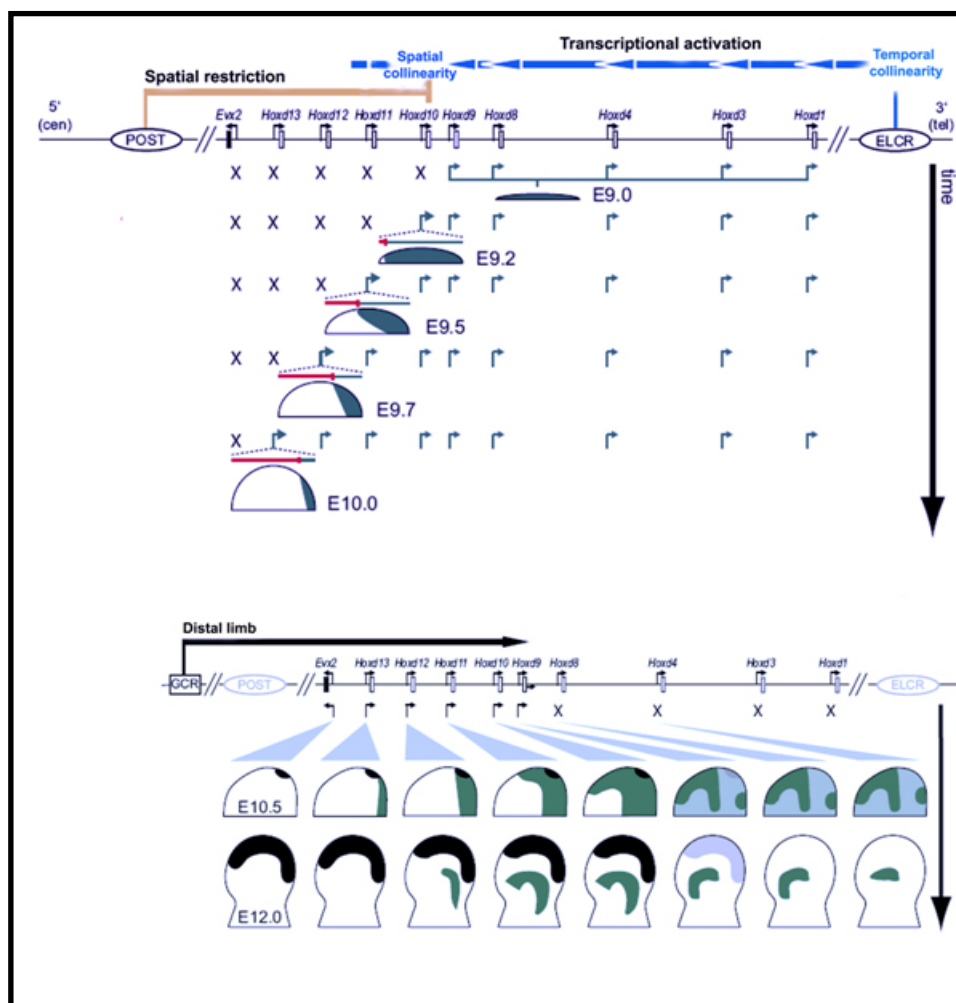


**Figure 8** – Model of collinear regulations during limb bud development. The first mechanism acts during limb budding, is time-dependent (temporal collinearity), and involves two regulatory influences originating from either side of the cluster. This early mechanism generates expression patterns along with forelimb bud outgrowth. Temporal collinearity in the limb is executed by regulatory sequences located telomeric to the cluster, and the beginning of the transcription for a given gene depends on its distance to these regulatory sequences. Spatial restriction of transcripts in the posterior bud is implemented by a distinct regulatory mechanism relying on sequences positioned centromeric to the cluster. Spatial collinearity is the outcome of both influences: the temporal aspect likely plays a secondary role in defining progressive A-P expression boundaries for successive genes. Thus, posterior restriction is maximal for those genes located close to the regulatory sequence and it becomes progressively less efficient with increasing relative distance, leading to a minimal anterior repression for *Hoxd10* gene.

The second wave of expression is independent of the previous and controlled by the Global Control Region (GCR) (Spitz *et al.*, 2003), which drives expression of five adjacent genes in tandem in the presumptive digit domain. This presumptive domain in mouse appears at day 10.5 and is wholly expanded by day 12, labelling the future distal elements. At the same time, the early collinear domain develops such that, at day 10.5, 3'-located genes (like *Hoxd8* or *Hoxd4*) are still expressed throughout the bud. 5'-located genes keep the same collinear arrangement, derived from the early wave of expression. At day 12, a proximal domain is observed at the level of the radius/ulna. The shape and polarity of this domain, for each gene, is directly derived from that observed at day 10.5, indicating that the radius/ulna domain at day 12 is only the product of the domain observed at day 10.5, which is itself derived from the early collinear mechanisms acting on the forelimb bud between days 9 and 10. During the second phase, they may continue to regulate expression in the radius/ulna domains or, alternatively, a maintenance system could substitute. These two independent waves of activation are necessary and sufficient to supply the full *Hoxd* gene patterns during early limb development. *Adapted from Tarchini and Duboule, 2006.*

### **1.5 The role of Mitogen Activated Protein Kinase / Extracellular Signal-Regulated Kinase (MAPK/ERK) signalling in limb development**

Intracellular responses to FGFs are mediated by several signal transduction cascades, including the MAPK and the phosphatidylinositol-3-OH kinase (PI(3)K)/Akt pathways (Javerzat *et al.*, 2002). Kawakami and colleagues (2003) found that *MAPK phosphatase 3 (mkip3)*, a gene encoding a dual-specificity phosphatase that is known to be a negative regulator of the MAPK/ERK pathway (Muda *et al.*, 1996; Groom *et al.*, 1996; Mourey *et al.*, 1996; Smith *et al.*, 1997) is a downstream factor of the FGF8



signalling pathway during limb development, whose induction is mediated through the PI(3)K pathway (Kawakami *et al.*, 2003). High levels of ERK phosphorylation are observed in the AER, but not in the mesenchyme, where *mkp3* is expressed (the non-ridge ectoderm and distal mesenchyme are weakly positive for pERK staining). In contrast, Akt is phosphorylated in the mesenchyme but not in the AER (Figure 9). Ectopic expression of *mkp3* in the AER perturbs its integrity and function. Misexpression of constitutively active *Mek1*, a specific ERK activator, as well as downregulation of *mkp3* by siRNA, resulted in cell death in the mesenchyme. These studies suggest that MKP3 has a key role in mediating the anti-apoptotic signalling of AER-derived FGF8 by downregulating the MAPK pathway at the level of ERK phosphorylation. This highlights a complex intracellular regulation of FGF signalling that is essential for limb development (Kawakami *et al.*, 2003; Eblaghie *et al.*, 2003).

In 2003, Corson and collaborators performed whole-mount immunohistochemistry with phospho-ERK antibodies to map the spatial and temporal patterns of ERK activation during early postimplantation mouse development. They analyzed the location, timing, distribution, duration and intensity of ERK signalling during mouse embryogenesis (5-10.5 days post-coitum). They observed that as the limb bud grows, a gradient of the di-phosphorylated forms of ERK1 and ERK2 (dp-ERK) is seen in the mesenchyme directly beneath the AER, and suggested the existence of FGF signalling from the surface ectoderm to the mesenchyme (Corson *et al.*, 2003).

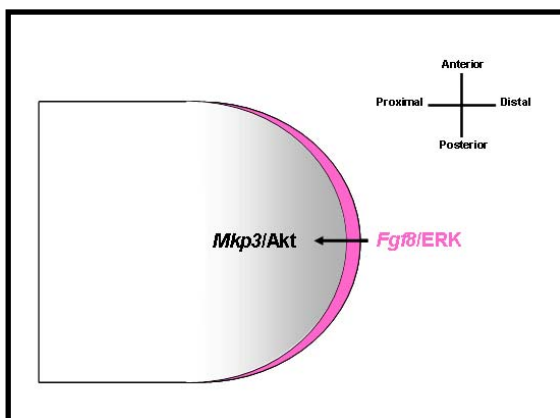


**Figure 9** – Illustration of the expression patterns of the *fgf8* and ERK activity (pink) and *mkp3* and Akt activity (black).

### 1.6 The role of Notch signalling pathway in limb bud element formation

Notch signalling, a conserved and essential pathway employed repeatedly by multiple developmental and cellular processes, has also been implicated in regulating vertebrate limb development. Some studies provide data that are compatible with a role of the Notch signalling pathway in the development of the forelimb distal mesenchyme.

## ***Introduction***

---

In the chick, *notch1* is expressed in the anterior two-thirds of the limb distal mesenchyme (Vargesson *et al.*, 1998). *hairyl1*, a downstream target of the Notch signalling pathway, is expressed in the chick limb distal mesenchyme and misexpression studies of this gene implicate Notch signalling pathway in the regulation of the overall chick limb size (Vasiliauskas *et al.*, 2003). The same is observed in misexpression studies with *delta1* (a ligand of the Notch signalling pathway), that result in abnormal skeletal limb development (Crowe *et al.*, 1999). In the mouse, *serrate1/jagged1* and *hes1* are expressed in the mouse distal limb mesenchyme (Francis *et al.*, 2005; McGlinn *et al.*, 2005) and a close similarity between the expression patterns of chicken *hairyl1*, *hairyl2* and the mouse *hes1*, *serrate1/jagged1* can be observed. *Hes1*-, *serrate1/jagged1*-null mouse embryos die during embryogenesis and no studies on limb formation are reported in the literature.

Loss of *presenilin* (the enzyme responsible for the proteolytic activation of Notch) from the mouse limb mesenchyme (Pan *et al.*, 2005) leads to a phenotype where digits appear to be truncated with some distal phalanx missing (Pan *et al.*, 2005). The authors state the possibility that *presenilin* deficiency in the mesenchyme affects endochondral skeletal differentiation in a Notch-independent manner.

The Notch signalling pathway is also implicated in the development of the AER and in interdigital apoptosis (fused digits phenotype). Mutants of some components of the canonical Notch signalling pathway such as *notch1* knockout mice (Francis *et al.*, 2005); *serrate2/jagged2* (Notch ligand) knockout mice (Jiang *et al.*, 1998; Sidow *et al.*, 1997) and *notch1;notch2* double knockout mice (Pan *et al.*, 2005) have mild phenotypes in the forelimbs but significant and reproducible phenotypes at hindlimb levels. In fact, these mutants do not have a phenotype in the formation of skeletal elements or in the formation of their boundaries, in agreement with the fact that, in the mouse, these genes are exclusively expressed in limb AER and completely absent from mouse limb distal mesenchyme (*notch1* - Francis *et al.*, 2005, *serrate2/jagged2* - Sidow *et al.* 1997 and Francis *et al.*, 2005).

## **2. THE SOMITOGENESIS MOLECULAR CLOCK**

During the first stages of vertebrate development, the embryo's axial structures (notochord and neural tube) are flanked by presomitic mesoderm (PSM), which is progressively subdivided into round epithelial spheres of cells named somites. Somites

arise into an anterior to posterior direction, from the upper part of the PSM, in tandem. Gastrulation proceeds in the posterior part of the embryo generating new cells that incorporate PSM, guaranteeing its elongation. Somites are transient embryonic structures that, though morphologically similar, have different anterior-posterior positional information which is supported by a commitment to their final fate. Somites give rise to all overt segmented structures of the vertebrate body, such as vertebrae, intervertebral disks and ribs, to all body skeletal muscles (except for the head) and to the dermis of the dorsal skin.

Somitogenesis occurs in a very coordinated manner, involving tight spatial and temporal regulation. In the chick embryo a new pair of somites is formed every 90 minutes, culminating in a total of 52 somite pairs. The time required to form a pair of somites, as well as the final somite pair number, is constant and characteristic for each species. This fact suggests the existence of an internal clock-like machinery controlling both the rhythm and duration of somitogenesis, in a species-specific manner (reviewed by Saga and Takeda, 2001; Pourquié, 2001; Freitas *et al.*, 2005; Andrade *et al.*, 2005).

## **2.1 The emergence of the segmentation clock era**

A molecular clock linked to vertebrate segmentation and somitogenesis was first proposed by Cooke and Zeeman in 1976, as the theoretical “Clock and Wavefront” model (Cooke and Zeeman, 1976). This model predicted the existence of a biochemical oscillator within PSM cells, which would be synchronized with respect to their oscillations. The cells were proposed to oscillate between a permissive and a non-permissive state for somite formation. A wavefront of differentiation was also suggested, expanding posteriorly throughout the embryo, and giving cells the competence to differentiate. When a group of “competent” cells oscillated to a permissive state, a new somite was formed.

The first molecular evidence for an intrinsic clock operating in avian PSM cells was obtained in 1997, with the discovery of the dynamic expression pattern of the chick *hairy1* gene. Whilst performing *in situ* hybridization experiments in order to study the expression of the chick homologue of the *Drosophila* segmentation gene *hairy*, Palmeirim and co-workers (1997) made a surprising observation: in embryos with the same somite number, i.e., that did not differ by more than 90 minutes in their development, a great variety of *hairy1* expression patterns in the PSM was obtained. This research showed that *hairy1* was expressed in a very dynamic manner in the chick

## Introduction

---

PSM. To characterize this dynamic behavior, the authors employed several experimental embryology techniques. In a first approach, embryos were cut in two halves, along the a-p axis of the embryo and while one half were immediately fixed, the other was further incubated for different periods of time. Then, both halves were hybridized with the *hairy1* probe. The comparison of the expression patterns between both control and experimental halves clearly showed that *hairy1* expression varied within the PSM cells, and that 30 minutes of incubation was sufficient to wholly change the *hairy1* expression pattern. On the contrary, the same expression pattern was acquired when the experimental half was incubated for 90 minutes. The authors concluded that *hairy1* was cyclically expressed in the PSM with a periodicity of 90 minutes, corresponding to the time of formation of one pair of somites (Figure 10A; Palmeirim *et al.*, 1997).

Further experiments demonstrated that *hairy1* cyclic expression is an intrinsic property of the PSM, not depending on any surrounding tissue or on a signal arising from the gastrulation site (Palmeirim *et al.*, 1997). In a first analysis, *hairy1* expression pattern appeared like a caudal-rostral wave along the PSM. However, this only corresponded to a “kinematic” wave since it is not perturbed in isolated pieces of PSM, suggesting that each cell oscillates independently from its neighboring cells. The wave-like pattern arises from the fact that neighboring cells are faintly out-of-phase with respect to their autonomous oscillations.

The evidences available to date suggest that each cell in the PSM undergoes a pre-determined number of *hairy1* oscillations, from the time it emerges from the primitive streak to the time when it is incorporated into a somite. At any given time, the cell has the information of the relative position it occupies at the axial level of the PSM, which is given by the number of cycles of gene expression it has already undergone (Figure 10B). Thus, the molecular clock may be translating time into positional information along the A-P axis of the embryo PSM (reviewed by Freitas *et al.*, 2005 and Andrade *et al.*, 2005).

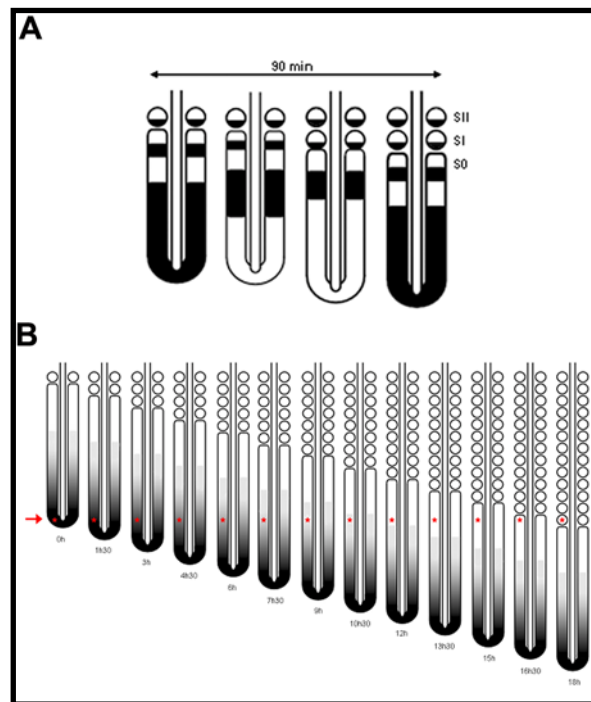


**Figure 10** - Schematic representation of the dynamic and cyclic nature of *hairy1* expression. (A) Variability of *hairy1* gene expression during the formation of a new somite pair. The posterior region of chick embryos with 15 to 20 somite pairs is illustrated. (B) Each cell in the PSM undergoes a pre-determined number of *hairy1* oscillations, from the time it emerges from the primitive streak to the time when it is incorporated into a somite. Since the PSM contains 12 prospective somites, the cell undergoes 12 cycles of *hairy1* expression until it is incorporated into a somite.

S0: somite in formation; S1: newly formed somite; SII: previously formed somite. *Adapted from Andrade et al., 2005.*

## 2.2 The clock since its discovery until nowadays

Since the discovery made by Palmeirim and colleagues (1997), new genes have been found to have the same type of gene expression oscillations in the chick embryo PSM: *hairy2*, a gene that encodes a transcription factor closely related to *hairy1* (Jouve *et al.*, 2000); *lunatic fringe*, encoding a secreted protein (McGrew *et al.*, 1998; Aulehla and Johnson, 1999) and the transcription factor *hey2* (Leimeister *et al.*, 2000). Similar cycling genes expressed during somitogenesis have been found in other vertebrates: *lunatic fringe* (*Lfn*) (Forsberg *et al.*, 1998; Aulehla and Johnson, 1999), *hes1* (Jouve *et al.*, 2000), *hey2* (Leimeister *et al.*, 2000), *hes7* (Bessho *et al.*, 2001; Bessho *et al.*, 2003)

## Introduction

---

and *nkd1* (Ishikawa *et al.*, 2004) in mouse; *her1* (Holley *et al.*, 2000; Sawada *et al.*, 2000), *delta C* (Jiang *et al.*, 2000) and *her7* (Oates and Ho, 2002) in zebrafish; *esr9* and *esr10* in xenopus (Li *et al.*, 2003); *her7* and *hey1* in medaka (Elmasri *et al.*, 2004).

The majority of the cycling genes found in vertebrates are intimately related to the Notch signalling pathway (reviewed in Rida *et al.*, 2004 and Freitas *et al.*, 2005). The WNT pathway, however, was recently implicated in the segmentation clock. *axin2*, a negative regulator of Wnt3a signalling, exhibits an oscillatory expression pattern in the mouse PSM (Aulehla *et al.*, 2003). *axin2* oscillations persist in Notch pathway mutants, whereas *axin2* and *lunatic fringe* oscillations are disrupted in *wnt3a* mutants, indicating that WNT signalling could act upstream of the Notch signalling pathway (Aulehla *et al.*, 2003). Furthermore, it has recently been demonstrated that *snail1* and *snail2* mRNA is cyclically expressed in the mouse and chick presomitic mesoderm, respectively, and that these *snail* gene oscillations are independent of Notch signalling, requiring WNT and FGF signaling (Dale *et al.*, 2006). Another gene that also exhibits cycles of expression in the mouse PSM is the *dact1* (Suriben *et al.*, 2006), a member of the Dact (Dpr/Frd) gene family, which encode conserved Dishevelled (Dvl)-binding regulators of WNT signaling pathway (Fisher *et al.*, 2006). The oscillation of *dact1* occurs in phase with the WNT signalling component *axin2*, and out of phase with the Notch signalling component *lfng* (Suriben *et al.*, 2006).

Negative feedback regulation has been identified for the mouse *hes1* and *hes7* genes. Studies at the protein level confirmed that these gene products presented oscillations with the same periodicity found for their mRNAs. Additionally, they inhibited their own promoters creating negative feedback loops (reviewed in Rida *et al.*, 2004 and Freitas *et al.*, 2005). An additional negative feedback regulation has been described for the *lunatic fringe* gene in chick (Dale *et al.*, 2003). Lunatic fringe protein oscillates in PSM cells, periodically inhibiting Notch signalling, and consequently down-regulates *lunatic fringe* expression. These negative feedback loops may represent important elements in the segmentation clock mechanism. Using mathematical modelling, Monk showed that oscillatory gene expression results essentially from transcriptional delays, and that the oscillation period is determined by the delay in transcription and by both protein and mRNA half-lives (Monk, 2003). In agreement, Hes7 protein instability was recently shown to be vital for the segmentation clock (Hirata *et al.*, 2004).

---

### 2.3 The role of Notch signalling pathway in somite formation

Several mutations that affect somitogenesis have been described in zebrafish and mice (Freitas *et al.*, 2005). Most of these mutations are in components of the canonical Notch signalling pathway and cause a progressive disruption of somitogenesis along the A-P axis. In the posterior part of the embryo, somites are irregular in size and shape presenting malformations in intersomitic boundaries (Pourquié, 2001). Interestingly, the formation of anterior somites occurs normally in these mutants (even in the *Notch1;Notch2* double knockout mice). In contrast, mouse embryos lacking *Presenilin* (the enzyme responsible for the proteolytic activation of Notch) have no somites at all (neither anterior nor posterior somites), suggesting that the earliest stages of somitogenesis require a  $\gamma$ -secretase-independent activity of presenilin (Huppert *et al.*, 2005). The study of *Notch1;Notch2*-, and of  $\gamma$ -secretase components, as *Nicastrin*-, *Pen-2*-, and *APH-1a* -deficient embryos performed in Kopan's laboratory (Huppert *et al.*, 2005), together with other observations (Aulehla *et al.*, 2003; Ishikawa *et al.*, 2004), lead the authors to propose that three different pathways - Canonical Notch, WNT and Presenilin - play redundant roles during anterior somitogenesis. In addition, since the authors were not able to detect a consistent Notch activation signal in the very posterior part of PSM where cycling of Notch target genes is initiated, they propose that the canonical Notch signalling pathway may not be required to initiate the segmentation clock. Instead, the initiation of the segmentation clock could be under control of Wnt3a, Hes1, Hes7, a Notch-independent contribution of Presenilin or a yet unidentified player (Huppert *et al.*, 2005). In fact, cyclic mRNA expression of *snail1* and *snail2* in the mouse and chick presomitic mesoderm requires WNT and FGF signaling and is independent of the Notch signaling pathway (Dale *et al.*, 2006).

### 2.4 The Wavefront - the partner of the Clock

The "Clock and Wavefront" model postulates the existence of a wavefront of cell differentiation that extends posteriorly throughout the embryo (Cooke and Zeeman, 1976). In 2001, Dubrulle *et al.* showed that there is a gradient of *fgf8* transcripts beginning from the embryo tail bud and fading in the direction of the highest part of the PSM tissue (Dubrulle *et al.*, 2001). The observed graded distribution of *fgf8* mRNA was shown to result from progressive mRNA decay, rather than from different transcription levels (Dubrulle and Pourquie, 2004). *wnt3a* was shown to present a PSM expression pattern similar to that of *fgf8*. *wnt3a* is proposed to act upstream of *fgf8* and may operate

together with, or *via*, the *fgf8* gradient (Aulehla *et al.*, 2003). A PSM cell positioned close to the tail bud bears high FGF/WNT signalling levels, which sustain cells in an undifferentiated state. Cellular levels of FGF/WNT gradually diminish along time, permitting the cell to activate its differentiation program as it achieves the appropriate threshold of FGF/WNT activity. Consequently, the anterior limit of *fgf8/wnt3a* gradient is proposed to establish the prospective somitic boundary location (Dubrulle *et al.*, 2001; Aulehla *et al.*, 2003). When the maturation wavefront is experimentally shifted anteriorly by placing an FGF8-coated bead in the mid-PSM, smaller somites form. Conversely, FGF8 inhibition at the same level induces the formation of larger somites (Dubrulle *et al.*, 2001). Thus, FGF8 maintains posterior PSM cells in an immature state, negatively regulating differentiation in chick PSM, and modifications in the slope of the *fgf8* gradient alters the location of intersomitic boundaries (Dubrulle *et al.*, 2001).

Recently, Delfini and co-workers (2005) have investigated the intracellular effectors of FGF signalling during avian segmentation. They present evidence for a gradient of ERK activation established in response to FGF signalling, showing that the maturation of the PSM is directly regulated by ERK activity. Additionally, they show that the MAPK/ERK pathway enforces a posterior-anterior gradient of cell motility. The gradual decrease of cell movements along the PSM may allow mesenchymal PSM cells to organize themselves appropriately at the beginning of the segmentation program (Delfini *et al.*, 2005).

Contrasting with the expression patterns described above, the *Raldh2* gene encoding retinoic acid (RA)-synthesizing enzyme, is expressed in the more anterior part of PSM and in the somites (Swindell *et al.*, 1999). Diez del Corral and collaborators have shown that FGF and RA pathways are mutually inhibitory and promote opposing effects in the PSM tissue. These maintain the necessary balance between naive/proliferative and differentiating PSM cells, exerting a strict control on somite boundary positioning (Diez del Corral *et al.*, 2003).

### 2.5 *Hox* genes and the segmentation clock

Expression of the genes from the four *Hox* clusters along the A-P axis of the vertebrate embryo is one of the major determinants of morphological identity of the vertebrae (Burke, 2000). Within each cluster, the genes are arranged in a sequence that reflects their order of expression during development (temporal collinearity) (Dollé *et*



*al.*, 1989) and the position of the anterior boundary of their expression domains along the A-P body axis (spatial collinearity) (Gaunt *et al.*, 1988; Graham *et al.*, 1989). This nested distribution of *Hox* genes along the A-P axis results in each vertebral precursor being endowed with a unique combinatorial expression of *Hox* genes that controls their A-P identity (Kessel and Gruss, 1991; Wellik and Capecchi, 2003). In amniote embryos, activation of genes along the *Hox* clusters occurs sequentially in the primitive streak and the tail bud during axis elongation (Deschamps and van Nes, 2005).

*Hox* genes are expressed in the presomitic mesoderm, as well as in the somites and their differentiated derivatives. Previous studies demonstrated a linkage between *Hox* gene activation in the presomitic mesoderm and the segmentation clock (Dubrulle *et al.*, 2001; Zakany *et al.*, 2001). The experiments performed by Dubrulle and collaborators (2001) suggest a two-step mechanism responsible for assigning precise *Hox* gene combinatorial expression to somites. In a first step, the clusters would progressively acquire their configuration prior to their entrance in PSM, by a mechanism that could be linked to stem cell proliferation. In a second step, the definitive expression of *Hox* genes would be allocated to each prospective somite as it becomes determined. This second phase is coupled to the segmentation clock, since increasing the number of oscillations in PSM cells results in a posteriorization of these cells (Dubrulle *et al.*, 2001). Another demonstration for *Hox* gene activation by the segmentation clock results from the work performed by Zakany and collaborators (2001) that demonstrated a dynamic expression of *Hox* genes in the anterior mouse PSM (Zakany *et al.*, 2001). Such a mechanism could explain how individual somites acquired their regional identity. Recently, Limura and Pourquié (2006) demonstrated that *Hoxb* genes are first activated in a temporal collinear fashion in precursors located in the epiblast lateral to the primitive streak. This suggests that collinear activation of *Hoxb* genes regulates the flux of cells from the epiblast to the streak and thus directly controls the establishment of the characteristic nested gene expression domains in the somites. This means that establishment of the spatial collinearity in the embryo is directly controlled by the *Hox* genes themselves (Limura and Pourquié, 2006). This work seems to bring a new highlight to the first step proposed by Dubrulle and collaborators (2001) discussed above.

In another study, Cordes and colleagues (2004) have produced transgenic mice expressing a dominant negative form of the Notch ligand *Delta1* in the presomitic mesoderm. These mutant mice displayed alterations of vertebral identities consistent

with homeotic transformations. Consistent with this analysis, the anterior expression borders of the *Hoxb6* and *Hoxc5* genes were shifted, suggesting that the exact positioning of the anterior limit of *Hox* gene expression requires accurately regulated Notch activity in the presomitic mesoderm. Also, both *Lfng* null mice and mice expressing the *Lfng* gene constitutively in the presomitic mesoderm exhibited changes in vertebral identities and reductions of the numbers of segments in the cervical and thoracic regions, suggesting anterior shifts of axial identity. These results indicate that precisely regulated levels of Notch activity as well as cyclic *Lfng* activity are critical for positional specification of vertebral identities along the A-P body axis (Cordes *et al.*, 2004).

*Hoxa10* gene transgenic misexpression in the presomitic mesoderm conferred *Hox* group 10 patterning identity to the somite, producing vertebrae without ribs (Carapuço *et al.*, 2005). Such phenotype was not produced if the *Hoxa10* gene was expressed only in the formed somites. When the *Hoxa11* gene was expressed using the same transgenic promoters, misexpression in the presomitic mesoderm gave *Hox* group 11 identity to the somites, resulting in partial homeotic transformation toward a sacral vertebral identity. Expression of *Hoxa11* in the somites, in contrast to the situation with *Hoxa10*, did result in a detectable phenotype in which lumbar vertebrae exhibited characteristics of caudal vertebrae. The discovery that *Hox* gene misexpression in the presomitic mesoderm transformed vertebral identity of the resulting somite was supported by analyses of mutants of the *Gbx2* gene, which encodes a homeobox-containing protein expressed in the presomitic mesoderm but not in the somites. *Gbx2*-deficient mouse embryos displayed *Hox*-like homeotic transformations of the axial skeleton without detectable alteration of the anterior boundaries of *Hox* gene expression in the embryo (Carapuço *et al.*, 2005). The discovery that inactivation of the *Gbx2* gene produced a typical *Hox* mutant phenotype in the axial skeleton without any apparent effect on *Hox* gene expression provides extra support to the view that homeotic genes can provide patterning instructions in the presomitic mesoderm (Carapuço *et al.*, 2005).

### 2.6 The molecular clock in two dimensions

Work performed in Palmeirim's lab shows that the segmentation clock is already operating in the prospective PSM territory. The expression patterns of the molecular clock components *hairy1*, *hairy2* and *lunatic fringe* in chick embryos present a very

dynamic expression in this territory (Freitas *et al.*, 2001). The expression patterns observed in the prospective PSM tissue resembled a “wave” of cyclic gene expression, similar to the one described in the PSM. By performing detailed fate map studies it was shown that different regions of the prospective PSM territory give rise to distinct PSM compartments: cells located anteriorly give rise to medial PSM cells (prospective medial-PSM domain: PM-PSM), while more posterior cells develop into lateral PSM domain (prospective lateral-PSM domain: PL-PSM). These observations implied that, simultaneous to the A-P gene expression “wave” that occurs in the PSM, another “wave” of expression is in progress in the most posterior part of the embryo, travelling along the future medial-lateral PSM axis (Freitas *et al.*, 2001). Therefore, an asynchrony in cyclic gene expression can be observed between the medial and lateral portions of the PSM, which is evidenced by the appearance of cross-stripes (Figure 11). These studies showed that the molecular clock associated to vertebrate embryo segmentation is providing cellular positional information in at least two dimensions: along both A-P and medial-lateral PSM axis (Freitas *et al.*, 2001).

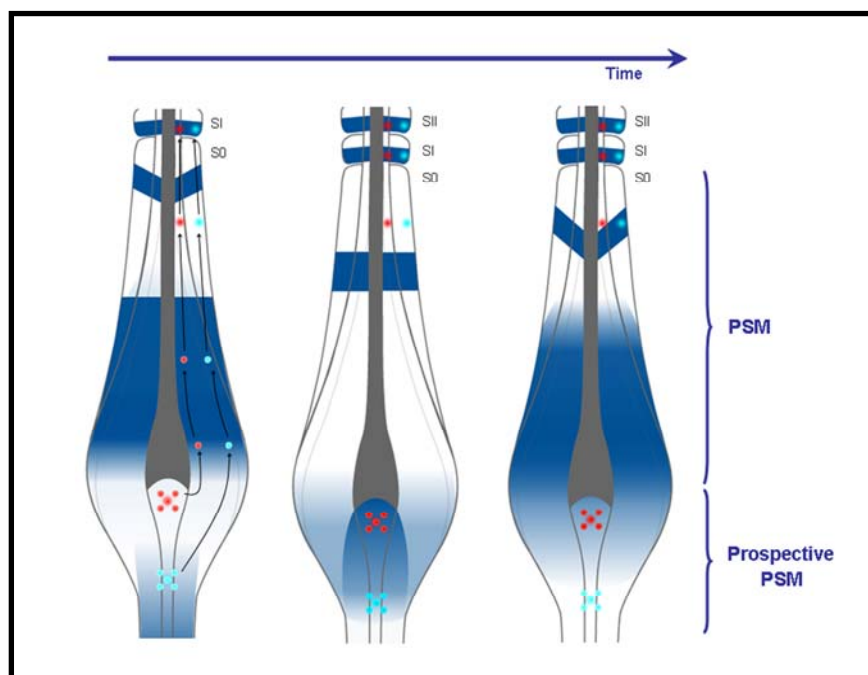


**Figure 11** - Illustration of *hairy1* dynamic expression observed along the time of formation of one somite-pair. Dynamic gene expression occurs in both the PSM and its prospective territory. Lateral PSM cells originate from PL-PSM (light blue), and medial PSM cells originate from PM-PSM (red). Arrows in the first panel show the positions occupied by these cells along time, until they are incorporated into a somite. An asynchrony in cyclic gene expression is observed both in the prospective and the PSM medial and lateral territories. This medial-lateral

asynchrony is evidenced in the PSM by the appearance of cross-stripes. S0: somite in formation; SI: newly formed somite; SII: previously formed somite. *Adapted from Andrade et al., 2005.*

### **2.7 Could the molecular clock be operating in other biological systems?**

Until now, all studies concerning cyclic gene expression have been performed exclusively in the somitogenesis process, which clearly takes place according to a strict temporal control. However, time control is certainly present during all embryonic processes and may even be considered a fourth developmental dimension.

Work performed by Hirata and co-workers (2002) has brought a new input to this field. The experiments performed by these authors showed that the administration of a single serum shock to stationary cultured cells could induce cyclic production of both *hes1* mRNA and Hes1 protein in several cell lines, such as myoblasts, fibroblasts, neuroblastoma and teratocarcinoma cells. The observed oscillations occurred with a 2 hour time period, corresponding to the periodicity of cyclic gene expression observed in the mouse embryo PSM. These findings lead the authors to postulate that, since Hes1 oscillations occur in many cell types, the molecular clock originally identified in the PSM, could be widely distributed and regulate timing in many biological systems (Hirata *et al.*, 2002).

---

## ***CHAPTER II***

### ***Material and Methods***



## **1. MATERIAL AND METHODS**

### **1.1 Eggs and embryos**

Fertilised chick (*Gallus gallus*) eggs obtained from commercial sources were incubated at 37.2°C in a 49% humidified atmosphere and staged according to the Hamburger and Hamilton (HH) classification (Hamburger and Hamilton, 1951).

### **1.2 RNA probes**

Antisense RNA probes were prepared as described: *hairy1* (Palmeirim *et al.*, 1997), *hairy2* (Jouve *et al.*, 2000), *mkp3* (Kawakami *et al.*, 2003), *gdf5* (Francis-West *et al.*, 1999), *MyoD* (Pourquié *et al.*, 1996) and *fgf8* (Crossley *et al.*, 1996). Intronic *mkp3* probe was prepared as described below.

#### **1.2.1 Antisense RNA probes synthesis**

The plasmids containing cDNA sequences used to generate the anti-sense mRNA probes was transformed into the *Escherichia coli* (*E. coli*) strain for further amplification and isolation, and stored at -70°C.

##### **1.2.1.1 Generation of competent bacteria**

Competent bacteria were prepared according to the calcium chloride (CaCl<sub>2</sub>) method. A glycerol cell culture stock of *E. coli* was defrosted and added to 100 ml of Luria Broth (LB) medium. This culture was incubated with vigorous shaking in an incubator- shaker for 3 hours at 37°C. To monitor the growth of the culture, the Optical Density (OD<sub>600</sub>) was determined every 30 minutes. On the beginning of the exponential phase the bacteria culture was relocated in tubes and incubated for 10 minutes on ice. The cells were collected by centrifuging at 1000 g for 10 minutes at 4°C. The pellet was resuspended in 10 ml of ice-cold 0.1 M CaCl<sub>2</sub> and incubated on ice. After another centrifugation the pellet was resuspended in 0.1 M CaCl<sub>2</sub>. Sterile glycerol was added to the final competent bacteria suspension to a final concentration of 15% (v/v). Competent bacteria aliquots were stored at -70°C.

## ***Materials and Methods***

---

### *1.2.1.2 Bacteria transformation*

Plasmids containing the DNA of interest were incubated with 50 µl of competent bacteria during 30 minutes on ice. A heat shock was applied at 42°C during 1 minute, followed by cooling on ice for 2 minutes. Next, 1 ml of LB medium was added to the bacteria solution. This mixture was incubated for 1 hour with agitation. Bacteria were plated in solid LB medium containing an appropriate antibiotic (100 µg/ml of ampicillin or kanamycin) to select the transformed bacteria and incubated overnight at 37°C.

### *1.2.1.3 Plasmid amplification*

A single colony of transformed bacteria was collected using a micropipette tip and inoculated into an Erlenmeyer containing 100 ml of liquid LB medium with 100 µg/ml of ampicillin or kanamycin at 37°C in an incubator-shaker overnight. The bacteria were collected by centrifuging at 5000 g during 30 minutes at 4°C.

### *1.2.1.4 Plasmid isolation*

After centrifugation, plasmid DNA extraction was carried out using the QIAfilter Plasmid Mini, Midi or Maxi Kit (QIAGEN) according to the protocol suggested by the manufacturer.

### *1.2.1.5 Plasmid linearization*

Among 3 to 10 µg of the plasmid were linearized for 3 hours at 37°C with the appropriate restriction enzymes and buffers commercially supplied. After digestion the efficiency of the restriction was verified in a 1% agarose gel using 1/20 of the digestion reaction volume. After that, the QIAquick Gel Extraction Kit (QIAGEN) was used to eliminate proteins from the restriction reaction according to the protocol suggested by the manufacturer. The purified digestion reaction was checked in a 1% agarose gel using 1/20 of the total volume.

### *1.2.1.6 Agarose gel electrophoresis*

Agarose was dissolved upon heating in 1x TAE buffer, to a final concentration of 1% and the gel solution was next discharged into a mould. Ethidium bromide was added to the gel to allow fluorescent visualization of the DNA fragments under UV light. The agarose gel was submerged in 1x TAE buffer in a horizontal electrophoresis equipment. The DNA samples and molecular weight markers for fragment size



determination were mixed with bromophenol blue loading buffer and loaded into the sample wells. Electrophoresis was performed at 5 to 20 V/cm of gel length until the appropriate resolution was attained. Afterward, the gel was placed in a UV light box to analyse the DNA separation pattern through comparison with the known molecular weight marker.

#### *1.2.1.7 In vitro FITC or DIG-labelled anti-sense RNA probe transcription*

Single stranded RNA probes were generated by *in vitro* transcription from the linearized DNA template using the appropriate SP6 (Roche), T3 (Roche) or T7 (Promega) RNA polymerase, which synthesises RNA complementary to the DNA template. Transcription was carried out at 37°C (for SP6 is carried out at 40°C) during 3 hours. In an RNase free tube, 14 µl of H<sub>2</sub>O ultrapure, 8 µl of 5x transcription buffer, 4 µl of 0.1 M dithiothreitol (DTT), 2 µl of 10x DIG RNA labelling mix (Roche) or 10x FITC RNA labelling mix (Roche), 1 µg of linearized plasmid, 2 µl of RNA polymerase and 2 µl of RNase inhibitor (RNAsin) (Promega) to avoid RNA degradation were added under RNase free conditions. Once the incubation was over, the tube with the transcription reaction was placed on ice. To stop the reaction 4 µl of DNase I (Promega) was added in order to remove the plasmid DNA, and 2 µl of RNAsin were added followed by 30 minutes of incubation at 37°C. Precipitation was carried out by adding 200 µl of TE, 20 µl of 4 M LiCl and 600 µl of EtOH 100% for 45 minutes at -80°C. The tube was centrifuged at 12000 g during 30 minutes at 4°C. The supernatant was removed using a needle. The pellet was washed with 1 ml of EtOH 70% and centrifuged at 12000 g during 15 minutes at 4°C. The supernatant was for a second time carefully removed with a needle. The pellet, after drying, was resuspended in an appropriate volume of ultrapure water. A 1% agarose gel was run in order to ensure the amount of synthesised RNA probe, which was subsequently stored at -20°C.

#### *1.2.2 Cloning of intronic *mkp3* probe*

Polymerase chain reactions (PCR) on chicken genomic DNA were used to amplify the fourth *mkp3* intron, using the sense oligo 5'-AGCAGAACCCCCATTCCCTTCT-3' and the antisense oligo 5'-CCAGCATGGAAATCCTGCA-3'. The PCR reaction was composite by 1 µl of chicken genomic DNA, 1 µl of primer sense, 1 µl of primer antisense, 3 µl of MgCl<sub>2</sub>, 1 µl of dNTPs, 0.3 µl of Taq polymerase, 37.7 µl of ultrapure H<sub>2</sub>O and 5 µl of buffer. The

## Materials and Methods

PCR amplification was carried out using the following conditions: 1 cycle at 96°C for 3 minutes, and 35 cycles at 94°C for 45 seconds, followed by a graded specific annealing temperature (55°C/56,9°C/61.1°C/65°C) for 45 seconds and 72°C for 45 seconds. After that the PCR reactions stay at 4°C. The selected PCR reaction to continue the protocol was the sample that has an annealing temperature of 61.1°C. A 1% agarose gel was run to ensure the PCR reaction sample.

The DNA fragment generated was cloned into the pCR<sup>®</sup>II-TOPO<sup>®</sup> vector (Invitrogen). The linkage of the DNA fragment in the vector was carried out at room temperature (RT) for 30 minutes in a tube where 4 µl of DNA fragment generated, 1 µl of Salt solution and 1 µl of the pCR<sup>®</sup>II-TOPO<sup>®</sup> vector was added. All the protocols described above, since bacteria transformation until the RNA probe transcription was performed. Antisense *mkp3* intronic RNA probe was produced by linearizing pCRII-MKP3 intron vector (Figure 12) with BamHI and transcribing with T7 polymerase.

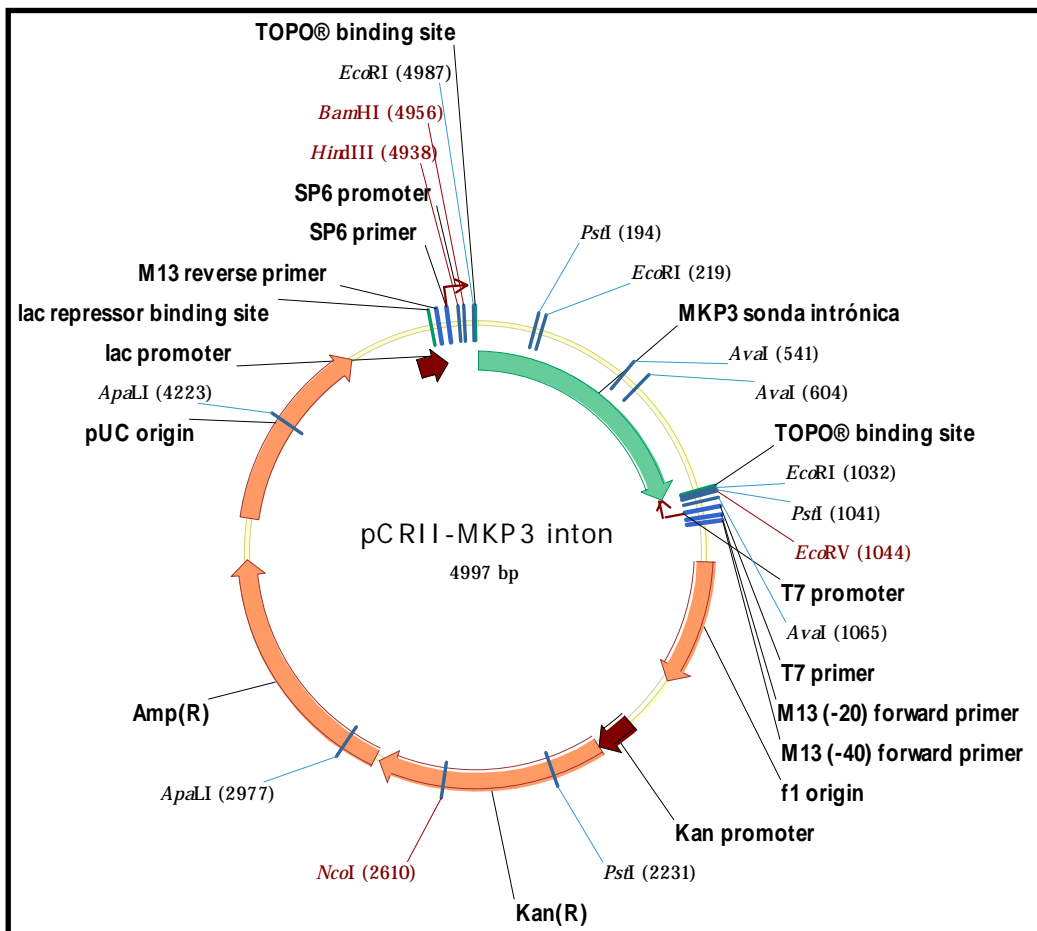


**Figure 12** – Representation of the pCRII-MKP3 intron vector circular map.

### **1.3 RNA extraction and reverse transcription**

Limb buds at stage HH24 were dissected into three portions of equivalent size along the P-D axis. Total mRNA was extracted from 5 distinct batches of each portion of the limb using the RNeasy Mini Kit Protect (Qiagen, Germany). Total mRNA quantification was done by spectrophotometry (NanoDrop Technologies, Inc., USA). Total RNA was digested with DNase RNase-Free (Promega, USA) according to manufacturer's instructions.

### **1.4 Quantitative real-time RT-PCR**

Quantitative real-time RT-PCR was performed as previously described (Nogueira-Silva *et al.*, 2006). Primer design was based on available sequences in *GenBank* (NCBI-NLM-PubMed-Gene). The following intron-spanning primers were used, sense and antisense, respectively: MKP3 5'-ATCTCTTTCATAGATGAAGCGCGG-3' and 5'-TGAGCTTCTGCATGAGGTAGGC-3'; FGF8 5'-CTGATCGGCAAGAGTAACGGC-3' and 5'-CCATGTACCAGCCCTCGTACTTG-3'; RALDH2 5'-CAAGGAGGAGATTTTTGGGCCTGTTC-3' and 5'-GGCCTTGTTTATGTCATTTGTAAAGACAGC-3'; the primers used for the reference gene 18S Ribosomal RNA were: 5'-TGCTCTTAACTGAGTGTCCTCCGC-3' and 5'-CCCGTTTCCGAAAACCAACAA-3'. Primer sets standard amplification curves were made for MKP3, FGF8, RALDH2 and 18S Ribosomal RNA with cDNA samples from chick limb buds at stage HH24, setting  $r=0.99$ . In all the samples, gene expression was normalized for 18S Ribosomal RNA and for limb region 1 values.

#### **1.4.1 Statistical Analysis**

All quantitative data are presented as mean  $\pm$  SEM. Statistical analysis was performed by one-way ANOVA on ranks and the Student-Newman-Keuls test was used for post-test analysis. Statistical significance was set at  $p<0.05$ .

### **1.5 *In situ* hybridization**

#### **1.5.1 Whole-mount**

Embryos and limb buds were fixed overnight at 4°C in fresh 4% formaldehyde 2mM EGTA in phosphate-buffered saline (PBS), rinsed in PBT (PBS, 0.1% Tween 20),

## ***Materials and Methods***

---

dehydrated through a methanol series and stored in 100% methanol at -20°C. Whole-mount *in situ* hybridization was performed according to the procedure described by Henrique and collaborators (1995).

### *1.5.1.1 Whole-mount in situ hybridization protocol*

#### Pre-treatments and Hybridization (1<sup>st</sup> day):

1. Rehydrate embryos through:

- Wash 1x MeOH /PBT ( 75% / 25% )
- Wash 1x MeOH /PBT ( 50% / 50%)
- Wash 1x MeOH /PBT ( 25% / 75%)

Allowing embryos to settle

2. Wash 2x with PBT

3. Incubate with 20 mg/ml Proteinase K (PK) in PBT:

For chick embryos, time of incubation in minutes = stage number (HH) until stage HH15. (Example: 10 minutes for a stage HH10 embryo). After this stage see table below for the PK incubation time.

<b>Stage (HH)</b>	<b>Minutes</b>	<b>PK</b>
16 - 18	25	20 mg/ml
19 - 20	30	20 mg/ml
21 - 25	35	20 mg/ml
26	40	20 mg/ml
27 - 29	45	20 mg/ml
30 - 31	50	20 mg/ml
32 - 35	55	20 mg/ml

4. Remove PK, rinse briefly with 2x PBT

5. Post-fix the embryos for at least 20 minutes

6. Rinse and wash 2x with PBT

7. Rinse 1x with PBT/Hybridization mix solution (Hybmix) (1:1). Let embryos settle.

8. Rinse 2x with Hybmix solution. Let embryos settle

9. Replace again the Hybmix solution and incubate  $\geq$  1h, at 70°C
10. Add your pre-warmed RNA probe. Immediately place at 70°C
11. Incubate overnight at 70°C (incubate also the Hybmix solution)

Post-Hybridization Washes (2<sup>nd</sup> day):

11. Rinse 2x with pre-warmed (70°C) Hybmix solution
12. Wash 1x 30 minutes with pre-warmed Hybmix solution, at 70°C
13. Wash 10 minutes with pre-warmed Hybmix:MABT solution (1:1), at 70°C
14. Rinse 2x with MABT solution
15. Wash 1x 15 minutes with MABT solution
16. Incubate 1 hour with MABT + Blocking Reagent (BR) + Goat serum (GS)
17. Incubate overnight, at room temperature (RT) with MABT + BR + GS + anti-DIG alkaline-phosphatase-conjugated antibody (Roche) (1:2000)

Post-antibody Washes and Histochemistry (3<sup>rd</sup> day):

18. Rinse 3x with MABT solution
19. Wash 3x for at least 1h with MABT solution
20. Wash 2x 10 minutes with NTMT solution
21. Incubate with revelation solution (NTMT solution+NBT+BCIP) (Roche) for DIG labeled anti-sense RNA probes and/or with (NTMT solution+INT+BCIP) (Roche) for FITC labelled anti-sense RNA probes at 37 °C, in the dark
22. Once colour had developed as desired, wash 3x with PBT
23. Store at 4°C in PBT + Azide

<p>For embryos bigger than stage HH21 the protocol should be extent to 4-5 days: the 3<sup>rd</sup> and 4<sup>th</sup> day should be washes with MABT, only.</p>
--

### 1.5.2 Tissue sections

Limb buds were sectioned using a Leica CM3000 cryostat after gelatine/sucrose inclusion (25  $\mu$ m section thickness). *In situ* hybridisation on tissue sections was performed as described in Strahle and colleagues (1994).

#### 1.5.2.1 On sections *in situ* hybridization protocol

## ***Materials and Methods***

---

### First day of protocol

1. Rinse the sections 1x in PBS for 5 minutes at RT
2. Digest in PK - PBS solution for 14 minutes at 37°C  
Stock solution: 20 mg/ml; diluted 1:1000 (10 µl/100ml)
3. Rinse in PBS 1x 2 minutes at RT
4. Postfix in Paraformaldehyde (PAF) 4% 1x 20 minutes at RT
5. Rinse in PBS 1x 5 minutes at RT
6. Equilibrate in SSC 2x solution pH 7.5, 1x 10 minutes at RT
7. Hybridise in Hybridization mix – probe 1%, overnight at 70°C  
Put 100 µl of Hybmix plus probe per slide (with coverslip) in a damp box with Formamid 50% - SSC 2% (wrap the box to avoid evaporation).

### Second day of protocol

8. Wash in Formamid 50% - SSC 1% - Tween20 0.1%, 1x 15 minutes plus 2x 30 minutes at 70°C
9. Wash in MABT solution 2x 30 minutes at RT
10. Pre-incubate in MABT - Blocking Reagent 2% - Goat Serum 20%, 1h30 at RT  
Put 400 µl per slide (without coverslip)
11. Incubate in MABT - Blocking Reagent 2% - Goat Serum 20%, overnight at RT  
Antibody diluted 1:2000; Put 100 µl per slide (with coverslip)

### Third day of protocol

12. Wash in MABT solution 4x 30 minutes at RT
13. Equilibrate in NTM solution 1x 30 minutes at RT
14. Stain in NTM - NBT - BCIP and/or NTM - INT - BCIP at 37°C
15. Once colour had developed as desired, wash 3x with PBT
16. Store at 4°C in PBT + Azide

## **1.6 *In ovo* embryonic manipulations**

### 1.6.1 Determination of the formation time of the forelimb second phalanx

Multiple batches of 90 fertilised eggs were incubated during 48 hours. A window was cut in the incubated egg shell, indian ink was injected into the subgerminal cavity and the vitelline membrane was pulled apart using a tungsten microscalpel. The precise

number of completely formed somites was registered for all embryos. This allowed us to temporally order the embryos with a maximum error of 1.5 hours. All eggs were then sealed and re-incubated in the same conditions. After 110-116 hours of incubation (time necessary to reach digit formation stages), the wings of surviving embryos (n=180) were fixed and hybridised with a *gdf5* antisense RNA probe and the number of *gdf5*-positive digit stripes was recorded for each embryo.

#### 1.6.2 Determination of the *hairy2* expression cycle time period

A window was cut in the incubated eggs and the vitelline membrane was removed. With a microscalpel, the right wings of embryos at different developmental stages (stage HH24 to 26) were removed, washed in PBS and fixed immediately in 4% formaldehyde. The operated embryos were re-incubated for different time periods: 1.5 hours (n=23), 3 hours (n=37), 5.5 hours (n=33), 6 hours (n=38), 6.5 hours (n=30), 9 hours (n=39), 11.5 hours (n=26), 12 hours (n=71) and 12.5 hours (n=19), after which the left wing was removed and processed the same way. Both wings were hybridised simultaneously ensuring the same conditions.

#### 1.6.3 AER removal

A window was cut in the incubated eggs and the vitelline membrane was removed. The AER was microsurgically removed (n=24) from the wing buds of stage HH20-21 embryos using a tungsten needle, the embryos were re-incubated for 4 hours and an *in situ* hybridisation with the *hairy2* probe was performed.

#### 1.6.4 Bead implants

AG1-X2 ion exchange beads (Biorad) were incubated in 4 mg/ml SU5402 (a drug known to specifically block the kinase activity of FGF receptors) (Calbiochem) in DMSO. Control beads were incubated in DMSO. Heparin acrylic beads (Sigma) were incubated in 1 mg/ml FGF8 (R&D Systems) in phosphate buffered saline (PBS). Control beads were incubated in PBS.

A window was cut in fertilised eggs and the vitelline membrane was removed. Two types of bead implant experiments were performed:

(1) Beads soaked in FGF8 protein (n=20) and in PBS (n=17) were microsurgically implanted in the proximal limit of the zone of *mkp3* expression in the right limb buds of stage HH24 embryos. Some embryos (n=6) were incubated 4 hours and hybridized with

## Materials and Methods

---

*mkp3* probe. Others (n=37) were incubated until digit formation and Alcian Blue staining was performed to permit cartilage analysis. The length of the radius and ulna were measured in both the right and left limbs of each embryo. The results were analyzed with a paired t-test, where the length of each bone of the right limb (incubated with an FGF8-soaked bead) was compared with that of the equivalent bone in the left limb (untreated). As a control, a paired t-test was also used to compare the bone lengths of the right limb (incubated in PBS-soaked bead) and left limb (untreated) of control embryos. This experiment was also performed at later stages of limb bud development (stage HH27 and HH28). The same experiment was also performed using SU5402-soaked beads, using as a control beads soaked in DMSO. An *in situ* hybridization was performed using the *mkp3* probe (n=6).

(2) Beads soaked in FGF8 protein were microsurgically implanted in the right limb distal mesenchyme, underneath the AER at stage HH25 (n=4). The operated embryos were incubated during 12 hours and hybridised with the *hairy2* probe. As a control, beads soaked in PBS were implanted in the same place of the right limb of control embryos.

### 1.7 Alcian Blue staining

1. Dissect the embryos in PBS.
2. Wash the embryos in PBS.
3. Fix and coloration of the cartilage, the time of fix depend of the embryos age:

Embryo Age	Time of fix (hours)
8 weeks	16 hours
10 weeks	20 hours
15 weeks	30 hours
20 weeks	40 hours

Fresh Fix: 80 ml EtOH 100% + 20 ml Acetic acid 100% + 15 mg Alcian Blue 8GX (Sigma)

4. Dehydrate in a minim of 3 washes of EtOH 100%.
5. Transparent tissue and bone coloration:

Embryo Age	KOH per 100ml of H <sub>2</sub> O	Alizarine Red S
------------	-----------------------------------	-----------------



		(Sigma)
< 10 weeks	0.5 g	-
10 weeks	0.5 g	10 mg
16 weeks	1 g	10 mg
21 weeks	3 g	10 mg

The time for the maceration of the tissues depends of the embryos age – 6 to 24 hours.

6. Rinse in 79 ml H<sub>2</sub>O + 20 ml Glycerol + 1 g KOH several times, until the tissue being completely transparent.

7. Dehydrate in a crescent series of glycerol (20% - 40% - 60% - 80% - 100%).

### **1.8 Tunel assay**

Apoptosis was analyzed in limb buds at stage HH24 after FGF8 and PBS bead implantation experiments using the Cell Death Detection Kit (Roche). Limb buds were fixed overnight in 4% paraformaldehyde (PFA) in PBS and then permeabilized with 0.5% Triton X-100 0.1% sodium citrate in PBS for 3 hours at 4°C, followed by washes in PBS. The limbs were incubated overnight at 37°C with the Tunel solution mix and then washed at least 3 times in PBS.

### **1.9 Immunohistochemistry (IHC)**

Two kinds of IHC were performed:

(1) Whole-mount IHC was performed in limb buds at stage HH24 after FGF8 and PBS bead implantation to analyze cell proliferation. The limb buds were fixed in 4% PFA in PBS and permeabilized with 0.5% Triton X-100 in PBS for 4 hours. Primary antibody incubation with the rabbit anti-phospho-histone H3 (UBI), used at 1/100, was performed overnight at 4°C, followed by washes in PBS. The secondary antibody used was Alexa Fluor 488 – conjugated goat anti-rabbit IgG (Molecular Probes), used at 1/1000. The incubation was performed overnight at 4°C, followed by PBS washes. The limb buds were post-fixed in 4% PFA overnight at 4°C.

(2) Forelimb buds were collected from stage HH25 chick embryos and immediately fixed in 4% paraformaldehyde in 0.1 M phosphate buffer (PB) with 0.12 mM CaCl<sub>2</sub> and 4% sucrose overnight at 4°C, washed in buffer only, and then in PB with 15% sucrose, both overnight at 4°C. Embryos were then incubated in PB with 15% sucrose and 7.5%

## ***Materials and Methods***

---

gelatin for 1 hr at 30°C, immediately frozen in liquid nitrogen chilled isopentane, and stored at -80°C until sectioned. Approximately 10-µm-thick serial sections were collected on Super Frost slides, and blocked for 30 min with 10% normal goat serum in PBS containing 1% bovine serum albumin. The primary anti-FGF8 antibody (KM1334 from BioWa, Inc.; Tanaka *et al.*, 1998; Shimada *et al.*, 2005) was diluted at 1:500 in the blocking solution and incubated overnight at 4°C, followed by washing in PBS, and detected with Alexa Fluor 488-conjugated anti-rabbit IgG, all F(ab')<sub>2</sub> fragments (Molecular Probes) diluted 1:1000 in blocking solution, followed by PBS washes. Slides were stained with 4',6-Diamidino-2-phenylindole (DAPI, Sigma), mounted in Vectashield (Vector Laboratories) and sealed after cover-slipping.

### **1.10 Imaging**

All *in situ* hybridization experimental embryos were photographed as whole-mounts in PBT with 0.1% azide, using a Sony DXC-390P-3CCD colour video camera coupled to a Leica MZFLIII microscope. The experimental embryos from the Tunel assay and whole-mount immunohistochemistry were photographed using a Pascal Zeiss confocal microscope. Embryos processed for immunohistochemistry in sections were photographed using an Olympus DP70 camera coupled to an Olympus BX61 microscope with epifluorescence. Images were treated in Adobe Photoshop CS.

### **1.11 Cell lines**

#### **1.11.1 Chicken Fibroblasts Preparation**

1. Incubate eggs for 10 days.
2. Dissect the embryos in PBS. The head and all the viscera have to be removed.
3. Put the embryos in a syringe (without needle) and apply pressure 2x, put the embryos mass in a plate. Eight embryo's per plate.
4. Incubate for 20 minutes with 20 ml of trypsin (Sigma).
5. Remove the cells debris.
6. Add 20 to 25 ml of complemented DMEM medium (Sigma).
7. Centrifuge 5 minutes at 1000 g.
8. Resuspend the pellet in 20 ml of complemented DMEM medium.
9. Place the cells solution in a plate with 10 cm of diameter.
10. Incubate at 37°C, 5% CO<sub>2</sub>.
11. Ten hours after, wash the plate with PBS and put fresh DMEM medium.

12. If the cells on the plate are confluent make the dilution 1:2.
13. At P1 confluence freezes the cells.

*1.11.1.1 Protocol to dilute the cells*

1. Remove the medium from the plate.
2. Wash with PBS at RT.
3. Put 2 ml of trypsin (Sigma) (for a 10 cm plate, the trypsin volume depends of plate size), 2 minutes or more at 37°C until the cells detach from the plate.
4. To inhibit trypsin add 3x the trypsin volume of medium (with serum). Mix carefully.
5. Put this mixture in a new plate and incubate at 37°C, 5% CO<sub>2</sub>.

*1.11.1.2 Protocol for cell freeze*

1. Remove the medium from the plate.
2. Wash 2x with PBS.
3. Add trypsin (the volume depends of the plate diameter, 2 ml for a 10 cm plate) to detach the cells from the plate, 2 minutes or more at 37°C.
4. Add 3x trypsin volume of medium (with serum). Mix gently.

To count the cells in a hemocytometer

5. Take a few µl of the cells in suspension to an eppendorf, made the following solution: 50 µl of cell + 50 µl of tripan blue (1:1), 1 minute at RT.
6. Take 20 µl of this solution and put in a hemocytometer.
7. Count viable cells in each quadrant of the hemocytometer, dead cells show a blue staining. The formula to found the number of cells x 10<sup>4</sup>/ml is:  
Number of cells = quadrant A + quadrant B + quadrant C + quadrant D x dilution factor  
The standard number of cells to freeze is ~1x10<sup>6</sup> cells/ml
8. Centrifuge the cell suspension 3 minutes at 1200 g.
9. Resuspend in the freezing solution with the volume calculate above and freeze (put first at -80°C and then in liquid nitrogen).

**1.12 Virus stock preparation**

1. Defreeze the cells and propagate until reach a good confluence (70% - 80% confluence).
2. Transfect the cells using the reagent Transfast (Promega).

Transfection protocol for a 10 cm plate:

## ***Materials and Methods***

---

3. Leave the cells plate 15 minutes at RT.
4. Remove the culture medium and add the following solution: 2000 µl of medium without serum (just with Glutamine and Penicilin/Streptomisine) + 28 µl of Transfast + 4-8 µg of plasmid.
5. 1 hour at 37°C.
6. Add 4 ml of supplemented medium.
7. Incubate at 37°C, 5% CO<sub>2</sub> at least for 2 days, lead the cells propagate.
8. When the cells reach a good confluence, dilute the cells until have 4 plates of 15 cm diameter/virus type.
9. When these cells have a 70% confluence, remove the medium used and add OPTIMEM medium (Sigma) (12.5 ml/plate). 1 day at 37°C, 5% CO<sub>2</sub>.
10. Remove the OPTIMEM medium from the plate to a 50 ml Falcon, centrifuge 5 minutes at 1000 g and place the supernatant in a new 50 ml Falcon, kept at 4°C.
11. Repeat this for 2 days until have 3 Falcons of 50 ml/type of virus.
12. Filter the viral solution, using a 0.45 µm filter.
13. Centrifuge 3 hours at 40000 g.
14. Discard the supernatant and resuspend the viral pellet in 50 µl of OPTIMEM medium. Make 20 µl aliquots, kept at -80°C.

### **1.13 Buffers and Solutions**

#### **PBS (1L)**

- NaCl            8 gr
- KCl             0.2 gr
- Na<sub>2</sub>HPO<sub>4</sub>    1.44 gr
- KH<sub>2</sub>PO<sub>4</sub>     0.24 gr

Add ultrapure water until reach 1L

Adjust the pH to 7.4 with HCl

#### **PBT**

- 0.1% Tween20 in PBS

#### **TAE buffer**

- 40 mM Tris.acetate
- 2.0 mM EDTA (pH=8.5)

#### **TE buffer**

- 1.0 mM EDTA

- 10 mM Tris.HCl (pH=8.0)

**Paraformaldehyde fixing solution (4%)**

- 4 gr of paraformaldehyde in 100 ml of PBS

**Luria Broth (LB) bacterial growth medium**

- 1% w/v bacto-tryptone

- 0.5% w/v bacto-yeast extract

- 1% w/v NaCl

**Whole-mount *in situ* hybridization solutions**

Whole-mount fix

- 4% formaldehyde in PBS, 2mM EGTA (pH=8.0), adjust pH to 7.5 with 1.0 M NaOH

Whole-mount postfix

- 4% formaldehyde in PBT, 0.1% gluteraldehyde

Hybridization mix

- 50% formamide

- 1.3x SSC (pH=5)

- 5.0 mM EDTA (pH=8)

- 50 µg/ml torula yeast RNA

- 0.2% Tween20

- 0.5% CHAPS

- 100 µg/ml Heparin

MABT solution

- 0.1 M Maleic acid

- 0.15 M NaCl

Adjust pH to 7.5 with 1.0 M NaOH

Blocking solution

- 20% Goat Serum

- 2% Blocking Reagent (Roche)

In MABT solution

NTMT solution

- 0.1 M NaCl

- 0.1 M Tris.HCl (pH=9.5)

- 0.4 M MgCl<sub>2</sub>

- 1% Tween20

## ***Materials and Methods***

---

### Detection Buffer

- 0.35 mg/ml NBT/INT

- 0.175 mg/ml BCIP

In NTMT

### **On section *in situ* hybridization solutions**

#### Whole-mount postfix

- 4% formaldehyde in PBT, 0.1% glutaraldehyde

#### Hybridization mix

- 1x Salt: 10x Salt solution (per 200 ml)

- 22.8 gr NaCl

- 2.8 gr Tris.HCl

- 0.268 gr Tris base

- 1.56 gr NaH<sub>2</sub>PO<sub>4</sub>·2H<sub>2</sub>O

- 1.42 gr NaH<sub>2</sub>PO<sub>4</sub>

- 20 ml 0.5M EDTA

- Ultrapure H<sub>2</sub>O

- 50% Formamide

- 10% Dextran Sulfate

- 1 mg/ml Yeast RNA

- 1x Denhart solution

- Ultrapure H<sub>2</sub>O

#### MABT solution

- 0.1 M Maleic acid

- 0.15 M NaCl

Adjust pH to 7.5 with 1.0 M NaOH

#### NTM solution

- 0.1 M NaCl

- 0.1 M Tris.HCl (pH=9.5)

- 0.4 M MgCl<sub>2</sub>

#### Detection Buffer

- 0.35 mg/ml NBT/INT

- 0.175 mg/ml BCIP

In NTM

### **Supplemented medium for culture cells**

DMEM medium supplemented with:

- 10% Foetal Calf Serum
- 2% Chick Serum
- 1% Glutamine
- 1% Penincilin/Streptomicine

OPTIMEM medium supplemented with:

- 10% Foetal Calf Serum
- 2% Chick Serum
- 1% Glutamine
- 1% Penincilin/Streptomicine

Freezing medium

- 10% DMSO
- 90% Foetal Calf Serum





---

## **CHAPTER III**

### ***Results***

- 1. Study of the expression pattern of the somitogenesis molecular clock hairy1 and hairy2 during forelimb development*
- 2. A molecular clock operates during proximal-distal limb outgrowth in the chick embryo*
- 3. Is a wavefront traveling along the distal limb mesenchyme?*



The current chapter presents a compendium of the most relevant results obtained. The work developed throughout this thesis aimed at answering the following question: Is the Clock and Wavefront model proposed for somitogenesis also applicable to limb bud outgrowth and patterning? Our first approach was to characterise the expression patterns of the somitogenesis molecular clock components *hairyl* and *hairy2* during limb bud development. We found that a molecular clock is operating during limb bud development: *hairy2* expression cycles in chondrogenic precursor cells with a periodicity of 6 hours and two cycles of *hairy2* expression are performed as one autopod limb element is laid down. We also searched for molecular gradients along the limb P-D axis that could be acting as “wavefront”. We hypothesise that the *mkp3* gene could be acting as a “wavefront” in the limb bud, with a similar behaviour to that of *fgf8* in PSM. Like in the somitogenesis process, smaller limb elements can be obtained when a proximal shift in FGF8 activity is induced. We also suggest that FGF8 regulates *hairy2* gene expression in the distal limb mesenchyme.

## ***1. STUDY OF THE EXPRESSION PATTERNS OF THE SOMITOGENESIS MOLECULAR CLOCK COMPONENTS HAIRY1 AND HAIRY2 DURING FORELIMB DEVELOPMENT***

### **1.1 *hairyl* is expressed during forelimb development**

*hairyl* expression pattern was analyzed from the beginning of limb bud formation (stage HH15) until stages of digit formation (stage HH32) (Figure 13). *hairyl* transcripts are detected as soon as stage HH15 in the presumptive limb region flanking somites 15 to 20 (Figure 13A). From stage HH16 to HH19, *hairyl* expression can be detected uniformly distributed within the forelimb (Figure 13B,C) and at stage HH19 an intense central stripe of *hairyl* expression with a proximal to distal direction becomes visible (Figure 13C). From stage HH20 to HH26, *hairyl* expression is observed in distal forelimb mesenchyme and forms a stripe that goes from this region to the proximal part of the forelimb (Figure 13D-G). *hairyl* expression is also observed in the anterior part of the forelimb at these stages (Figure 13D-G). From stage HH29 to HH32, *hairyl* transcripts are expressed in the interdigital zone of the wing (Figure 13H).

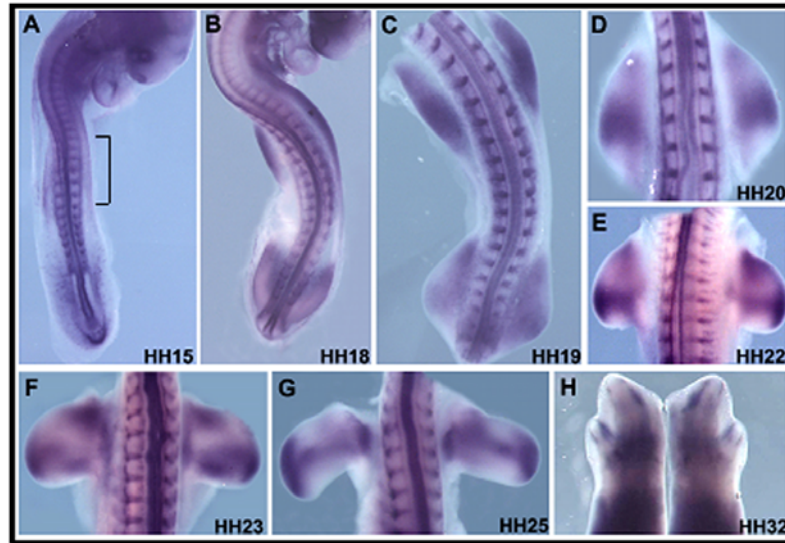


**Figure 13** – *hairy1* expression pattern during forelimb development. (A) *Hairy1* expression is detected at stage HH15 in the presumptive forelimb zone (bracket). (B, C) At stages HH18–HH19, *hairy1* transcripts are observed uniformly within the forelimb bud. At stage HH19 *hairy1* expression becomes stronger within a stripe with a proximal to distal direction. (D – G) *hairy1* transcripts are detected in the distal limb mesenchyme and within a stripe observed from the more distal part to the most proximal part of the limb at stages HH20 though HH25. At these stages, *hairy1* expression can be also observed in the anterior part of the forelimb. (H) At stage HH32, *hairy1* expression is observed at the level of the interdigital zone. All pictures show a dorsal view.

### 1.2 *hairy2* is expressed during forelimb development

We analyzed *hairy2* expression during forelimb development from limb bud initiation (stage HH14) to digit formation (stage HH32) (Figure 14). *hairy2* transcripts are first detected at stage HH14 in the presumptive forelimb region flanking somites 15 to 20 (Figure 14A). At stages HH16 and HH17, *hairy2* transcripts are uniformly expressed within the early wing bud (Figure 14B,C). From stage HH18 onwards, *hairy2* expression becomes localized to distinct expression domains: (1) *hairy2* transcripts are detected in the AER from its formation at stage HH18 (Martin, 1998) until its progressive disappearance at stage HH32 (Sanz-Ezquerro and Tickle, 2003) (Figure 14D–N; black arrow in G); (2) from stages HH18 to HH28, *hairy2* is expressed in a posterior limb bud area including the ZPA (Figure 14C–H and 14J–L; white arrow in G); (3) along all stages, *hairy2* transcripts are also present in dorsal and ventral mesenchymal domains containing the limb muscles precursors cells as visualised by

*MyoD* expression (Figure 14G,I, asterisks). *hairy2* expression was never found in the limb core, the region that contains the differentiating chondrogenic cells (Figure 14I, square); (4) *hairy2* expression is observed in the forming digits joints (Figure 14N); and (5), interestingly, in some embryos *hairy2* transcripts are found in the distal limb mesenchyme (Figure 14H,J; black arrows) while others lack this expression domain. This led us to focus our attention for the expression of the *hairy2* gene on this region.

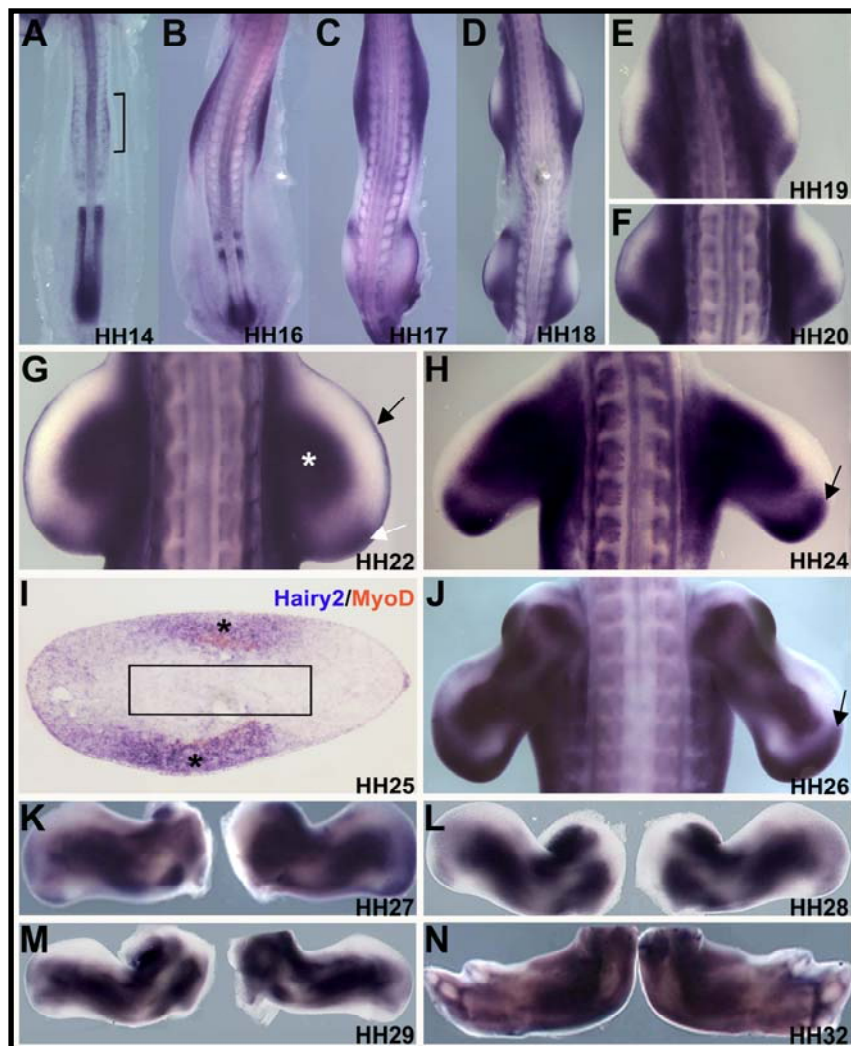


**Figure 14** - *hairy2* expression pattern during forelimb development. (A) *hairy2* transcripts are first detected at stage HH14 in the presumptive forelimb region (bracket). (B,C) At stages HH16 and HH17, *hairy2* transcripts are uniformly expressed within the early wing bud. From stage HH18 onwards, *hairy2* expression becomes localized to distinct expression domains: (1) *hairy2* transcripts are detected in the AER from its formation at stage HH18 until its progressive disappearance at stage HH32 (D-N; black arrow in G); (2) from stages HH18 to HH28, *hairy2* is expressed in a posterior limb bud area including the ZPA (C-H and J-L; white arrow in G); (3) along these stages, *hairy2* transcripts are also present in dorsal and ventral mesenchymal

## Results

---

domains containing the limb muscles precursors cells as visualised by *MyoD* expression (G,I, asterisks). *hairly2* expression was never found in the limb core, the region that contains the differentiating chondrogenic cells (I, empty rectangle); (4) *hairly2* expression is observed in the forming digits joints (N); and (5) in some embryos *hairly2* transcripts are found in the distal limb mesenchyme (H,J; black arrows) while others lack this expression domain (Figure 15). All pictures show a dorsal view.

## 2. A MOLECULAR CLOCK OPERATES DURING PROXIMAL-DISTAL LIMB OUTGROWTH IN THE CHICK EMBRYO

### 2.1 *hairly2* is dynamically expressed along the limb proximal-distal axis

A closer analysis of our results showed that, although two forelimbs of the same embryo always presented the same *hairly2* expression pattern, forelimbs of different embryos at the same stage of development, showed variable *hairly2* expression patterns in the distal mesenchyme (up to 400  $\mu\text{m}$  from the AER). Figure 15 shows representative patterns of this dynamic *hairly2* expression in forelimb buds, at stages HH20 (Figure 15A-C), HH24 (Figure 15D-F), HH25 (Figure 15G-I), HH26 (Figure 15J-L) and HH28 (Figure 15M-O), that were hybridized under precisely the same conditions. In some of these wings, the distal domain under the AER was clearly negative (Figure 15A,D,G,J,M), while in others, *hairly2* was strongly expressed in this same region (Figure 15C,F,I,L,O), and various intermediate patterns could also be observed (Figure 15B,E,H,K,N). The *hairly2* expression in the ZPA was always present. This variability in *hairly2* expression patterns is clear from stages HH20 to HH28. At stages HH20-22, the region presenting variable *hairly2* expression is localized between the central mesenchyme and the ZPA (Figure 15P), from stages HH23-26 is displaced to a more anterior region becoming located between the central mesenchyme and the AER (Figure 15Q), being restricted to the posterior part of the distal limb mesenchyme at stages HH27-28 (Figure 15R). According to the fate map of Vargesson and collaborators, the regions presenting cyclic *hairly2* expression throughout all these forelimb stages, correspond to the regions containing the chondrogenic precursor cells (Vargesson *et al.*, 1997). Thus, changes in the *hairly2* expression domain fit with the fate maps of Vargesson and collaborators and can be attributed to the expansion and fanning out of populations initially expressing *hairly2* (Vargesson *et al.*, 1997). After stage HH30 we could not ascertain whether the *hairly2* expression observed at digit tips corresponds to a

dynamic expression pattern or to the progressive appearance of interphalangeic joints (Figure 14N). Before stage HH20 we were also unable to clearly identify variations in *hairy2* expression. As a control, we hybridized some limbs with a *scleraxis* probe in parallel with the *hairy2* hybridized limbs. No variations in the expression pattern of *scleraxis* were observed among the different limbs (data not shown).

In conclusion, from stages HH20 to 28, the distal limb mesenchyme, containing undifferentiated chondrogenic precursor cells, displays variable *hairy2* expression patterns reminiscent of that previously described in the PSM. This suggests that *hairy2* is dynamically expressed in cartilage precursor cells during the laying down of limb skeletal elements, but stops being expressed in the differentiating chondrogenic cells.

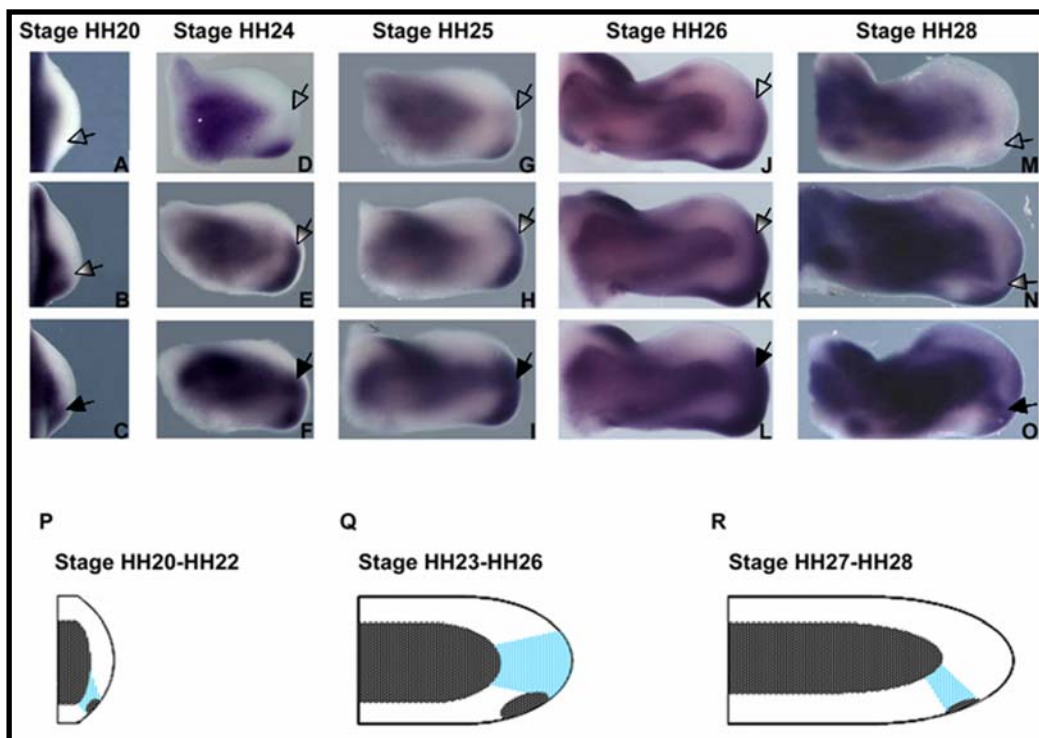


**Figure 15** - Dynamic *hairy2* expression in the distal limb mesenchyme. Representative *hairy2* expression patterns at stages HH20 (A-C), HH24 (D-F), HH25 (G-I), HH26 (J-L) and HH28 (M-O) illustrate the variations in *hairy2* expression observed in the forelimb distal mesenchyme. (A,D,G,J,M) Hollow arrows point to the absence of *hairy2* expression in the distal limb mesenchyme. (C,F,I,L,O) Filled arrows point to *hairy2* expression in the distal limb mesenchyme. (B,E,H,K,N). Partially filled arrows indicate an intermediate pattern. Bottom: (P-R) Schematic representation of the region where *hairy2* is dynamically expressed (blue) from stages HH20 to HH28. Right wings' dorsal view.

### 2.2 The formation time of a forelimb digit cartilaginous element is 12 hours

In the PSM, *hairy2* expression occurs with a cycle of 1.5 hours, corresponding to the formation time of one somite (Jouve *et al.*, 2000). If *hairy2* has similar cyclic expression in undifferentiated chondrogenic precursors of the forelimb bud, we would expect the period to be related to the time of limb skeletal element formation. However, the formation time of the limb skeletal elements is unknown. Therefore, our first step towards identifying the period of *hairy2* expression cycles was to determine the formation time of a limb skeletal element.

Joint formation can be used to define the boundaries of skeletal elements. Thus, the time between the formation of the proximal and distal joints of a skeletal element represents its formation time. The joint marker *gdf5* labels, as stripes, the formation of the second and the third autopod limb joints as well as the tip of the third phalanx (Storm and Kingsley, 1996; Francis-West *et al.*, 1999). Since it has been suggested that the third phalanx is formed by a mechanism independent of the one leading to the formation of the other phalanxes (Sanz-Ezquerro and Tickle, 2003), we concentrate on the formation time of the second phalanx. To determine the formation time of the second phalanx, we incubated multiple batches of 90 eggs for 48 hours, opened them and counted the number of somites in each embryo. This allowed us to order the embryos by their developmental age with a maximum error of 1.5 hours. The embryos were then re-incubated under identical conditions and during the same time period, until digit formation stages (Figure 16). After incubation, the embryonic limbs were fixed and analyzed by *in situ* hybridization with the digit joint marker *gdf5* (Francis-West *et al.*, 1999). In some batches, the formation of both joints delimiting the second phalanx was caught. In all these cases (n=13), the period of time that passed between the formation of the first and the second joint was longer than 10h30m and shorter than 13h30m, the average being 12 hours. In two cases, the time that passed was exactly 12 hours (Figure 16, arrows). These results strongly suggest that the forelimb second phalanx takes 12 hours to be formed.



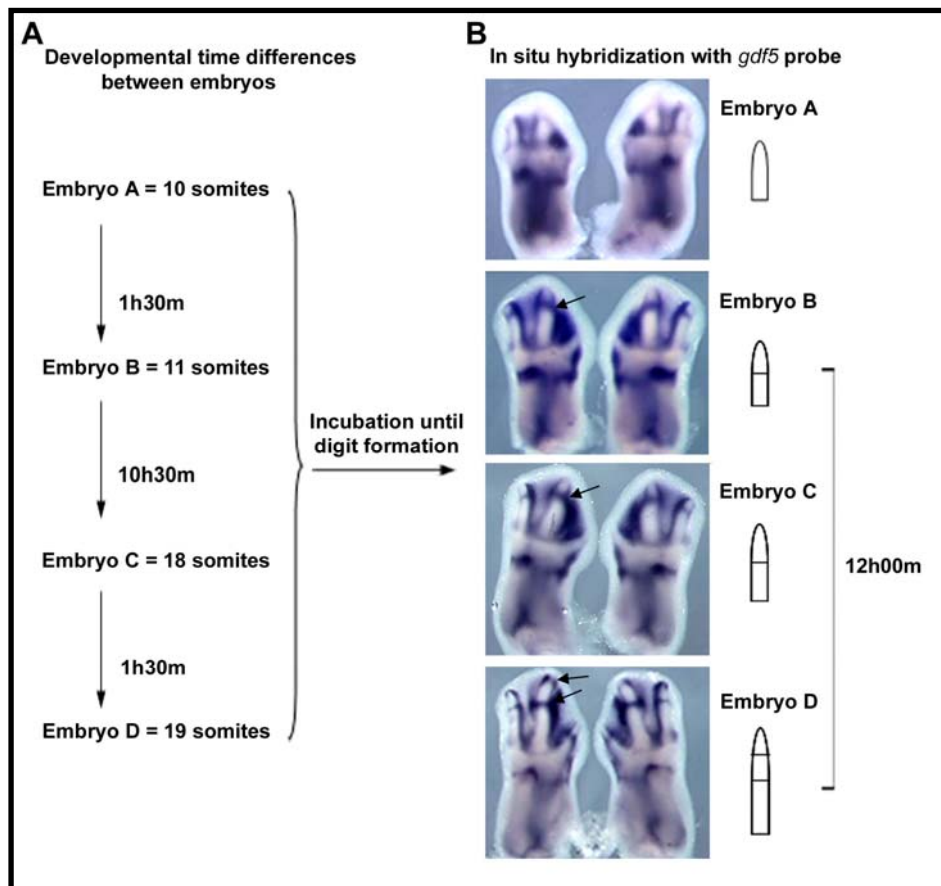


**Figure 16** - Estimating the formation time of an autopod limb element. (A) Schematic representation of the strategy used to estimate the formation time of the second phalanx of forelimb digit 3. (B) *gdf5* expression pattern in forelimbs of embryos A-D (arrows indicate the *gdf5*-positive digit stripes). In batches where the onset of formation of both joints delimiting the second phalanx was caught, the developmental time of the corresponding embryos differed by 12 hours.

### 2.3 Cyclic *hairy2* expression has a 6 hour periodicity in the distal forelimb bud

We provide data suggesting that a forelimb digital element takes 12 hours to be formed. If our analogy to somitogenesis is correct, then the dynamic *hairy2* expression in undifferentiated chondrogenic precursor cells should cycle with a time-period that correlates with the digit formation time. Thus, we surgically removed and fixed the right wings from stage HH24-26 embryos and re-incubated each embryo, with the left wing, for various lengths of time up to 12.5 hours (Figure 17). Both limbs pairs were then processed together for *hairy2* *in situ* hybridization. The percentage of wing pairs where the same expression pattern was observed in incubated and non-incubated wings was determined for each incubation period (Figure 17). At every developmental stage, the

## Results

graph reveals a clearly distinguishable peak at 12 hours of incubation, but, interestingly, there are also equally clear peaks at 6 hours. This experiment demonstrates that in stages HH24, HH25 and HH26, *hairy2* expression in the distal limb region (containing autopod chondrogenic precursor's cells) cycles with a 6 hour periodicity. We therefore conclude that, for every two cycles of *hairy2* expression, a chondrogenic autopod element is formed. This is different from somitogenesis where one element is formed per cycle.

In order to determine the time spent in each phase of the *hairy2* cycle, we analyzed the *hairy2* expression pattern in the limb distal mesenchyme of a total of 383 embryos and found that, 22% presented a completely negative pattern, 19% presented an intermediate pattern, and 59% presented a positive pattern. Based on a cycle time of 6 hours, these would correspond approximately to 1h20m with a negative pattern, 1h10m with an intermediate pattern, and 3h30m with a positive pattern.

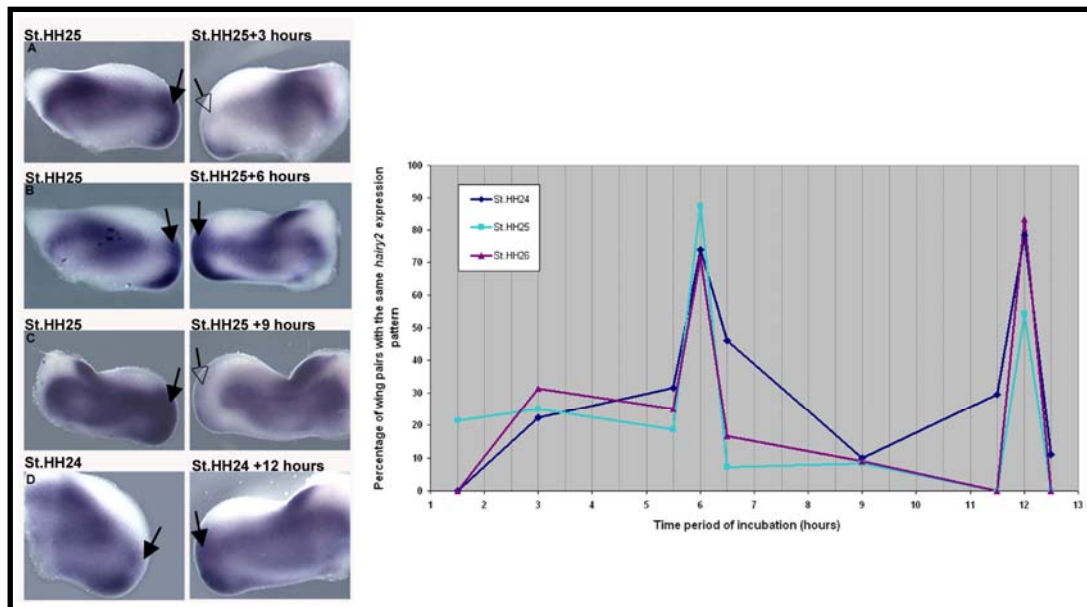


**Figure 17** - Periodicity of *hairy2* cyclic expression along limb P-D axis. Comparison of the P-D *hairy2* expression pattern between two wings of the same embryo in which the right wing was surgically removed and immediately fixed while the left wing was re-incubated (*in ovo*) for different time periods. Both wings were hybridized in the same tube, ensuring the same conditions. The *hairy2* expression pattern in the left wing was either different (A and C) or similar (B and D) to that in the right wing. The graphs show the percentage of wing pairs with the same *hairy2* expression pattern for each incubation time. Two clearly distinguishable peaks are observable at 6 hours and 12 hours. Hollow and filled arrows point to the absence or the presence of *hairy2* expression in the distal limb mesenchyme, respectively. All pictures show a dorsal view.

### 3. IS A WAVEFRONT TRAVELING ALONG THE DISTAL LIMB MESENCHYME?

#### 3.1 Mkp3 and FGF8 - functional partners in the distal limb mesenchyme.

In the somitogenesis process a wavefront of cell differentiation that extends posteriorly throughout the embryo can be observed. Cells in the posterior-most PSM tissues have been proposed to be maintained undifferentiated by high levels of FGF signalling and to activate their differentiation program only when they reach the appropriate threshold of FGF activity, as they become located more distantly to the tail bud and FGF levels gradually diminish (Vasiliauskas and Stern, 2001). Thus, the anterior limit of FGF gradient is proposed to establish the prospective somitic boundary location. Dubrulle and Pourquié (2004) have shown that the autonomous establishment of a caudal *fgf8* gradient in the PSM is based on progressive mRNA decay. In limb bud, as has been previously described, *fgf8* mRNA is expressed in AER (Mahmood *et al.*, 1995; Figure 18A). Moreover, by performing immunohistochemistry for the FGF8 protein in limb bud, we detected strong immunoreactivity in the AER (Figure 18B, C).

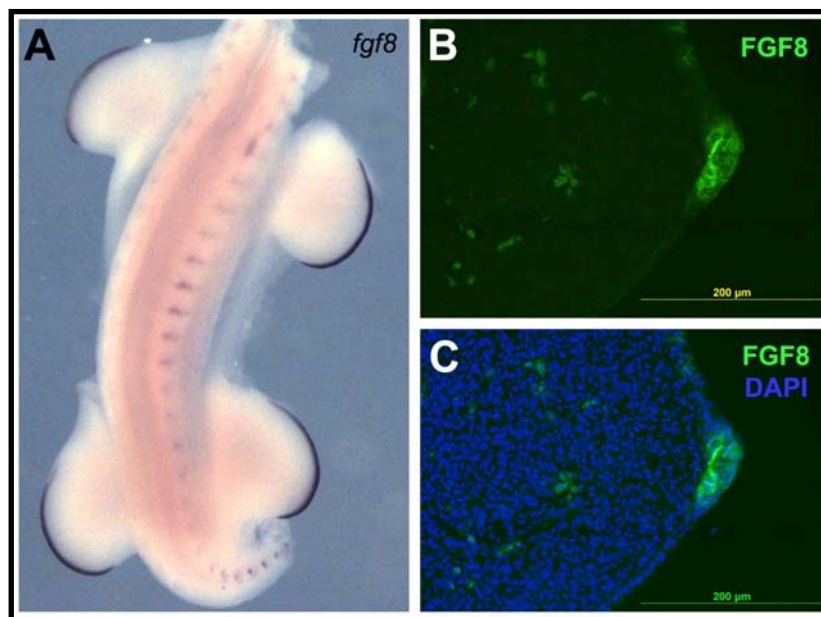


**Figure 18** - *fgf8* mRNA and FGF8 protein detection in the chick limb bud. (A) *fgf8* gene expression in the AER of stage HH23 chick limbs. (B) Longitudinal section of stage HH25 forelimb bud confirms the production of FGF8 protein (green) by the AER. (C) Same section as B, counterstained with DAPI.

## Results

We provide data suggesting that the expression of *mkp3*, a downstream effector of FGF8 during limb bud development (Kawakami *et al.*, 2003) can mimic the PSM mRNA *fgf8* behaviour in limb bud. This gene is expressed in the distal limb bud mesenchyme (Kawakami *et al.*, 2003; Figure 20A-C), the zone where cells are in an undifferentiated state like in PSM. We performed *mkp3* *in situ* hybridization studies in chick limb buds and observed that *mkp3* shows a graded distribution of its transcripts throughout the limb mesenchyme (Figure 19A). *mkp3* expression is stronger in the most distal part of the limb (underneath the AER), fading out in the direction of the more proximal part (Figure 19A). Real-time polymerase chain reaction (real-time RT-PCR) was performed to characterise the observed *mkp3* mRNA gradient in the limb bud. Limb buds at stage HH24 were dissected into three portions of equivalent size along the P-D axis (Figure 19A). Total mRNA was extracted from multiple batches of each portion of the limb (n=5) and *mkp3* mRNA content variation in the three regions was analysed by real-time RT-PCR. This high-resolution analysis clearly demonstrates a gradient of *mkp3* transcripts in the limb bud, in a distal to proximal direction (Figure 19B). Real-time RT-PCR experiments also showed that *fgf8* is strongly expressed in the distal tip of the limb bud, and no transcripts can be significantly measured in the more proximal limb regions (Figure 19B). Moreover, we could observe an opposing gradient of *raldh2* expression, which presents higher transcript levels in the proximal limb region (Figure 19C).

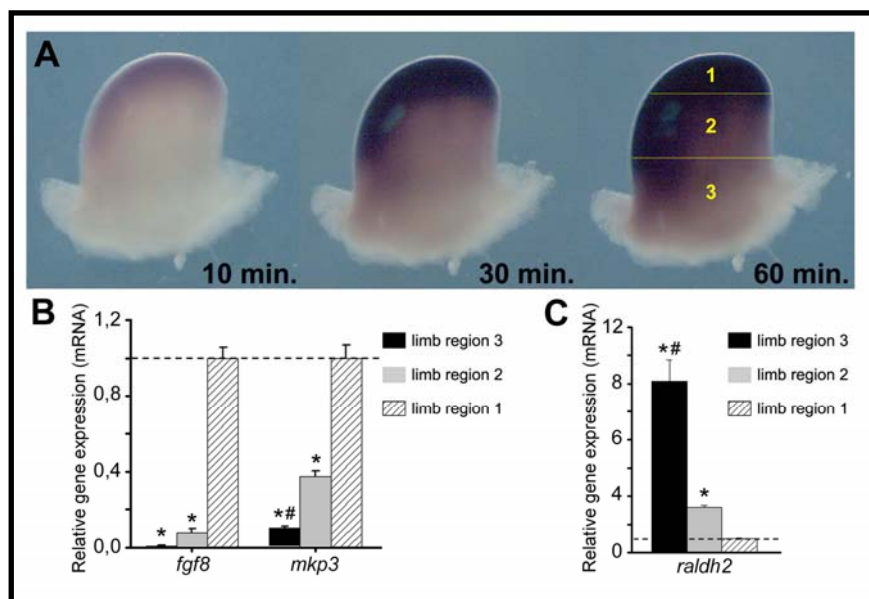


**Figure 19** - Characterization of the *mkp3* mRNA gradient in the chick limb bud. (A) Visualization of the *mkp3* mRNA gradient in stage HH24 chick wing bud mesenchyme. The

wing bud was photographed after increasing staining reaction times: 10 minutes, 30 minutes and 60 minutes. The three regions of wing bud collected for real-time RT-PCR are represented in the wing bud with 60 minutes of staining. (B) *mkp3* and *fgf8* mRNA levels in the different limb regions analyzed obtained by real-time RT-PCR, expressed in arbitrary units normalized for 18S Ribosomal RNA and for limb region 1 values (n=5 for each region); p<0.001: \*vs. limb region 1, # vs. limb region 2. (C) *raldh2* mRNA levels in the different limb regions analyzed obtained by real-time RT-PCR, expressed in arbitrary units normalized for 18S Ribosomal RNA and for limb region 1 values (n=5 for each region); p<0.05: \*vs. limb region 1, # vs. limb region 2.

Nevertheless, to observe if the *mkp3* expression gradient in limb bud mesenchyme is based on progressive mRNA decay as *fgf8* in PSM, we constructed an *mkp3* intronic probe and monitored the production of *mkp3* nascent transcripts in chick limb bud using riboprobes directed against intronic sequences of the *mkp3* gene (Figure 20). Whereas *mkp3* expression detected by the exonic probe is spans through a wide area of the limb mesenchyme (Figure 20A-C), cells recognized by the intronic probe were strictly localized just at the more distal part of the limb, even after a long exposure time to developing solution (Figure 20D-F). These results suggest that similar to the *fgf8* behaviour in PSM, the *mkp3* gradient in the limb distal mesenchyme is supported on progressive mRNA decay.

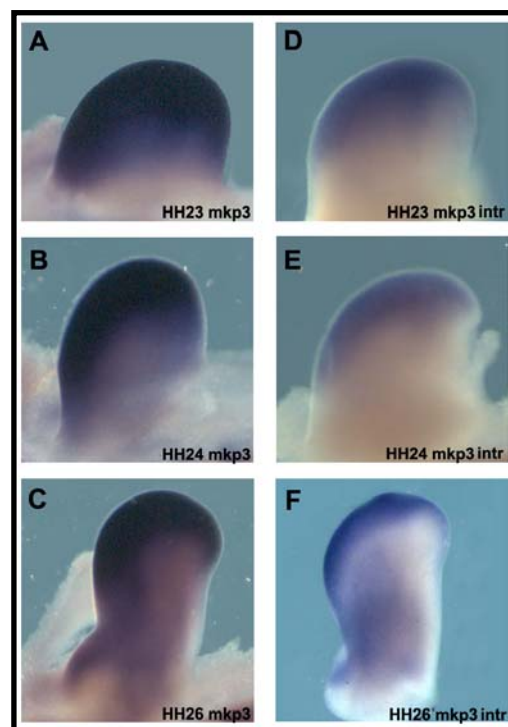


**Figure 20** – Expression patterns obtained using *mkp3* exonic versus *mkp3* intronic probes. (A-C) In stages HH23, HH24 and HH26, *mkp3* expression is detected by the exonic probe, showing

## Results

---

that transcripts are present in distal limb mesenchyme. (D-F) In stages HH23, HH24 and HH26, expression recognized by the intronic probe was restricted to the more distal part of the limb. The *in situ* hybridization was performed for both probes at the same time ensuring the same conditions and with the same time of labelling.

### 3.2 A proximal shift in *mkp3* expression causes a size reduction of limb skeletal elements

During somitogenesis, somite size is determined by the number of cells that escape FGF8 influence every 1.5 hours. Thus, somite size can be altered by manipulating FGF8 availability (Dubrulle *et al.*, 2001). In order to challenge the hypothesis of a parallelism between somite formation and limb skeletal element formation, the effect of FGF8 on limb skeletal element size was evaluated by placing FGF8-soaked beads in the right wing, at the proximal end of the *mkp3* expression domain, the FGF8 downstream effector (Kawakami *et al.*, 2003), the left wing being the control. This experiment was performed in stage HH24 wing buds, when the zeugopod distal end is being laid down. Eggs were re-incubated until all skeletal elements were formed and the limbs were stained with Alcian Blue to reveal the skeletal elements. Under these conditions, the radius and ulna were significantly shorter than in control wings ( $p=0.027$  for radius;  $p<0.0001$  for ulna; Figure 21). In contrast, in embryos where a PBS-soaked bead was implanted in the right wing, no differences in bone length were observed. When a FGF8-soaked bead is placed by the same method in later stages, when phalanx are being laid down (experiment performed at stages HH26-HH27), some phalanx are smaller in digit 3 and digit 4. Thus, we propose that when an FGF8-coated bead is applied, i.e. when the zone of FGF8 influence (represented by *mkp3* expression) is shifted proximally (Figure 21E), the limb skeletal elements under formation become shorter (Figure 21F). Similarly to what occurs during somitogenesis, sustained FGF8 activity in cells that are normally escaping its influence could make them unable to integrate the forming element, leading to smaller elements.

In an attempt to further investigate the role of FGF signalling in limb bud development, we placed SU5402 (a drug known to specifically block the kinase activity of FGF receptors) -soaked beads at stage HH24 right wing buds at the proximal end of *mkp3* expression domain. The results obtained shown that, when an *in situ* hybridization was performed for *mkp3*, a downregulation in *mkp3* expression levels is observed in this



region (Figure 22). Unfortunately the embryos die when we re-incubated them to look for the skeletal element size; consequently no results are obtained in this experiment.

Preliminary experiments using TUNEL assay and rabbit anti-phospho-histone H3 immunohistochemistry lead us to hypothesize that no increase in cell death or decrease in cell proliferation occurs around the FGF8-soaked bead, suggesting that the shortened structures are not resultant of this effects. However, an optimization of the protocol has to be performed to confirm this result.

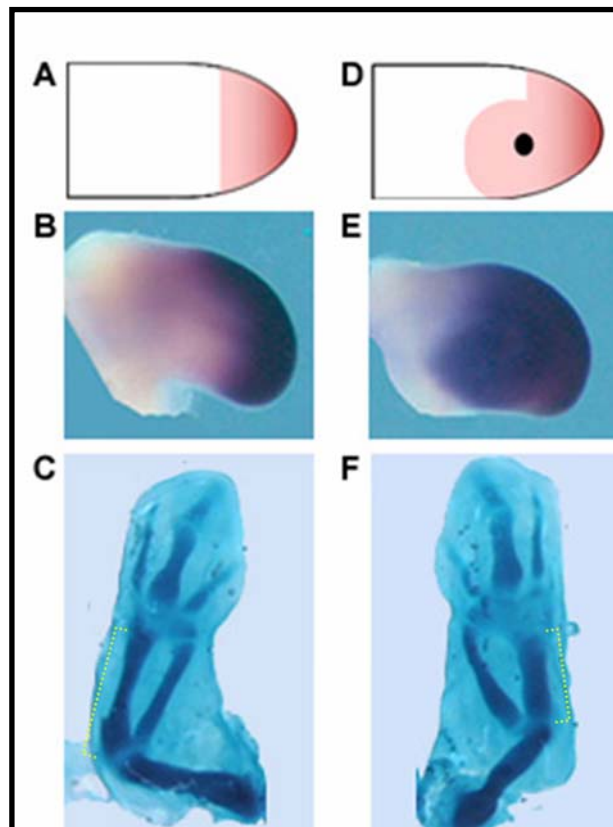


**Figure 21** - Proximal extension of the *mkp3* domain results in a shortening of skeletal elements in the forelimb. (A-C) Control limb: (A) schematic representation of *mkp3* gene expression in the limb distal mesenchyme of stage HH24 embryo. (B) *mkp3* pattern of expression in the limb distal mesenchyme of stage HH24 embryo and (C) skeletal preparation of a control left limb of stage HH31 embryo. (D-F) Experimental limb: (D) scheme showing the location of the *in ovo* implanted FGF8-soaked bead and its effect on *mkp3* expression in the right limb of stage HH24 embryo. (E) The *mkp3* expression pattern in the limb distal mesenchyme 4 hours after incubation with an FGF8-soaked bead located at the proximal limit of *mkp3* expression. (F) Skeletal preparation of the right wing of the experimental embryo 72 hours after FGF8 bead implantation. The overall skeletal pattern is complete and digit pattern formation occurred normally, however the radius and ulna of the right (FGF8-treated) wing were smaller (yellow brackets) compared to the left wing. All pictures show a dorsal view.

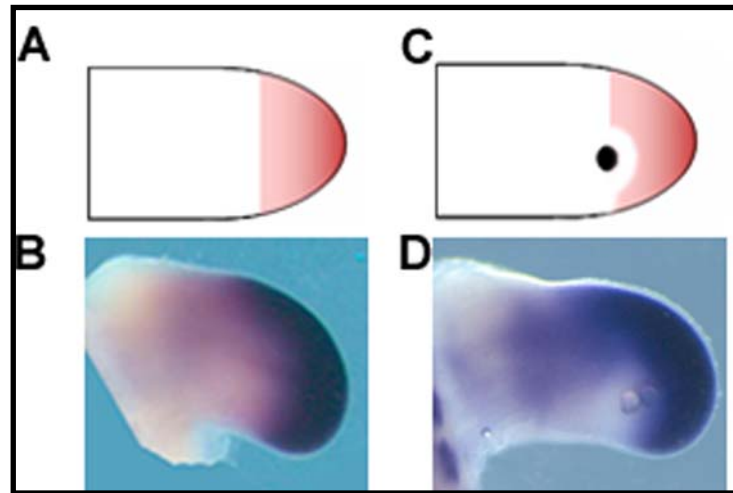


**Figure 22** – *mkp3* expression pattern under influence of the FGF inhibitor SU5402. (A) Schematic representation of *mkp3* gene expression in the limb distal mesenchyme of stage HH24 embryo. (B) *mkp3* expression pattern in the limb distal mesenchyme of stage HH24 embryo. (C) Schematic representation showing the location of the *in ovo* implanted SU5402-soaked bead and its effect on *mkp3* expression in the right limb of stage HH24 embryo. (D) *mkp3* expression pattern 4 hours after incubation with SU5402-soaked bead. All pictures show a dorsal view.

### 3.3 FGF8 regulates *hairy2* gene expression in distal limb mesenchyme

It has been suggested that *fgf8* expressed by the tail bud maintains posterior PSM cells in an undifferentiated state (Dubrulle *et al.*, 2001). Whether this “undifferentiated state” involves maintenance of cyclic gene expression remains to be determined. Limb distal mesenchymal cells are also maintained in an undifferentiated state by *fgf8* produced by the AER and this *fgf8* source can be experimentally removed by AER ablation (Mahmood *et al.*, 1995). AER ablations were performed *in ovo* at stage HH20-21 limbs and after a 4 hours incubation period the embryos were processed for *hairy2 in situ* hybridization. Our results show that, 4 hours after AER removal, *hairy2* expression in the distal limb mesenchyme has completely disappeared (Figure 23A), indicating that AER-produced factors are necessary for *hairy2* expression in this region. In addition, ZPA *hairy2* expression also disappeared (Figure 23A), agreeing with the reported loss of ZPA identity after AER ablation (Anderson *et al.*, 1993, 1994; Vogel and Tickle, 1993; Niswander *et al.*, 1994; Laufer *et al.*, 1994). To test whether *hairy2* is indeed regulated by FGF8 activity, we implanted FGF8-soaked beads in the distal mesenchyme, underneath the AER, at stage HH25 forelimbs and observed *hairy2*



expression 12 hours later. The results showed an increase of *hairy2* expression near the beads when compared to the control left wings (Figure 23B). We conclude that FGF8 activity positively regulates *hairy2* expression in the distal limb mesenchyme.

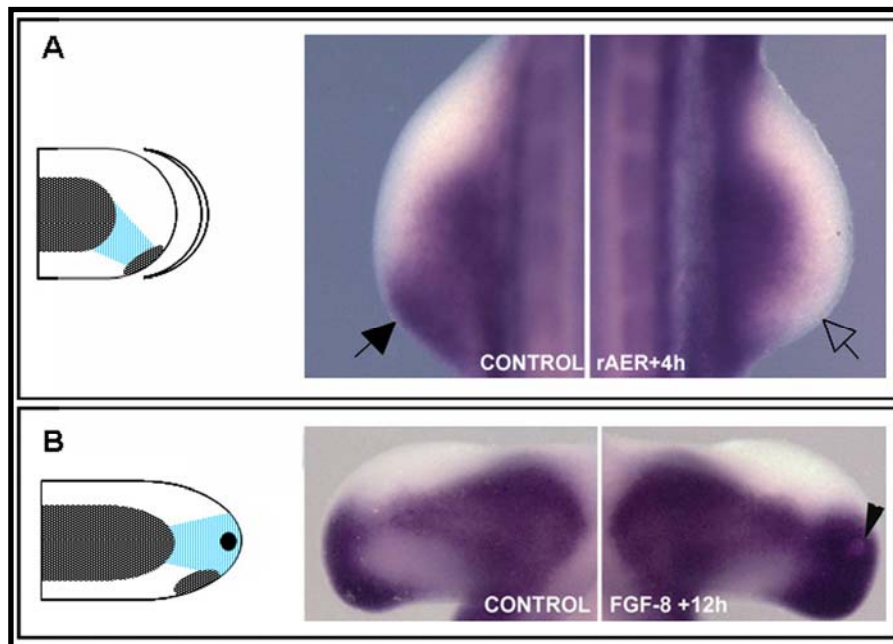


**Figure 23** - The effect of FGF8 on *hairy2* expression. (A) The AER was removed from the right wings of stages HH20-21 embryos as shown in the schematic representation, while the left wings were left intact. Four hours after AER removal, *hairy2* expression is downregulated in the distal limb mesenchyme and the ZPA of the right wing, while the left wing shows expression in both domains. Hollow and filled arrows point the absence or the presence of *hairy2* expression in the distal limb mesenchyme, respectively. (B) FGF8-soaked beads were implanted underneath the AER of right wings of stage HH25 embryos as shown in the schematic representation, while the left wings were left intact. A reinforced *hairy2* expression is observed in the right wing as compared to the left wing, after a 12 hour incubation period. rAER=removal of AER; FGF8=application of FGF8-coated bead. All pictures show a dorsal view.



---

## **CHAPTER IV**

### ***General Discussion***

*1. hairy2 is cyclically expressed in limb bud cartilaginous progenitor cells with an oscillation period that correlates with the formation time of an autopod limb element*

*2. Cyclic hairy2 expression and the acquisition of temporal information*

*3. Notch signaling pathway and proximal-distal limb outgrowth*

*4. Could a wavefront be traveling during limb bud development?*

*5. FGF8 activity and the regulation of limb element size*

*6. Compendium parallelisms*



The results presented in this thesis unveil some parallelisms between the molecular events controlling somitogenesis and limb element formation. The data obtained demonstrate that a molecular clock is working during P-D limb outgrowth and that the periodicity of this clock correlates with the formation time of a limb element. Our results also suggest that a wavefront could be travelling during limb bud development and that the gradient of *mkp3* expression under the influence of FGF8 could be regulating limb element size. Additionally, this thesis raises the exciting possibility that the molecular clock operates in many other tissues with tissue-specific time periods, controlling the formation of various morphological units. Since time control is essential to coordinate cells during all developmental processes in multicellular organisms, it is conceivable that this molecular behaviour is widespread, but only detectable when synchrony is maintained between adjacent cells.

***1. HAIRY2 IS CYCLICALLY EXPRESSED IN LIMB BUD CARTILAGINOUS PROGENITOR CELLS WITH AN OSCILLATION PERIOD THAT CORRELATES WITH THE FORMATION TIME OF AN AUTOPOD LIMB ELEMENT***

Oscillatory expression of several genes has been described in presomitic cells and its functional relevance for vertebrate segmentation investigated (reviewed by Freitas *et al.*, 2005; Rida *et al.*, 2004). However, although this phenomenon has been extensively studied in recent years, the function of the molecular clock during somitogenesis is still unclear. In 2002, Hirata and collaborators showed that in response to a serum shock, periodic expression of *Hes1* (the mouse *hairy2* homologue) can be triggered in a variety of cultured cell lines (Hirata *et al.*, 2002), suggesting that the segmentation clock could play a role in other cell types and biological processes. *In vivo*, however, this phenomenon of oscillatory gene expression has only been reported in presomitic cells and it is not clear whether it also operates during the formation of other embryonic structures. In this thesis, we report the cyclic expression of *hairy2* in the distal part of stage HH20-28 embryo forelimb mesenchyme, corresponding to an area containing undifferentiated autopod chondrogenic precursor cells. Since, *hairy2* expression is never detected in the central core of the limb where the already-specified cartilaginous elements are localized, we propose that cartilaginous precursor cells perform *hairy2* cycles while they are undifferentiated, ceasing this cyclic behaviour when they start the chondrogenic differentiation program.

By performing *in ovo* microsurgery experiments, we showed that *hairy2* expression is cyclic in phalanx chondrogenic precursor cells and that it has a 6 hour periodicity. Interestingly, the 6 hour time-period is distinct from the 1.5 hour period reported for *hairy2* in somite precursor cells, but it is a multiple of 1.5 hours. In fact, the possibility of the existence of cyclic gene expression with a periodicity different from, but multiple of 1.5 hours has been predicted in the “Clock and Trail model”, proposed by Kerszberg and Wolpert (2000). The authors concentrate on the somitogenesis clock and argue that it is unlikely that an oscillator of this type consists only of one single component. A model is presented where period-doubling oscillations can arise from an oligomerisation mechanism between transcription factors that act both by activating or inhibiting genes, including themselves. The authors argue for the existence of cycles that are different from, but multiples of 1.5 hours, and that these cycles could specify hemi-somites (45 minutes), somites (90 minutes), or even pairs of somites (180 minutes) (Kerszberg and Wolpert, 2000).

During somitogenesis, each clock gene expression cycle underlies the formation of a new somite pair. In the limb, the formation time of skeletal elements was unknown. Previous work suggested that each of the seven limb element primordial would take about the same length of time to be laid down and would then proliferate differentially (Wolpert *et al.*, 1975). The work performed in this thesis showed that the formation time of the second phalanx is likely to be 12 hours, by measuring the time between the formation of the second and third joint of digit 3. Consequently, the formation of the entire set of seven limb elements would take 3.5 days, which is in accordance with the time required to form a chick forelimb (3-4 days; Hamburger and Hamilton, 1951).

During somitogenesis, each PSM cell undergoes many molecular clock gene cycles before escaping the FGF8 influence and becoming committed to incorporate a somite. One somite forms every time the molecular clock wave sweeps the PSM, but each PSM cells “experiences” those waves many times. Similarly, we propose that limb distal mesenchyme cells perform several *hairy2* expression cycles before being incorporated into a limb skeletal element. Every 12 hours, a batch of cells forms a new limb element. This means that one limb skeletal element is formed by a set of cells with “n” and “n+1” *hairy2* cycles. In fact, in the case of somitogenesis, the bones that result from the somite (i.e. the vertebrae) are formed by the sclerotomal cells from the posterior compartment of one somite and the anterior compartment of the immediately posterior somite. Thus every vertebra is also formed by a set of cells with “n” and “n+1”

molecular clock gene cycles. As a consequence of the work here presented was the formulation of a comparative model of molecular clock gene expression cycles underlying the formation of trunk and limb skeletal segments, presented in Figure 24.

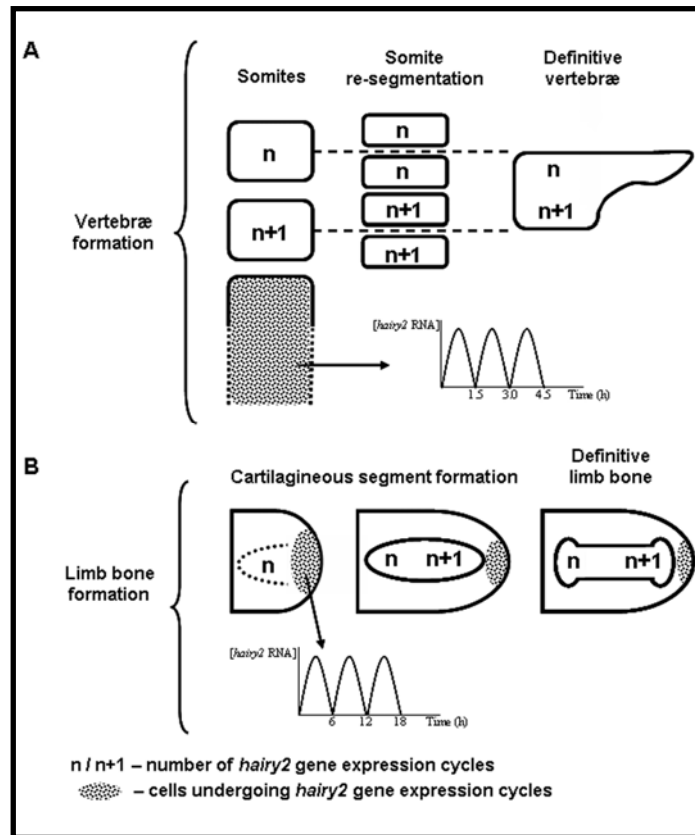


**Figure 24** - Comparative model of molecular clock gene expression cycles underlying the formation of trunk and limb skeletal segments. (A) Schematic representation of somite re-segmentation that underlies vertebrae formation, evidencing *hairy2* expression cycles in somite precursor cells and showing that each vertebra is composed of cells that previously underwent “n” and “n+1” molecular clock gene expression cycles. (B) Schematic representation of the process of limb bone formation evidencing *hairy2* expression cycles in chondrogenic precursor cells, proposing that each limb element is composed by cells that previously underwent “n” and “n+1” molecular clock gene expression cycles.

## 2. CYCLIC HAIRY2 EXPRESSION AND THE ACQUISITION OF TEMPORAL INFORMATION

Vertebrate limbs are formed by elements sequentially arranged along the P-D axis. The progress zone model (Summerbell *et al.*, 1973) postulates that PZ cells acquire P-D positional information progressively and that they must display synchronized oscillations related to the periodic transcription of some gene (Kerszberg

and Wolpert, 2000; Tickle and Wolpert, 2002). The important difference between this model and the early specification model (Dudley *et al.*, 2002) is in the timing of P-D specification. The progress zone model proposes progressive P-D specification while the early specification model suggests that all cell fates are already specified within the early limb bud and that progressive P-D segment formation results from a temporally regulated expansion of the progenitor populations in each domain (Dudley *et al.*, 2002). Based on our results, we propose that cells in the distal limb region record the number of *hairy2* oscillations they undergo while in this region, which provides them with a temporal value. This temporal value could either be translated into positional value (according to the progress zone model) or it could determine the time-point of progenitor population expansion (proposed by the early specification model). Thus our proposal that *hairy2* expression provides temporal information is compatible with both models.

### **3. NOTCH SIGNALLING PATHWAY AND PROXIMAL-DISTAL LIMB OUTGROWTH**

Most of the mutations that affect the somitogenesis clock are in components of the canonical Notch signalling pathway. These mutations cause a progressive disruption of intersomitic boundary formation along the A-P axis, although the formation of rostral somites occurs normally (Freitas *et al.*, 2005; Pourquié, 2001). In contrast, mouse embryos lacking *presenilin* have no somites at all, suggesting that formation of rostral somites requires presenilin activity which is independent of the Notch signalling pathway (Huppert *et al.*, 2005). The presence of anterior somites in embryos mutated for *Notch1:Notch2*-, and in components of the  $\gamma$ -secretase, such as *Nicastrin*-, *Pen-2*- and *APH-1a* , lead Huppert and collaborators to propose that three pathways (canonical Notch, WNT and presenilin) play redundant roles during anterior somitogenesis (Huppert *et al.*, 2005).

The limb phenotype of mouse embryos lacking *Notch1*, *Notch1:Notch2*, *jagged2/serrate2* of the canonical Notch pathway, clearly implicate the Notch signalling pathway in the development of the AER and in interdigital apoptosis (Francis *et al.*, 2005; Jiang *et al.*, 1998; Sidow *et al.*, 1997; Pan *et al.*, 2005). This is in agreement with the fact that these genes are exclusively expressed in mouse limb AER and that expression is completely absent from mouse limb distal mesenchyme (Francis *et al.*, 2005; Sidow *et al.*, 1997).



Several studies provide data that are compatible with a role of the Notch signalling pathway in the development of the forelimb distal mesenchyme as previous mentioned in the introduction chapter. In the chick, *notch1* and *hairy1* are expressed in the limb distal mesenchyme (Vargesson *et al.*, 1998; our unpublished data; Vasiliauskas *et al.*, 2003), the same happens with the expression patterns of the *serrate1/jagged1* and *hes1* in the mouse (Francis *et al.*, 2005; McGlinn *et al.*, 2005). *hes1*-, *serrate1/jagged1*-null mouse embryos die during embryogenesis and no studies on limb formation have been reported in the literature. Therefore certain differences may exist between mouse and chick with regard to the exact Notch components involved in limb development.

Loss of *presenilin* from the mouse limb mesenchyme (Pan *et al.*, 2005) leads to a phenotype that is completely different from the one of mouse embryos lacking the Notch signalling components described above. Mutant embryos have clinched forelimb digits (which may result from problems in the formation of inter-element boundaries), some digits appear to be truncated and some distal phalanxes are missing (Pan *et al.*, 2005). This corresponds to a phenotype that we would expect after a perturbation in the limb molecular clock. The limb phenotypes in *presenilin*-null embryos may thus reflect an activity of Presenilin that is independent of Notch signalling, as reported for somitogenesis by Huppert and collaborators (2005), and discussed above. Therefore, the study of *presenilin*-null embryos has revealed the existence of Notch-independent functions of presenilin both in anterior somites and in forelimbs. Taking all this into consideration, one could argue that there is a potential parallelism between the formation of rostral somites and forelimb skeletal elements.

#### **4. COULD A WAVEFRONT BE TRAVELING DURING LIMB BUD DEVELOPMENT?**

In 2001, Dubrulle and colleagues showed that there is a gradient of *fgf8* transcripts starting from the embryo tail bud and fading in the direction of the uppermost part of the PSM (Dubrulle *et al.*, 2001). This graded distribution of *fgf8* mRNA was demonstrated to result from progressive mRNA decay, rather than from different transcription levels (Dubrulle and Pourquié, 2004). In this thesis we show that in the limb bud FGF8 protein and *fgf8* mRNA is detected in AER. We also show that in limb bud mesenchyme, *mkp3*, a downstream effector of FGF8 (Kawakami *et al.*, 2003), have a graded distribution of its transcripts under the influence of FGF8, beginning in

## General Discussion

---

the most distal part of the limb (right underneath the AER) and fading out in the direction of the more proximal part of the limb.

To further characterise limb bud *mkp3* expression gradient we constructed an intronic probe for *mkp3* and looked for the distribution of *mkp3* nascent transcripts. We observed that cells recognized by the intronic probe were strictly localized at the more distal part of the limb, mimicking the effect obtained with the intronic *fgf8* probe in the PSM. This result demonstrates that the graded distribution of *mkp3* in distal limb mesenchyme is a result of RNA decay.

Concerning these results we propose a model for *mkp3* expression pattern in the chick limb bud (schematized in Figure 25): FGF8 protein produced in the AER induces *mkp3* gene transcription in the cells located immediately underneath, in the distal limb mesenchyme. As cell division and limb outgrowth proceeds, these cells are progressively displaced away from the FGF8 source. At a certain distance from the AER, *mkp3* transcription is no longer induced, but *mkp3* mRNA molecules are still present in these cells and decay over time. This results in a spatial gradient of mRNA expression in the chick limb bud. Our description of the *mkp3* expression gradient in the chick limb bud is reminiscent to the *fgf8* mRNA gradient present in the chick presomitic mesoderm. These results suggest for the first time that a similar process can be operating during limb bud development.

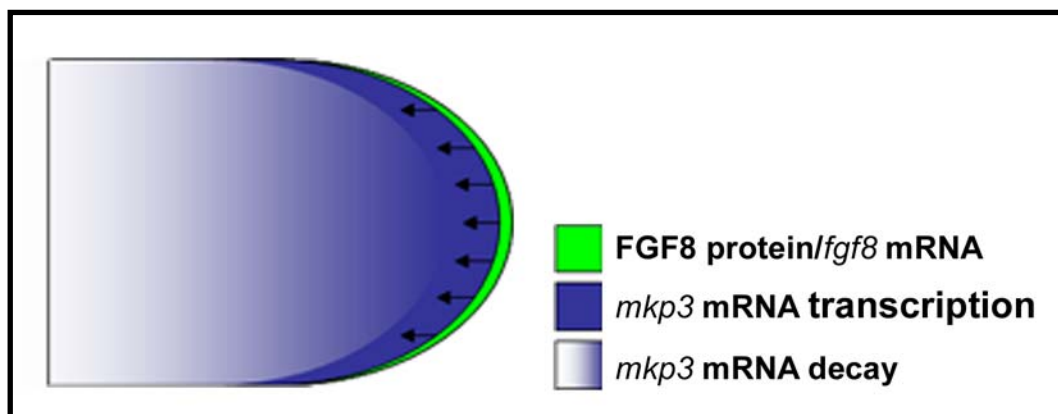


**Figure 25** - Model proposed for *mkp3* expression pattern in the chick limb bud (*see text for details*).

Similarly to what happens with the PSM wavefront, other genes appear to be implicated in the hypothetic limb wavefront. In the PSM, it was recently shown that *wnt3a* is present in an analogous pattern to that of *fgf8*, and it has been proposed that it could act upstream of *fgf8* and may operate together with or via the *fgf8* gradient (Aulehla *et al.*, 2003). In the limb bud, *fgf8* and *wnt3a* expression is confined to AER, but other genes involved in these same pathways are expressed in a gradient in the limb bud distal mesenchyme. This is the case for *mkp3* (downstream effector of FGF8) mentioned above, and *wnt5a* (Kawakami *et al.*, 1999), which acts through the canonical WNT pathway, similarly to *wnt3a*. This led us to believe, in a parallelism with PSM events, that the FGF/WNT signalling pathways could be working together in the limb bud to sustain cells in an undifferentiated state. Another interesting observation that reinforces our idea is the work recently described by Delfini and co-workers (2005) that presents evidences for a gradient of ERK activation established in response to FGF signalling, demonstrating that the maturation of PSM is directly regulated by MAPK/ERK activity. In the limb bud, high levels of ERK phosphorylation are observed in the AER but not in the mesenchyme (only a weak activity in the non-ridge ectoderm and distal mesenchyme are reported) (Kawakami *et al.*, 2003). Additionally, a study performed by Corson and collaborators (2003) has shown that ERK phosphorylation is observed in a graded distribution in the distal mesenchyme directly beneath the AER (Corson *et al.*, 2003). Kawakami and co-workers have also shown that Akt is phosphorylated in the limb mesenchyme but not in the AER (Kawakami *et al.*, 2003). MKP3 is an antagonist of ERK activity; this could be the reason why ERK activity is weak in distal limb mesenchyme (Kawakami *et al.*, 2003).

##### **5. FGF8 ACTIVITY AND THE REGULATION OF LIMB ELEMENT SIZE**

While the molecular clock is believed to regulate the periodicity of somite formation, somite size appears to be regulated by a gradient of FGF8 activity. An antagonism between FGF and RA signalling pathways is thought to operate during the development of several structures (see e.g. Irving and Mason, 2000; Schneider *et al.*, 1999). Similarly, during somitogenesis, FGF8 and RA are mutually inhibitory (Diez del Corral *et al.*, 2003). The antagonistic relationship that RA has on FGF8 activity has been proposed to regulate somite size. Thus, excess FGF8 activity in the PSM maintains cells in an undifferentiated state and inhibits their incorporation in a forming segment. This results in the formation of smaller somites, while the inhibition of FGF8 activity

results in larger somites (Dubrulle *et al.*, 2001). Interestingly, it has been shown that FGFs promote limb distalization by counteracting the RA pathway. This happens through inhibition of the proximalizing RA signal required to maintain the Meis activity, providing a molecular basis for the role of RA in specifying proximal limb fates in different vertebrates (Mercader *et al.*, 2000). Here we show that application of an FGF8-coated bead at the lower limit of the *mkp3* expression gradient leads to a size reduction of limb skeletal elements. A similar reduction in the length of radius and ulna after FGF2 and FGF4 application has been reported (Li *et al.*, 1996; Li and Muneoka, 1999). We therefore suggest that, as happens during somitogenesis, the confrontation between FGF and RA signalling pathways in the limb bud plays a role in allocating a certain number of cells to the initiation of the chondrogenic differentiation program, resulting in the regulation of limb element size.

We also show for the first time that FGF8 regulates *hairy2* expression. Ablation of the *fgf8* source (the AER) led to a complete downregulation of *hairy2* expression in the limb distal mesenchyme, while application of exogenous FGF8 resulted in an increase of the *hairy2* signal. These results suggest that in the limb distal mesenchyme, FGF8 controls the expression of *hairy2*. It would be interesting to determine if the same occurs in the PSM.

### **6. COMPENDIUM PARALLELISMS**

We propose that somitogenesis and limb bud are two parallel systems. Both have a zone where cells are maintained in an undifferentiated state (PSM and distal limb mesenchyme). In both these zones a molecular clock is operating regulating the periodicity of structure formation. We also suggest that these zones are maintained undifferentiated by the FGF/WNT signalling pathways that control the size of the elements formed. Recently, MAPK/ERK pathway has been implicated in this process. We moreover propose that RA and FGF have mutually inhibitory roles in limb bud development, similarly to what occurs during somitogenesis, playing a function in allocating a certain number of cells to the initiation of the chondrogenic differentiation program, resulting in the regulation of element size (Figure 26). This could be interpreted in evolutionary terms, since the embryo activates the same pathways when having to build an axis, the A-P axis in the case of somitogenesis or the P-D axis in the case of limb bud development.

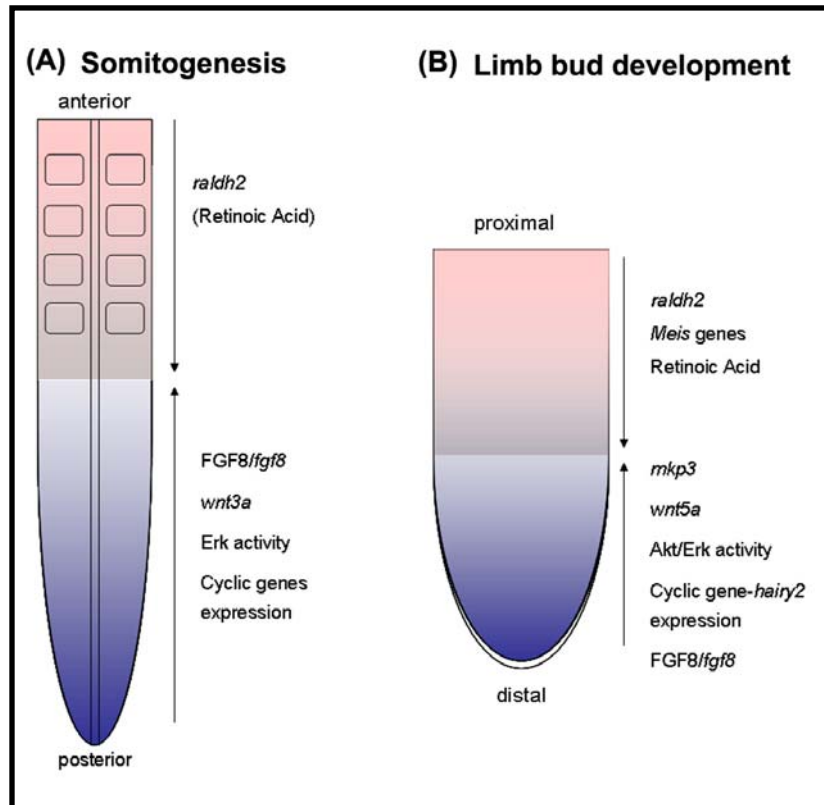


**Figure 26** – Parallelisms between somitogenesis and limb bud development during structure formation. (A) Schematic representation of the anterior-posterior (A-P) axis of an embryo demonstrating the main working signalling pathways. (B) Schematic representation of principal signalling pathways involved in limb bud proximo-distal (P-D) axis.



---

## ***CHAPTER V***

### ***Conclusions and Future Perspectives***





## **CONCLUSIONS**

The data presented in this thesis provide the first evidence for a molecular clock operating during limb outgrowth and patterning. The periodicity of this clock correlates with the formation time of a limb element, and our results also suggest that a maturation wavefront could be travelling during limb bud development. This unveils clear parallelisms between the molecular events controlling somitogenesis and limb element formation. Additionally, this work raises the exciting possibility that the molecular clock operates in many other tissues with tissue-specific time periods, controlling the formation of various morphological units. Since time control is essential to coordinate cells during all developmental processes in multicellular organisms, it is conceivable that this molecular behaviour is widespread, but only detectable when synchrony is maintained between adjacent cells.

The main findings of the present thesis are presented:

- The somitogenesis molecular clock components, *hairy1* and *hairy2* are expressed during forelimb development.
- *hairy2* is dynamically expressed in cartilage precursor cells during the laying down of limb skeletal elements, ceasing its expression in the differentiating chondrogenic cells.
- *hairy2* expression cycles with a 6 hour periodicity in the distal limb region (containing autopod chondrogenic precursor cells), at stages HH24, HH25 and HH26.
- The forelimb second phalanx takes 12 hours to be formed, suggesting that an autopod limb skeletal element is formed by cells with “n” and “n+1” *hairy2* expression cycles.
- The expression of *mkp3*, a downstream effector of FGF8 seems to mimic the PSM FGF8 behaviour during limb bud development.

## *Conclusions and Future Perspectives*

---

- Similarly to what occurs during somitogenesis, sustained FGF8 activity in cells that are normally escaping its influence could make them unable to integrate the forming element, leading to smaller elements.
- FGF8 activity positively regulates *hairy2* expression in the distal limb mesenchyme.

### ***FUTURE PERSPECTIVES***

Until now, little is known about how limb bud cells acquired positional information along the P-D axis. The work performed in this thesis brings new insights to this field of study, with the discovery that a molecular clock is operating during limb bud development in autopod chondrogenic cells. The autopod precursor cells perform cycles of 6 hours that are related with the formation of an autopod limb element.

This work unveils a new mechanism during limb bud development. In fact, the studies performed in this thesis open a completely novel line of investigation in the limb bud development field that could be further extrapolated to several developmental processes. However, much more work has to be performed until the machinery of this limb clock is completely understood.

Additional questions that should be addressed in future studies are:

- In the somitogenesis process *hairy1* was the first gene found to have a cyclic behaviour in PSM cells. After that, other genes have been identified presenting the same behaviour during the somitogenesis process. In limb bud it would be very interesting to observe if other genes, for example *hairy1*, have a cyclic expression pattern during limb bud development in a reminiscent way to *hairy2*.
- Since *hairy1* and *hairy2* genes in the somitogenesis process are inhibiting each other, it would be very interesting understand the interactions between *hairy1* and *hairy2* during limb bud development. Studies of *hairy2* gain- and loss-of-function using the retrovirus and adenovirus system can be performed in limb bud to evaluate the expression of *hairy1* and vice-versa.
- Another attractive point to be addressed in future work is the evaluation of limb bud phenotypes obtained in studies of *hairy1/hairy2* gain- and loss-of-function performed by retrovirus and adenovirus technology.

- The work performed in this PhD thesis shows that *mkp3* gene under influence of FGF8 is expressed as a gradient in the distal limb mesenchyme and has a similar behaviour to that of *fgf8* in PSM. However, another interesting experiment that could be performed to address this question is the study of the MKP3 protein distribution, to observe whether it shows the same distribution as *mkp3* mRNA. Since during limb bud development the RA and FGF have opposing effects it would be very interesting to observe the consequence of placing RA-soaked beads in the distal limb mesenchyme. By performing this experiment it will be possible to analyse the size of the forming structures and the RA effect in *mkp3* expression pattern and *hair2* expression pattern and oscillation period.
- We also demonstrated in this thesis that FGF8 treatment shortens the size of the forelimb. However, we have not examined how *hair2* oscillations are affected by FGF8 treatment. Is reduction of the limb size due to a shorter period of *hair2* oscillation? The existence of a correlation between limb size and the period of *hair2* oscillation would be a very good question to address. It would be also very interesting to see whether treatment with SU5402 (FGF inhibitor) would cause the opposite effect on both limb size and *hair2* oscillation period.
- Since the *hair2* genes are intimately related to the Notch signalling pathway, another attractive experiment that could be addressed is the inhibition of Notch signalling using DAPT and assess for effects on *hair2* expression and limb phenotypes.
- Another important line to be addressed is to observe if the homologues of these genes in other experimental animal models have the same behaviour during the formation of the appendages.

---

## *CHAPTER VI*

### *Papers*



**A molecular clock operates during proximal-distal limb outgrowth in  
the chick embryo**

Susana Pascoal, Cláudia R. Carvalho, Joaquín Rodríguez-León, Marie Claire Delphini,  
Delphine Duprez, Sólveig Thorsteinsdóttir and Isabel Palmeirim

*Development*

(Manuscript under revision)





## RESEARCH REPORT

A molecular clock operates during proximal-distal limb outgrowth in the chick embryo

Susana Pascoal<sup>1</sup>, Cláudia R. Carvalho<sup>2,5</sup>, Joaquín Rodríguez-León<sup>2,6</sup>, Marie Claire Delphini<sup>3</sup>, Delphine Duprez<sup>3</sup>, Sólveig Thorsteinsdóttir<sup>2,4</sup> and Isabel Palmeirim<sup>1‡</sup>

<sup>1</sup> Life and Health Sciences Research Institute (ICVS), School of Health Sciences, University of Minho, 4710-057 Braga, Portugal

<sup>2</sup> Instituto Gulbenkian de Ciência, R. Quinta Grande 6, 2780-156 Oeiras, Portugal.

<sup>3</sup> CNRS, UMR 7622, Biologie du développement, Université Pierre et Marie Curie, Campus de Jussieu, 9 quai Saint Bernard, Bâtiment C, 6ème Etage, Case 24, 75252 Paris Cedex 05 - France.

<sup>4</sup> Departamento de Biologia Animal, Centro de Biologia Ambiental, Faculdade de Ciências, Universidade de Lisboa, 1740-016 Lisboa, Portugal

<sup>5</sup> Present address: Departamento de Morfologia, ICB, Universidade Federal de Minas Gerais, 31270-901, Belo Horizonte, MG, Brazil.

<sup>6</sup> Present address: Center of Regenerative Medicine in Barcelona, Dr. Aiguader 80, 08003 Barcelona. Spain.

‡ Author for correspondence:

E-mail address: ipalmeirim@ecsaude.uminho.pt

Phone: +351 253 604865

Fax: +351 253 604831

Short title: The molecular clock and limb outgrowth

Key words: *hairy2* / Molecular clock / Limb development / Cycling genes / Vertebrate embryo

Total words count: 2905 words

## SUMMARY

Temporal control can be considered the fourth dimension in embryonic development. The identification of the somitogenesis molecular clock brought new insight into how embryonic cells measure time. We provide the first evidence for a molecular clock operating during limb outgrowth and patterning, by showing that the expression of the somitogenesis clock component *hairy2* cycles in limb chondrogenic precursor cells with a 6 hour periodicity. We determined the time period required to form an autopod skeletal limb element and propose that an autopod limb skeletal element is formed by cells with “n” and “n+1” *hairy2* expression cycles. We suggest that temporal control exerted by cyclic gene expression can be a widespread mechanism providing cellular temporal information during vertebrate embryonic development.

## INTRODUCTION

Embryo limb development requires precise orchestration of cell proliferation and differentiation in time and space (Tickle, 2004). Limb skeletal elements are laid-down as cartilaginous primordia in a proximal-distal (p-d) sequence. Chick wing elements are laid-down with the same size and grow differentially (Wolpert et al., 1975). Two models seek to explain cell fate specification along the p-d limb axis. Although fundamentally different, both models imply the existence of a limb bud distal zone where cells reside until they reach the time to differentiate-Progress Zone (PZ) Model (Summerbell et al., 1973) or to expand-Early Specification Model (Dudley et al., 2002; Sun et al., 2002). However, how these cells measure time remains unknown.

Time control during embryo development is particularly evident during somitogenesis. Chick presomitic cells were shown to undergo several cycles of *hairy1* gene expression, providing molecular evidence for the existence of a molecular clock underlying the rhythm of somitogenesis (Palmeirim et al., 1997). An increasing number of genes have been implicated in the molecular clock machinery (Pourquié, 2001; Freitas et al., 2005), namely *hairy2*, encoding a transcriptional repressor closely related to *hairy1* (Jouve et al., 2000). All studies regarding embryonic cyclic gene expression have focused on somitogenesis. Nevertheless, Hirata et al. (2002) showed that periodic expression of *Hes1* (mouse *hairy2*

homologue) can be triggered in a variety of cultured cell lines. This led us to postulate that a molecular clock could play a role in the temporal control of other embryonic structure formation.

## **MATERIALS AND METHODS**

### **Eggs and embryos**

Fertilized chick (*Gallus gallus*) eggs were incubated at 37.2°C in a 49% humidified atmosphere and staged according to the Hamburger and Hamilton (HH) classification (1951).

### **RNA probes and in situ hybridization**

RNA probes were prepared as described: *hairy2* (Jouve et al., 2000), *gdf5* (Francis-West et al., 1999) and *MyoD* (Pourquié et al., 1996). Whole-mount and tissue sections in situ hybridization were performed according to Henrique et al. (1995) and Strahle et al. (1994), respectively.

### **In ovo manipulations**

*Formation time of the forelimb second phalanx:* Multiple batches of 90 fertilized eggs were incubated during 48 hours. A window was cut in the egg shell, Indian ink was injected into the subgerminal cavity and the vitelline membrane was pulled apart using a tungsten microscalpel. The precise number of completely formed somites was registered, allowing us to order the embryos by their developmental age with a maximum error of 1.5 hours. All eggs were then sealed and re-incubated under the same conditions. After 110-116 hours of incubation (time necessary to reach digit formation stages), the wings of surviving embryos (n=180) were fixed and hybridized with a *gdf5* antisense RNA probe and the number of *gdf5*-positive digit stripes was recorded for each embryo (Fig. 3B, arrows). The number of stripes and the age of each embryo were compared within each batch.

*Time period of the hairy2 expression cycle:* A window was cut in the incubated eggs and the vitelline membrane was removed. With a microscalpel, the right wings of embryos at different developmental stages (stages HH24-26) were removed, washed in PBS and fixed immediately in 4% formaldehyde. The operated embryos were re-incubated for different time periods: 1.5 hours (n=23), 3 hours (n=37), 5.5

hours (n=33), 6 hours (n=38), 6.5 hours (n=30), 9 hours (n=39), 11.5 hours (n=26), 12 hours (n=71) and 12.5 hours (n=19), after which the left wing was removed and processed the same way. Both wings were hybridized simultaneously ensuring the same conditions.

All experimental embryos were photographed as whole-mounts in PBT with 0.1% azide, using a Sony DXC-390P-3CCD colour video camera.

## RESULTS AND DISCUSSION

We analyzed *hairy2* expression during forelimb development, from limb bud initiation to digit formation (Fig. 1). A closer analysis of our results showed that, although forelimbs of the same embryo always presented the same *hairy2* expression pattern, forelimbs of different embryos at the same stage of development, showed variable *hairy2* expression patterns in the distal mesenchyme (up to 400  $\mu\text{m}$  from the Apical Ectodermal Ridge-AER). Figure 2 shows representative patterns of *hairy2* expression in forelimb buds hybridized under precisely the same conditions. In some wings the distal domain under the AER was negative (Fig. 2A,D,G,J,M), while in others *hairy2* was strongly expressed in this same region (Fig. 2C,F,I,L,O). Various intermediate patterns could also be observed (Fig. 2B,E,H,K,N). This variability in *hairy2* expression patterns is clear from stages HH20 to HH28. The region showing variable *hairy2* expression is located between the limb central mesenchyme and the Zone of Polarizing Activity (ZPA) at stages HH20-22 (Fig. 2P), is displaced to a more anterior region becoming located between the central mesenchyme and the AER at stages HH23-26 (Fig. 2Q), and is restricted to the posterior part of the distal limb mesenchyme at stages HH27-28 (Fig. 2R). According to previous fate maps (Saunders, 1948; Vargesson et al., 1997), the displacement of the region presenting dynamic *hairy2* expression corresponds to the expansion and fanning out of the chondrogenic precursor cell population. After stage HH30 we could not ascertain whether the *hairy2* expression observed at digit tips corresponds to a dynamic expression pattern or to the progressive appearance of interphalangeic joints (Fig. 1N). Before stage HH20 we were also unable to clearly identify variations in *hairy2* expression. As a control, limbs were hybridized with a *scleraxis* probe in parallel with the *hairy2* hybridized limbs. No variations were observed among the different *scleraxis* hybridised limbs (data not shown). In conclusion, our data suggest

that from stages HH20 to HH28, *hairy2* is dynamically expressed in chondrogenic precursor cells during the laying down of limb skeletal elements, but stops being expressed in the differentiating chondrogenic cells.

If *hairy2* has a cyclic expression in chondrogenic precursors of the forelimb bud, we would expect the period of these cycles to be related with the time of limb skeletal element formation. Therefore, our first step towards identifying the period of *hairy2* expression cycles was to determine the formation time of a limb skeletal element.

The time between the formation of the proximal and distal joints of a skeletal element represents its formation time. The joint marker *gdf5* labels, as stripes, the formation of the second and the third autopod limb joints as well as the tip of the third phalanx (Francis-West et al., 1999). Since it has been suggested that the third phalanx is formed by a mechanism that differs from the formation of the other phalanxes (Sanz-Ezquerro and Tickle, 2003), we determined the formation time of the second phalanx. Batches of 90 eggs were incubated for 48 hours, opened and the number of somites counted. This allowed us to order the embryos by their developmental age with a maximum error of 1.5 hours. The embryos were then re-incubated under identical conditions and for the same time, until digit formation stages (Fig. 3A,B). After incubation, the embryonic limbs were fixed and analyzed using the digit joint marker *gdf5* (Francis-West et al., 1999). In some batches, the formation of both joints delimiting the second phalanx was observed. In all these cases (n=13), the period of time between the formation of the first and the second joint was longer than 10h30m and shorter than 13h30m, the average being 12 hours. In two cases, this time period was exactly 12 hours (Fig. 3B, arrows). These results strongly suggest that the forelimb second phalanx takes 12 hours to be formed. Considering previous work that suggested that each of the seven limb element primordia requires the same time to be laid down (Wolpert et al., 1975), the formation of the entire set of seven limb elements would take 3.5 days. In fact, this is in accordance with the time required to form a chick forelimb (3-4 days; Hamburger and Hamilton, 1951).

To determine if *hairy2* expression cycles with a time-period correlating with digit skeletal element formation, embryo right wings were surgically removed, fixed and each embryo was re-incubated for various lengths of time (Fig. 3C). Limb pairs were processed together for *hairy2* in situ hybridization.

This study was performed at stages HH24-26, while the autopod chondrogenic precursor cells are located in the limb distal mesenchyme (Summerbell, 1974). The percentage of wing pairs (incubated/non-incubated) presenting the same expression pattern was determined for each incubation period (Fig. 3C). For every developmental stage, the resulting graph reveals a clear peak at 12 hours of incubation, the autopod element formation time. Interestingly, there is also an equally clear peak after 6 hours. This experiment demonstrates that at stages HH24-26, *hairy2* expression in autopod chondrogenic precursor cells cycles with a 6 hour periodicity. In order to determine the time spent in each phase of the *hairy2* cycle, we analyzed the *hairy2* expression pattern in the limb distal mesenchyme of a total of 383 embryos and found that 22% presented a completely negative pattern, 19% presented an intermediate pattern and 59% presented a positive pattern. Based on a cycle time of 6 hours, distal limb mesenchyme would present a negative pattern during approximately 1h20m, an intermediate pattern during 1h10m and a positive pattern during 3h30m.

During somitogenesis each PSM cell undergoes many 1,5h molecular clock gene expression cycles before becoming committed to incorporate a somite. One somite forms every time the molecular clock wave sweeps the PSM, but each cell “experiences” those waves many times. Similarly, we propose that limb distal mesenchyme cells perform several *hairy2* expression cycles before being incorporated into a limb skeletal element. Every 12 hours, a batch of cells forms a new limb element. This means that one limb skeletal element is formed by two sets of cells: one with “n” and another with “n+1” *hairy2* cycles. In fact, the bones that arise from somites (i.e. vertebrae) are formed by the sclerotomal cells from the posterior compartment of one somite and the anterior compartment of the immediately posterior somite. Thus, every vertebra is also formed by two sets of cells, with “n” and “n+1” molecular clock gene expression cycles (Fig. 4).

Although oscillatory expression of several genes has been described in presomitic cells and its functional relevance for vertebrate segmentation investigated, the function of the molecular clock during somitogenesis is still unclear (Freitas et al., 2005; Rida et al., 2004). Here, we report cyclic *hairy2* expression in autopod chondrogenic precursor cells and propose that these cells perform *hairy2* expression cycles while undifferentiated, ceasing this cyclic behaviour when they start the chondrogenic

differentiation program, in a reminiscent way of what has been previously described during somitogenesis.

The PZ model postulates that PZ cells acquire p-d positional information progressively and that they must display synchronized oscillations related to the periodic transcription of some gene (Summerbell et al., 1973; Kerszberg and Wolpert, 2000; Tickle and Wolpert, 2002). The early specification model suggests that p-d segment formation results from a temporally regulated expansion of the already specified progenitor populations (Dudley et al., 2002). Based on our results, we propose that cells in the distal limb region register the number of *hairy2* oscillations they undergo while in this region. This provides them a temporal value that could either be translated into positional value (according to the PZ model) or it would determine the time-point of expansion (proposed by the early specification model). Our proposal that *hairy2* cyclic expression provides temporal information does not allow us to discriminate between these two models, but unveils the first molecular evidence for the existence of a molecular clock operating in these cells.

*Hairy2* is a downstream target of the Notch signalling pathway. Data compatible with a role for the Notch signalling pathway in the development of the forelimb distal mesenchyme has been provided: (1) in the chick, *notch1* and *hairy1* are expressed in the limb distal mesenchyme (Vargesson et al., 1998; Vasiliasuskas et al., 2003; our unpublished data); (2) *hairy1* misexpression implicate the Notch signalling pathway in the regulation of the chick limb size (Vasiliasuskas et al., 2003); (3) in the mouse, *serrate1/jagged1* and *hes1* are expressed in the distal limb mesenchyme (Francis et al., 2005; McGlinn et al., 2005). *Hes1*-, *serrate1/jagged1*-null mouse embryos die during embryogenesis and no studies on limb formation have been reported; (4) *presenilin* mutant embryos have clinched forelimb digits and lack some distal phalanxes (Pan et al., 2005). This corresponds to a phenotype that we would expect by perturbing the limb molecular clock.

In summary, we show for the first time that a molecular clock is working during p-d limb outgrowth, and that the periodicity of this clock correlates with the formation time of an autopod limb element. Accordingly, this work demonstrates that temporal control exerted by cyclic gene expression is not an exclusive property of the somitogenesis process, as previously thought. This leads us to the

exciting possibility that a molecular clock can be operating in many embryonic tissues with tissue-specific time periods, controlling the formation of various morphological units. Since time control is essential to coordinate cells during all developmental processes in multicellular organisms, it is conceivable that this molecular behaviour is widespread, but only detectable when synchrony is maintained between adjacent cells.

## REFERENCES

**Dudley, A.T., Ros, M.A. and Tabin, C.J.** (2002). A re-examination of proximodistal patterning during vertebrate limb development. *Nature* **418**, 539-544.

**Francis, J.C., Radtke, F. and Logan, M.P.** (2005). Notch1 signals through Jagged2 to regulate apoptosis in the apical ectodermal ridge of the developing limb bud. *Dev Dyn* **234**, 1006-1015.

**Francis-West, P.H., Abdelfattah, A., Chen, P., Allen, C., Parish, J., Ladher, R., Allen, S., MacPherson, S., Luyten, F.P. and Archer, C.W.** (1999). Mechanisms of GDF-5 action during skeletal development. *Development* **126**, 1305-1315.

**Freitas, C., Rodrigues, S., Saúde, L. and Palmeirim, I.** (2005). Running after the clock. *Int J Dev Biol* **49**: 317-324.

**Hamburguer, V. and Hamilton, H.L.** (1951). A series of normal stages in the development of the chick embryo. *J Morphol* **88**, 49-92.

**Henrique, D., Adam, J., Myat, A., Chitnis, A., Lewis, J. and Ish-Horowicz, D.** (1995). Expression of a Delta homologue in prospective neurons in the chick. *Nature* **375**, 787-790.

**Hirata, H., Yoshiura, S., Ohtsuka, T., Bessho, Y., Harada, T., Yoshikawa, K. and Kageyama, R.** (2002). Oscillatory expression of the bHLH factor Hes1 regulated by a negative feedback loop. *Science* **298**, 840-843.

**Jouve, C., Palmeirim, I., Henrique, D., Beckers, J., Gossler, A., Ish-Horowicz, D. and Pourquie O.** (2000). Notch signalling is required for cyclic expression of the hairy-like gene HES1 in the presomitic mesoderm. *Development* **127**, 1421-1429.



- Kerszberg, M. and Wolpert, L.** (2000). A clock and trail model for somite formation, specialization and polarization. *J Theor Biol* **205**, 505-510.
- McGlinn, E., van Bueren, K.L., Fiorenza, S., Mo, R., Poh, A.M., Forrest, A., Soares, M.B., Bonaldo, Mde F., Grimmond, S., et al.** (2005). Pax9 and Jagged1 act downstream of Gli3 in vertebrate limb development. *Mech Dev* **122**, 1218-1233.
- Palmeirim, I., Henrique, D., Ish-Horowicz, D. and Pourquie, O.** (1997). Avian hairy gene expression identifies a molecular clock linked to vertebrate segmentation and somitogenesis. *Cell* **91**, 639-648.
- Pan, Y., Liu, Z., Shen, J. and Kopan, R.** (2005). Notch1 and 2 cooperate in limb ectoderm to receive an early Jagged2 signal regulating interdigital apoptosis. *Dev Biol* **286**, 472-482.
- Pourquie, O., Fan, C.M., Coltey, M., Hirsinger, E., Watanabe, Y., Breant, C., Francis-West, P., Brickell, P., Tessier-Lavigne, M. and Le Douarin, N.M.** (1996). Lateral and axial signals involved in avian somite patterning: a role for BMP4. *Cell* **84**, 461-471.
- Pourquie, O.** (2001). Vertebrate somitogenesis. *Annu Rev Cell Dev Biol* **17**, 311-350.
- Rida, P.C., Le Minh, N. and Jiang, Y.J.** (2004). A Notch feeling of somite segmentation and beyond. *Dev Biol* **265**, 2-22.
- Sanz-Ezquerro, J.J. and Tickle, C.** (2003). Fgf signaling controls the number of phalanges and tip formation in developing digits. *Curr Biol* **13**, 1830-1836.
- Saunders, J.W.** (1948). The proximo-distal sequence of the origin of the parts of the chick wing and the role of the ectoderm. *J Exp Zool* **108**, 363-403.
- Strahle, U., Blader, P., Adam, J. and Ingham, P.W.** (1994). A simple and efficient procedure for non-isotopic in situ hybridization to sectioned material. *Trends Genet* **10**, 75-76.
- Summerbell, D., Lewis, J.H. and Wolpert, L.** (1973). Positional information in chick limb morphogenesis. *Nature* **244**, 492-496.
- Summerbell, D.** (1974). A quantitative analysis of the effect of excision of the AER from the chick limb-bud. *J Embryol Exp Morphol* **32**, 651-660.
- Sun, X., Mariani, F.V. and Martin, G.R.** (2002). Functions of FGF signalling from the apical ectodermal ridge in limb development. *Nature* **418**, 501-508.

- Tickle, C. and Wolpert, L.** (2002). The progress zone -- alive or dead? *Nat Cell Biol* **4**, E216-217.
- Tickle, C.** (2004). The contribution of chicken embryology to the understanding of vertebrate limb development. *Mech Dev* **121**, 1019-1029.
- Vargesson, N., Clarke, J.D., Vincent, K., Coles, C., Wolpert, L. and Tickle, C.** (1997). Cell fate in the chick limb bud and relationship to gene expression. *Development* **124**, 1909-1918.
- Vargesson, N., Patel, K., Lewis, J. and Tickle, C.** (1998). Expression patterns of Notch1, Serrate1, Serrate2 and Delta1 in tissues of the developing chick limb. *Mech Dev* **77**, 197-199.
- Vasiliauskas, D., Laufer, E. and Stern, C.D.** (2003). A role for hairy1 in regulating chick limb bud growth. *Dev Biol* **262**, 94-106.
- Wolpert, L., Lewis, J. and Summerbell, D.** (1975). Morphogenesis of the vertebrate limb. *Ciba Found Symp*, 95-130.

## **ACKNOWLEDGEMENTS**

We thank Raquel Andrade, Fernanda Bajanca, Leonor Saúde and Fernando Rodrigues for fruitful discussions and Mónica Ferreira for technical support. Financial support was provided by FCT/FEDER (POCTI/BCI/42040/2001), the EU/FP6-Network of Excellence-Cells into Organs, ICVS and by IGC. S.P. (SFRH/BD/8657/2002) and J.R-L. (SFRH/BPD/5511/2001) were supported by FCT. C.R.C. was supported by Calouste Gulbenkian Foundation.

## FIGURE LEGENDS

### Figure 1 – *Hairy2* expression pattern during forelimb development.

(A) *Hairy2* transcripts are first detected at stage HH14 in the presumptive forelimb region (bracket). (B,C) At stages HH16 and HH17, *hairy2* transcripts are uniformly expressed within the early wing bud. From stage HH18 onwards, *hairy2* expression becomes localized to distinct expression domains: (1) *hairy2* transcripts are detected in the AER from its formation at stage HH18 until its progressive disappearance at stage HH32 (D-N; black arrow in G); (2) from stages HH18 to HH28, *hairy2* is expressed in a posterior limb bud area including the ZPA (C-H and J-L; white arrow in G); (3) along all these stages, *hairy2* transcripts are also present in dorsal and ventral mesenchymal domains containing the limb muscles precursors cells as visualised by *MyoD* expression (G,I, asterisks). *Hairy2* expression was never found in the limb core, the region that contains the differentiating chondrogenic cells (I, empty rectangle); (4) *hairy2* expression is observed in the forming digits joints (N); and (5) in some embryos *hairy2* transcripts are found in the distal limb mesenchyme (H,J; black arrows) while others lack this expression domain (Figure 2). All pictures show a dorsal view.

### Figure 2 – Dynamic *hairy2* expression in the distal limb mesenchyme.

Representative *hairy2* expression patterns at stages HH20 (A-C), HH24 (D-F), HH25 (G-I), HH26 (J-L) and HH28 (M-O) illustrate the variations in *hairy2* expression observed in the forelimb distal mesenchyme. (A,D,G,J,M) Hollow arrows point to the absence of *hairy2* expression in the distal limb mesenchyme. (C,F,I,L,O) Filled arrows point to *hairy2* expression in the distal limb mesenchyme. (B,E,H,K,N). Partially filled arrows indicate an intermediate pattern. Bottom: (P-R) Schematic representation of the region where *hairy2* is dynamically expressed (blue) from stages HH20 to HH28. All pictures show right wings' dorsal view.

**Figure 3 – Estimating the formation time of an autopod limb element and periodicity of *hairy2* cyclic expression along limb p-d axis.**

(A) Schematic representation of the strategy used to estimate the formation time of the second phalanx of forelimb digit 3. 48h-incubated embryos were temporally ordered according to their somite number. After re-incubation until all limb skeletal elements were formed, their wings were hybridized for the joint marker *gdf-5*. (B) *Gdf5* expression pattern in forelimbs of embryos A-D (arrows indicate the *gdf5*-positive digit stripes). In batches where the onset of formation of both joints delimiting the second phalanx was caught, the developmental time of the corresponding embryos differed by 12 hours. (C) Comparison of the p-d *hairy2* expression pattern between two wings of the same embryo in which the right wing was surgically removed and immediately fixed while the left wing was re-incubated (in ovo) for different time periods. Both wings were hybridized in the same tube, ensuring the same conditions. The *hairy2* expression pattern in the left wing was either different (i and iii) or similar (ii and iv) to that in the right wing. The graphs (stages HH24, HH25 and HH26) show the percentage of wing pairs with the same *hairy2* expression pattern for each incubation time. Two clearly distinguishable peaks are observable, one at 6 hours and the other at 12 hours. Hollow and filled arrows point to the absence or the presence of *hairy2* expression in the distal limb mesenchyme, respectively. All pictures show a dorsal view.

**Figure 4 - Comparative model of the number of molecular clock gene expression cycles underlying the formation of trunk and limb skeletal segments.**

(A) Schematic representation of the process of somite re-segmentation that underlies vertebrae formation, showing that each vertebra is composed of cells that previously underwent “n” and “n+1” molecular clock gene expression cycles. (B) Schematic representation of the process of limb formation proposing that each limb bone is composed of cells that previously underwent “n” and “n+1” molecular clock gene expression cycles.

Fig.1

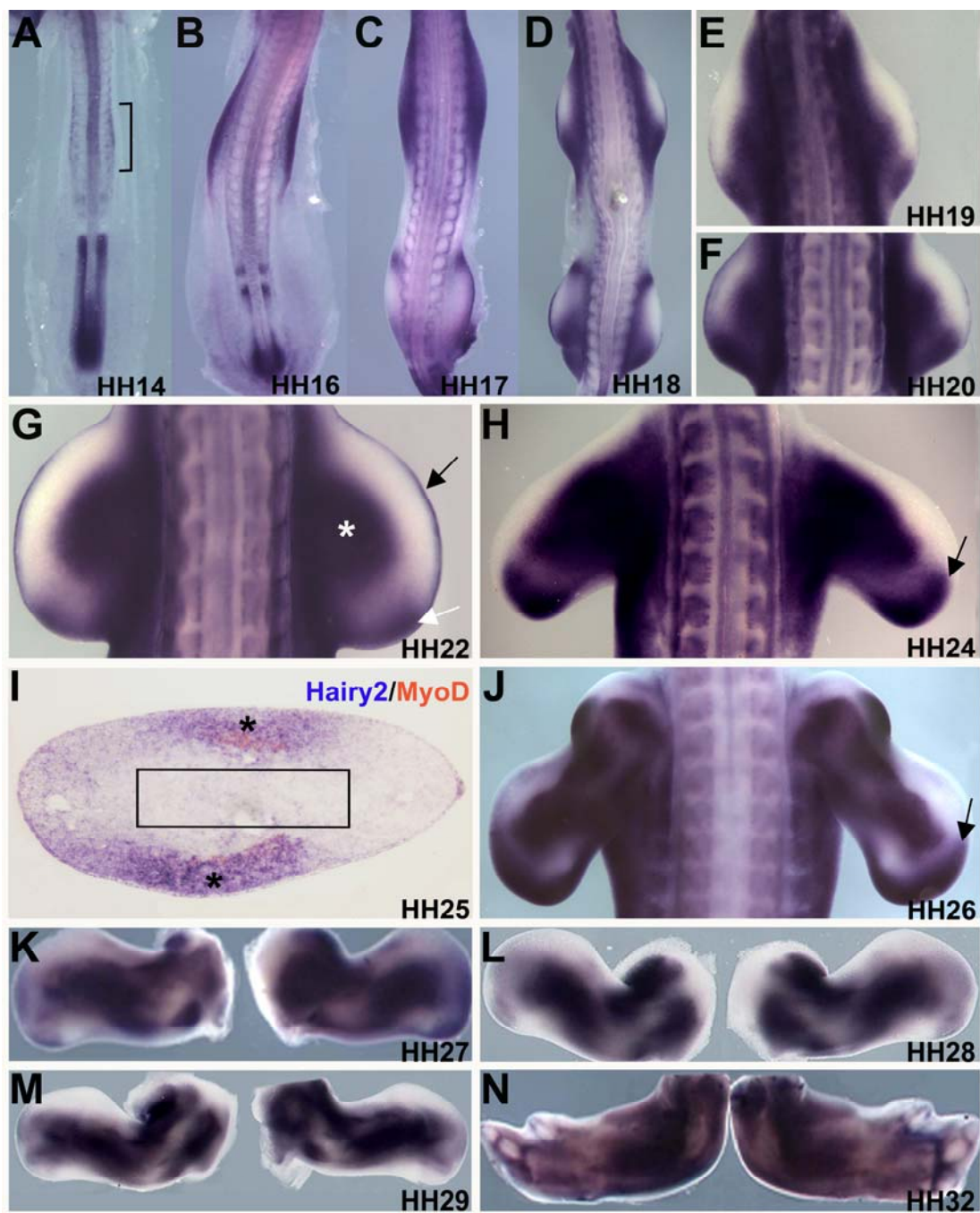


**Fig. 2**

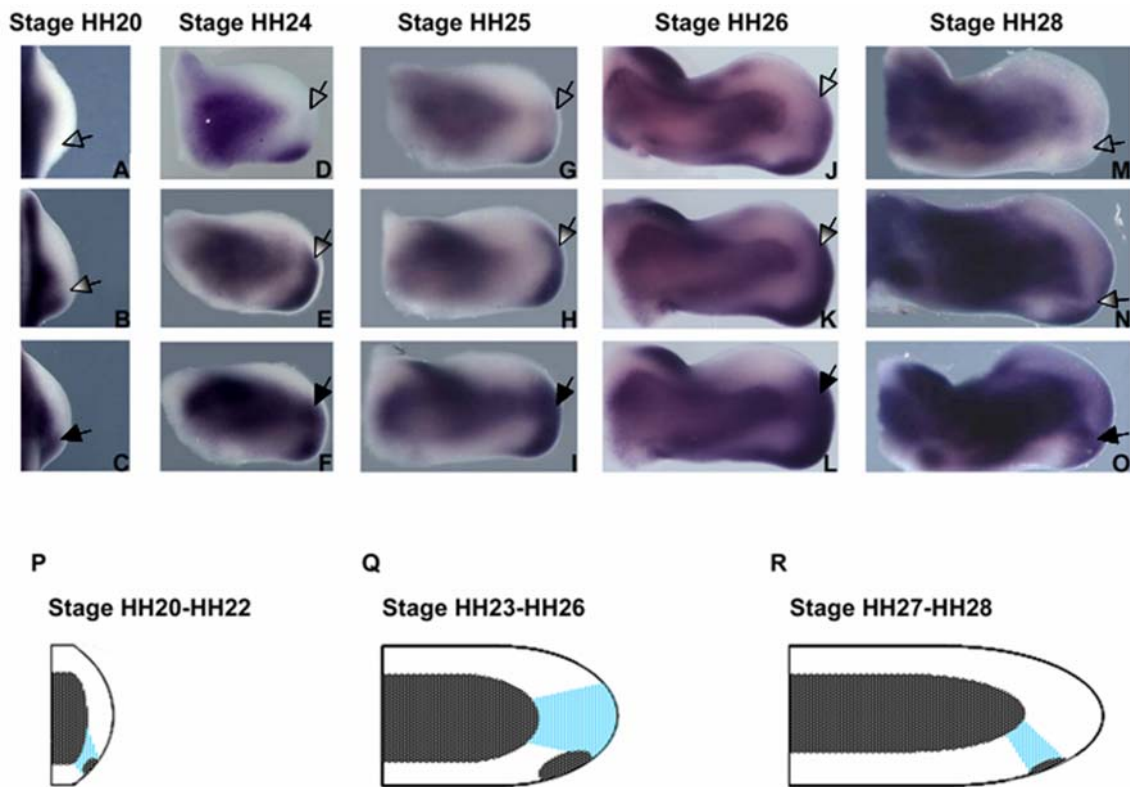


**Fig. 3**

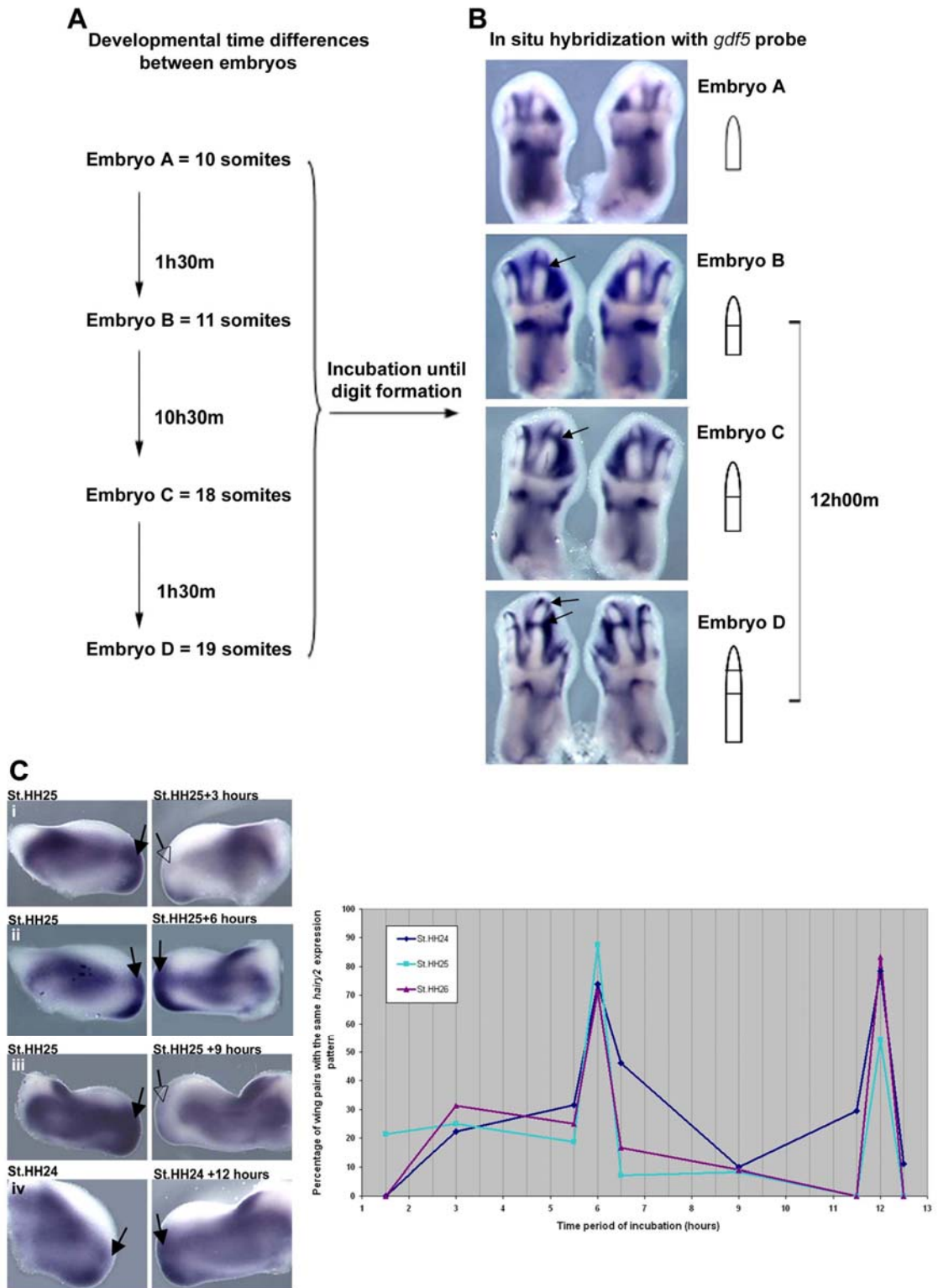
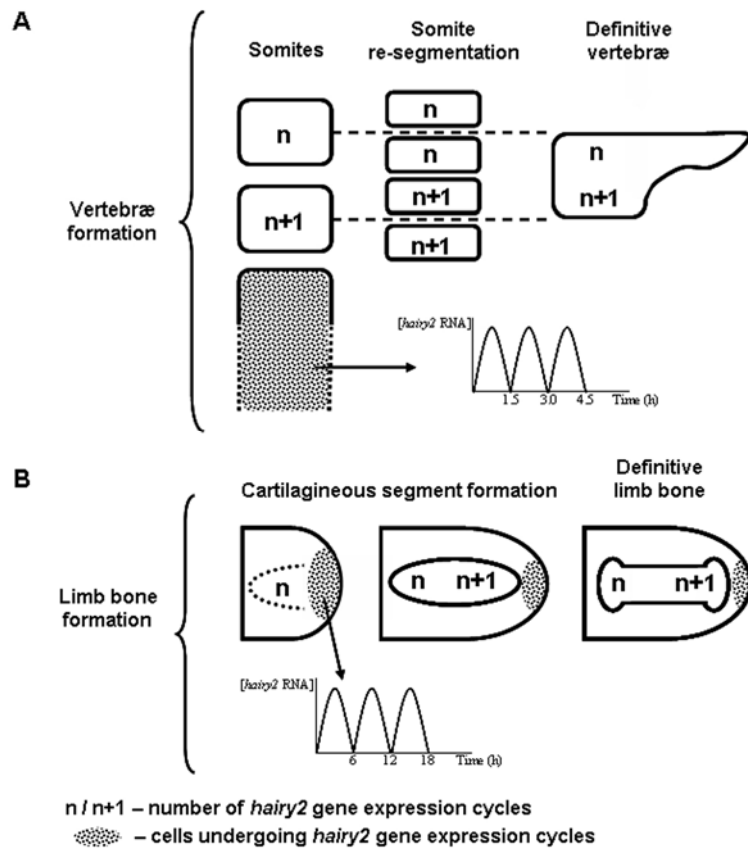


**Fig. 4**





**Progressive mRNA decay establishes an *mkp3* expression gradient in  
the chick limb bud**

Susana Pascoal, Raquel P. Andrade, Fernanda Bajanca and Isabel Palmeirim

*Biochemical and Biophysical Research Communications (BBRC), in press*



**Progressive mRNA decay establishes an *mkp3* expression gradient in the chick limb bud**

Susana Pascoal, Raquel P. Andrade, Fernanda Bajanca, Isabel Palmeirim‡

Life and Health Sciences Research Institute (ICVS), School of Health Sciences, University of Minho, 4710-057 Braga, Portugal

‡Author for correspondence:

E-mail address: ipalmeirim@ecsaude.uminho.pt

Phone: +351 253 604865

Fax: +351 253 604831

## ABSTRACT

The apical ectodermal ridge (AER) controls limb outgrowth and patterning, such that its removal causes changes in mesodermal gene expression, cell death and limb truncation. Fibroblast Growth Factor (FGF) family members are expressed in the AER and can rescue limb bud outgrowth after AER removal. Cells localized underneath the AER are maintained in an undifferentiated state by the FGFs produced by the AER. *MAPK phosphatase 3* (*mkp3*) is a downstream effector of FGF8 signalling during limb bud development and is expressed in the distal limb mesenchyme. The present work evidences a gradient of *mkp3* transcripts along the chick limb bud, in a distal to proximal direction. *mkp3* transcription occurs only in the most distal limb bud cells and its mRNA gradient throughout the limb results from progressive mRNA decay. We show that FGF8-soaked beads induce ectopic *mkp3* expression, indicating that AER-derived FGF8 protein may activate *mkp3* in the distal mesenchyme. Keywords: FGF8; *mkp3*; mRNA decay; mRNA gradient; limb bud distal mesenchyme; chick embryo development

## INTRODUCTION

Initiation of limb bud development occurs at defined positions in the flank of the embryo through differential cell proliferation of mesenchymal cells of two embryonic origins, lateral plate and somitic mesoderm. Fibroblast Growth Factors (FGFs) are essential during embryonic development namely, for the regulation of cellular proliferation and differentiation [1].

Intracellular responses to FGFs are mediated by several signal transduction cascades, including the MAPK and the phosphatidylinositol-3-OH kinase (PI(3)K)/Akt pathways [2]. The *MAPK phosphatase 3 (mkp3)* encodes a dual-specificity phosphatase, known to be a negative regulator of the MAPK/ERK pathway [3, 4, 5, 6]. Kawakami and colleagues (2003) found that *mkp3* is a downstream effector of the FGF8 signalling pathway during limb development, and that its induction is mediated through the PI(3)K pathway [7]. Thus, *mkp3* mediates the cellular response to FGF8 signalling in the vertebrate limb [7].

The growing limb mesenchyme is surrounded by ectoderm, whose distal tip forms a specialized epithelial structure, the apical ectodermal ridge (AER) [8]. AER removal leads to limb truncation, evidencing that the AER is responsible for proximaldistal (p-d) limb outgrowth and its activity keeps the subjacent mesoderm in an undifferentiated state [8, 9]. Several members of the FGF family, *fgf2*, *fgf4* and *fgf8* are expressed in the chick AER and rescue limb outgrowth and patterning following ridge removal [10, 11, 12].

FGFs are diffusible proteins whose signals are mediated by a group of four transmembrane proteins with intrinsic tyrosine kinase activity, known as FGF receptors (FGFRs) [13, 14]. FGFRs are expressed in a variety of tissues and organs throughout vertebrate development with a distinct expression pattern for each receptor. FGFR1, 2 and 3 exist in two alternative splice variants: IIIb and IIIc. FGF4 and FGF8 are produced by the limb epithelium AER

and preferentially bind to the IIIc isoforms [15], which are expressed in the mesenchyme [16, 17, 18].

In this work, we show that FGF8 protein produced in the AER induces the expression of its downstream effector *mkp3* in the distal limb mesenchyme. *mkp3* presents an expression gradient in the limb mesenchyme and we show that this gradient results from the decay of mRNA transcribed by the distal limb bud progenitors.

## **MATERIALS AND METHODS**

### **Eggs and embryos**

Fertilised chick (*Gallus gallus*) eggs obtained from commercial sources were incubated at 37.2°C in a 49% humidified atmosphere and staged according to the Hamburger and Hamilton (HH) classification [19].

### **RNA probes**

Antisense digoxigenin-labelled RNA probes *mkp3* [7] was prepared as previously described.

An intronic *mkp3 in situ* hybridisation probe was generated. Reverse transcription and polymerase chain reactions (RT-PCR) were used to isolate the fourth chick *mkp3* intron, using the sense oligo 5'-AGCAGAACCCCCATTCCCTTCT-3' and the antisense oligo 5'-CCAGCATGGAAATCCTGCA-3'. The DNA fragment generated was cloned into the pCR®II-TOPO® vector (Invitrogen) and plasmid DNA was isolated. Antisense *mkp3* intronic RNA probe was produced using standard procedures.

### **RNA extraction and reverse transcription**

Limb buds at stage HH24 were dissected into three portions of equivalent size along the p-d axis. Total mRNA was extracted from 5 distinct batches of each portion of the limb using the RNeasy Mini Kit Protect (Qiagen, Germany). Total mRNA quantification was done by spectrophotometry (NanoDrop Technologies, Inc., USA). Total RNA was digested with DNase RNase-Free (Promega, USA) according to manufacturer's instructions.

### **Quantitative real-time RT-PCR**

Quantitative real-time RT-PCR was performed as previously described [20]. Primer design was based on available sequences in *GenBank* (NCBI-NLM-PubMed- Gene). The following intron-spanning primers were used, sense and antisense, respectively: MKP3 5'-ATCTCTTTCATAGATGAAGCGCGG-3' and 5'-TGAGCTTCTGCATGAGGTAGGC-3'; FGF8 5'-CTGATCGGCAAGAGTAACGGC-3' and 5'-CCATGTACCAGCCCTCGTACTTG-3'; RALDH2 5'-CAAGGAGGAGATTTTTGGGCCTGTTC-3' and 5'-GGCCTTGTTTATGTCATTTGTAAAGACAGC-3'; the primers used for the reference gene 18S Ribosomal RNA were: 5'-TGCTCTTAACTGAGTGTCCTCCGC-3' and 5'-CCCGTTTCCGAAAACCAACAA-3'. Primer sets standard amplification curves were made for MKP3, FGF8, RALDH2 and 18S Ribosomal RNA with cDNA samples from chick limb buds at stage HH24, setting  $r=0.99$ . In all the samples, gene expression was normalized for 18S Ribosomal RNA and for limb region 1 values.

### **Statistical Analysis**

All quantitative data are presented as mean  $\pm$  SEM. Statistical analysis was performed by one-way ANOVA on ranks and the Student-Newman-Keuls test was used for post-test analysis. Statistical significance was set at  $p < 0.05$ .

### **Whole-mount *in situ* hybridization**

Embryos and limb buds were collected from stage HH24 and fixed overnight at 4°C in fresh 4% formaldehyde 2mM EGTA in phosphate-buffered saline (PBS), rinsed in PBT (PBS, 0.1% Tween 20), dehydrated through a methanol series and stored in 100% methanol at -20°C. Whole-mount *in situ* hybridization was performed according to the previously described procedure [21].

### **Immunohistochemistry (IHC)**

Forelimb buds were collected from stage HH25 chick embryos and immediately fixed in 4% paraformaldehyde in 0.1 M phosphate buffer (PB) with 0.12 mM CaCl<sub>2</sub> and 4% sucrose overnight at 4°C, washed in buffer only, and then in PB with 15% sucrose, both overnight at 4°C. Embryos were then incubated in PB with 15% sucrose and 7.5% gelatin for 1 hr at 30°C, immediately frozen in liquid nitrogen chilled isopentane, and stored at -80°C until sectioned. Approximately 10- $\mu$ m-thick serial sections were collected on Super Frost slides, and blocked for 30 min with 10% normal goat serum in PBS containing 1% bovine serum albumin. The primary anti-FGF8 antibody (KM1334 from BioWa, Inc.; [22, 23]) was diluted at 1:500 in the blocking solution and incubated overnight at 4°C, followed by washing in PBS, and detected with Alexa Fluor 488-conjugated anti-rabbit IgG, all F(ab')<sub>2</sub> fragments (Molecular Probes) diluted 1:1000 in blocking solution, followed by



PBS washes. Slides were stained with 4',6-Diamidino-2-phenylindole (DAPI, Sigma), mounted in Vectashield (Vector Laboratories) and sealed after cover-slipping.

### **Bead implants**

A window was cut in fertilised eggs and the vitelline membrane was removed. Heparin acrylic beads (Sigma) soaked in FGF8 protein at 1 mg/ml (R&D Systems) or PBS were microsurgically implanted in the proximal limit of the zone of *mkp3* expression in the right limb buds of stage HH24 embryos. The embryos (n=12) were incubated for 4 hours and hybridized with *mkp3* probe. The same experiment was performed using AG1-X2 ion exchange beads (Biorad) incubated in 4 mg/ml SU5402 (a drug known to specifically block the kinase activity of FGF receptors) (Calbiochem) or in DMSO (n=6).

### **Imaging**

Embryos processed for *in situ* hybridization were photographed in PBT/0.1% azide, using a Sony DXC-390P-3CCD colour video camera coupled to a Leica MZFLIII microscope. Embryos processed for IHC were photographed using an Olympus DP70 camera coupled to an Olympus BX61 microscope with epifluorescence. Images were treated in Adobe Photoshop CS.

## RESULTS AND DISCUSSION

We performed *mkp3 in situ* hybridization studies in chick limb buds and observed that *mkp3* shows a graded distribution of its transcripts throughout the limb mesenchyme (Figure 1). *mkp3* expression is stronger in the most distal part of the limb (underneath the AER), fading out in the direction of the more proximal part (Figure 1A). Real-time polymerase chain reaction (real-time RT-PCR) was performed to characterise the observed *mkp3* mRNA gradient in the limb bud. Limb buds at stage HH24 were dissected into three portions of equivalent size along the p-d axis (Figure 1A). Total mRNA was extracted from multiple batches of each portion of the limb (n=5) and *mkp3* mRNA content variation in the three regions was analysed by real-time RTPCR. This high-resolution analysis clearly demonstrates a gradient of *mkp3* transcripts in the limb bud, in a distal to proximal direction (Figure 1B).

Real-time RT-PCR experiments showed that *fgf8* is strongly expressed in the distal tip of the limb bud, and no transcripts can be significantly measured in the more proximal limb regions (Figure 1B). We could also observe an opposing gradient of *raldh2* expression, which presents higher transcript levels in the proximal limb region (Figure 1C). An antagonism between FGF and RA signalling pathways is thought to operate during the development of several structures (see e.g. [24, 25]). Namely, during somitogenesis, FGF8 and RA are mutually inhibitory [26]. In fact, it has been shown that FGFs promote limb distalization by counteracting the RA pathway. This happens through inhibition of the proximalizing RA signal required to maintain the Meis activity, providing a molecular basis for the role of RA in specifying proximal limb fates in different vertebrates [27].

To further characterise limb bud *mkp3* expression gradient, we constructed an intronic *in situ* hybridisation probe for *mkp3* (see Materials and Methods) that allows

the detection of *mkp3* nascent transcripts. Whereas *mkp3* expression detected by the exonic probe spans through a wide area of the limb mesenchyme (Figure 2A), cells recognized by the intronic probe were restricted to the most distal part of the limb, even after a long exposure time to developing solution (Figure 2B). These observations suggest that the *mkp3* mRNA gradient seen in the limb mesenchyme may not result from a gradient of active transcription, but from the progressive decay of the mRNA molecules produced by the distal limb progenitors.

Kawakami et al. (2003) proposed that *mkp3* is able to mediate cellular response to FGF8 signalling in the vertebrate limb by observing that FGF8-soaked beads can rescue the loss of *mkp3* expression resulting from AER removal [7]. As has been previously described, *fgf8* mRNA is expressed in the AER [28]. Moreover, we detected strong immunoreactivity for the FGF8 protein in the AER (Figure 3A, B). Thus, FGF8 produced at the AER is most likely capable of inducing *mkp3* expression in the closely located distal limb mesenchymal cells. To further address this issue, we placed FGF8-soaked beads in stage HH24 chick embryo right wings at the proximal end of the *mkp3* expression domain. After 4 hours of incubation, we observed ectopic *mkp3* expression extending proximally (Figure 4Aii). In order to validate our hypothesis, this experiment was repeated using SU5402-soaked beads, a drug known to specifically block the kinase activity of FGF receptors. As expected, SU5402 caused downregulation of *mkp3* expression (Figure 4Aiii).

The results obtained throughout this work lead us to propose the following model for *mkp3* expression pattern in the chick limb bud (schematized in Figure 4B): FGF8 protein produced in the AER induces *mkp3* gene transcription in the cells located immediately underneath, in the distal limb mesenchyme. As cell division and limb outgrowth proceeds, these cells are progressively displaced away from the FGF8 source. At a certain distance

from the AER, *mkp3* transcription is no longer induced, but *mkp3* mRNA molecules are still present in these cells and decay over time. This results in a spatial gradient of mRNA expression in the chick limb bud.

Our description of the *mkp3* expression gradient in the chick limb bud is reminiscent to the *fgf8* mRNA gradient present in the chick presomitic mesoderm. In fact, Dubrulle and Pourquié have shown a mechanism based on progressive RNA decay involved in the autonomous establishment of the caudal *fgf8* mRNA gradient [29]. Our work suggests for the first time that a similar process can be operating during limb bud development.

#### ***ACKNOWLEDGMENTS***

We wish to thank Cristina Nogueira-Silva for technical support in the real-time RT-PCR experiments and BioWa, Inc. for kindly providing the anti-FGF8 antibody. Financial support was provided by FCT/FEDER (POCTI/BCI/42040/2001) and by the EU/FP6-Network of Excellence-Cells into Organs. S.P. (SFRH/BD/8657/2002), R.P.A. (SFRH/BPD/9432/2002) and F.B. (SFRH/BPD/17368/2004) were supported by FCT, Portugal.

## REFERENCES

- [1] M. Goldfarb, Functions of fibroblast growth factors in vertebrate development, *Cytokine Growth Factor Rev.* 7 (1996) 311–325.
- [2] S. Javerzat, P. Auguste, A. Bikfalvi, The role of fibroblast growth factors in vascular development, *Trends Mol. Med.* 8 (2002) 483-489.
- [3] M. Muda, U. Boschert, R. Dickinson, J. C. Martinou, I. Martinou, M. Camps, W. Schlegel, S. Arkininstall, MKP-3, a novel cytosolic protein-tyrosine phosphatase that exemplifies a new class of mitogen-activated protein kinase phosphatase, *J. Biol. Chem.* 271 (1996) 4319-4326.
- [4] L. A. Groom, A. A. Sneddon, D. R. Alessi, S. Dowd, S. M. Keyse, Differential regulation of the MAP, SAP and RK/p38 kinases by Pyst1, a novel cytosolic dualspecificity phosphatase, *Embo J.* 15 (1996) 3621-3632.
- [5] R. J. Mourey, Q. C. Vega, J. S. Campbell, M. P. Wenderoth, S. D. Hauschka, E. G. Krebs, J. E. Dixon, A novel cytoplasmic dual specificity protein tyrosine phosphatase implicated in muscle and neuronal differentiation, *J. Biol. Chem.* 271 (1996) 3795- 3802.
- [6] A. Smith, C. Price, M. Cullen, M. Muda, A. King, B. Ozanne, S. Arkininstall, A. Ashworth, Chromosomal localization of three human dual specificity phosphatase genes (DUSP4, DUSP6, and DUSP7), *Genomics* 42 (1997) 524-527.

- [7] Y. Kawakami, J. Rodriguez-Leon, C. M. Koth, D. Buscher, T. Itoh, A. Raya, J. K. Ng, C. R. Esteban, S. Takahashi, D. Henrique, *et al*, MKP3 mediates the cellular response to FGF8 signalling in the vertebrate limb, *Nat. Cell Biol.* 5 (2003) 513-519.
- [8] J. Saunders, The proximo-distal sequence of the origin of the parts of the chick wing and the role of the ectoderm, *J. Exp. Zool.* 108 (1948) 363-403.
- [9] D. Summerbell, L. Wolpert, Precision of development in chick limb morphogenesis, *Nature* 244 (1973) 228-230.
- [10] J. F. Fallon, A. Lopez, M. A. Ros, M. P. Savage, B. B. Olwin, B. K. Simandl, FGF- 2: apical ectodermal ridge growth signal for chick limb development, *Science* 264 (1994) 104-107.
- [11] L. Niswander, C. Tickle, A. Vogel, I. Booth, G. R. Martin, FGF-4 replaces the apical ectodermal ridge and directs outgrowth and patterning of the limb, *Cell* 75 (1993) 579-587.
- [12] R. Mahmood, J. Bresnick, A. Hornbruch, C. Mahony, N. Morton, K. Colquhoun, P. Martin, A. Lumsden, C. Dickson, I. Mason, A role for FGF-8 in the initiation and maintenance of vertebrate limb bud outgrowth, *Curr. Biol.* 5 (1995) 797-806.
- [13] C. Basilico, D. Moscatelli, The FGF family of growth factors and oncogenes, *Adv. Cancer Res.* 59 (1992) 115-165.

- [14] D. E. Johnson, L. T. Williams, Structural and functional diversity in the FGF receptor multigene family, *Adv. Cancer Res.* 60 (1993) 1-41.
- [15] D. M. Ornitz, J. Xu, J. S. Colvin, D. G. McEwen, C. A. MacArthur, F. Coulier, G. Gao, M. Goldfarb, Receptor specificity of the fibroblast growth factor family, *J. Biol. Chem.* 271 (1996) 15292-15297.
- [16] P. W. Finch, G. R. Cunha, J. S. Rubin, J. Wong, D. Ron, Pattern of keratinocyte growth factor and keratinocyte growth factor receptor expression during mouse fetal development suggests a role in mediating morphogenetic mesenchymal-epithelial interactions, *Dev. Dyn.* 203 (1995) 223-240.
- [17] A. Orr-Urtreger, M. T. Bedford, T. Burakova, E. Arman, Y. Zimmer, A. Yayon, D. Givol, P. Lonai, Developmental localization of the splicing alternatives of fibroblast growth factor receptor-2 (FGFR2), *Dev. Biol.* 158 (1993) 475-486.
- [18] K. G. Peters, S. Werner, G. Chen, L. T. Williams, Two FGF receptor genes are differentially expressed in epithelial and mesenchymal tissues during limb formation and organogenesis in the mouse, *Development* 114 (1992) 233-243.
- [19] V. Hamburger, H. L. Hamilton, A series of normal stages in the development of the chick embryo, *Dev. Dyn.* 195 (1951) 231-272.

[20] C. Nogueira-Silva, M. Santos, M. J. Baptista, R. S. Moura, J. Correia-Pinto, IL-6 is constitutively expressed during lung morphogenesis and enhances fetal lung explant branching, *Pediatr Res.* 60 (2006) 530-536.

[21] D. Henrique, J. Adam, A. Myat, A. Chitnis, J. Lewis, D. Ish-Horowicz, Expression of a Delta homologue in prospective neurons in the chick, *Nature* 375 (1995) 787-790.

[22] A. Tanaka, A. Furuya, M. Yamasaki, N. Hanai, K. Kuriki, T. Kamiakito, Y. Kobayashi, H. Yoshida, M. Koike, M. Fukayama, High frequency of fibroblast growth factor (FGF) 8 expression in clinical prostate cancers and breast tissues, immunohistochemically demonstrated by a newly established neutralizing monoclonal antibody against FGF 8, *Cancer Res.* 58 (1998), 2053-2056.

[23] N. Shimada, T. Ishii, T. Imada, K. Takaba, Y. Sasaki, K. Maruyama-Takahashi, Y. Maekawa-Tokuda, H. Kusaka, S. Akinaga, A. Tanaka, K. Shitara, A neutralizing antifibroblast growth factor 8 monoclonal antibody shows potent antitumor activity against androgen-dependent mouse mammary tumors in vivo, *Clin. Cancer Res.* 11 (2005) 3897-3904.

[24] C. Irving, I. Mason, Signalling by FGF8 from the isthmus patterns anterior hindbrain and establishes the anterior limit of Hox gene expression, *Development* 127 (2000) 177-186.



- [25] A. Schneider, T. Mijalski, T. Schlange, W. Dai, P. Overbeek, H. H. Arnold, T. Brand, The homeobox gene NKX3.2 is a target of left-right signalling and is expressed on opposite sides in chick and mouse embryos, *Curr. Biol.* 9 (1999) 911-914.
- [26] R. Diez del Corral, I. Olivera-Martinez, A. Goriely, E. Gale, M. Maden, K. Storey, Opposing FGF and retinoid pathways control ventral neural pattern, neuronal differentiation, and segmentation during body axis extension, *Neuron* 40 (2003) 65-79.
- [27] N. Mercader, E. Leonardo, M. E. Piedra, A. C. Martinez, M. A. Ros, M. Torres, Opposing RA and FGF signals control proximodistal vertebrate limb development through regulation of Meis genes, *Development* 127 (2000) 3961-3970.
- [28] R. Mahmood, J. Bresnick, A. Hornbruch, C. Mahony, N. Morton, K. Colquhoun, P. Martin, A. Lumsden, C. Dickson, I. Mason, A role for FGF-8 in the initiation and maintenance of vertebrate limb bud outgrowth, *Curr Biol* 5 (1995) 797-806.
- [29] J. Dubrulle, O. Pourquie, fgf8 mRNA decay establishes a gradient that couples axial elongation to patterning in the vertebrate embryo, *Nature* 427 (2004) 419-422.

## FIGURES LEGENDS

### **Figure 1– Characterization of the *mkp3* mRNA gradient in the chick limb bud.** (A)

Visualization of the *mkp3* mRNA gradient in stage HH24 chick wing bud mesenchyme. The wing bud was photographed after increasing staining reaction times: 10 minutes, 30 minutes and 60 minutes. The three regions of wing bud collected for real-time RT-PCR are represented in the wing bud with 60 minutes of staining. (B) *mkp3* and *fgf8* mRNA levels in the different limb regions analyzed obtained by real-time RT-PCR, expressed in arbitrary units normalized for 18S Ribosomal RNA and for limb region 1 values (n=5 for each region); p<0.001: \*vs. limb region 1, # vs. limb region 2. (C) *raldh2* mRNA levels in the different limb regions analyzed obtained by real-time RT-PCR, expressed in arbitrary units normalized for 18S Ribosomal RNA and for limb region 1 values (n=5 for each region); p<0.05: \*vs. limb region 1, # vs. limb region 2.

### **Figure 2 - Expression patterns obtained using *mkp3* exonic versus *mkp3* intronic probes.** (A), *mkp3* expression is detected throughout the limb mesenchyme by the exonic

probe at stage HH24. (B) In the same stage, *mkp3* expression recognized by the intronic probe was restricted to the distal part of the limb. *In situ* hybridization was performed for both probes at the same time, ensuring the same conditions, including the same time of labelling.

### **Figure 3 – FGF8 protein is expressed in the AER.** (A) Longitudinal section of stage

HH25 forelimb bud confirms the production of FGF8 protein (green) by the AER. (B) Same section as A, counterstained with DAPI.

**Figure 4 – *mkp3* is unregulated by FGF8.** (A) *mkp3* expression pattern in the distal limb mesenchyme of stage HH24 embryo. (i) control (ii) 4 hours after incubation with an FGF8-soaked bead located at the proximal limit of *mkp3* expression; (iii) 4 hours after incubation with SU5402-soaked bead. (B) Model proposed for *mkp3* expression pattern in the chick limb bud (*see text for details*).

Figure 1

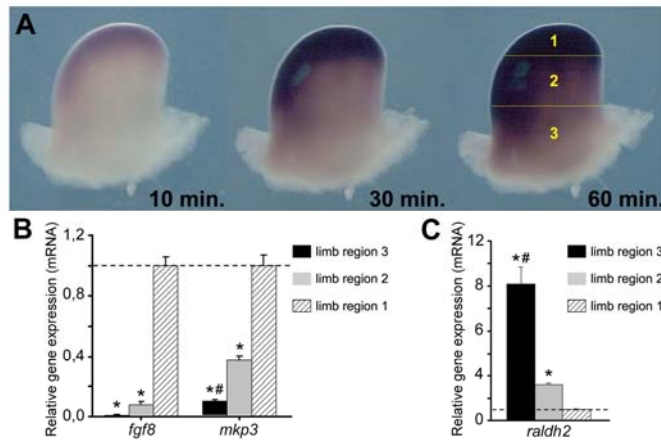


Figure 2

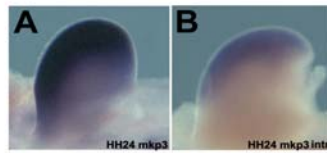


Figure 3

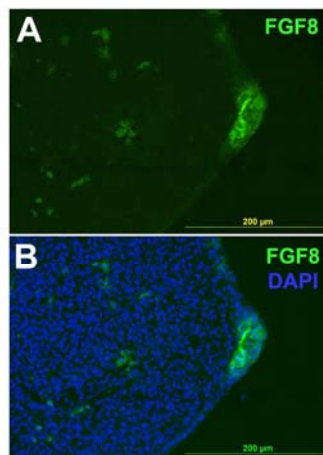
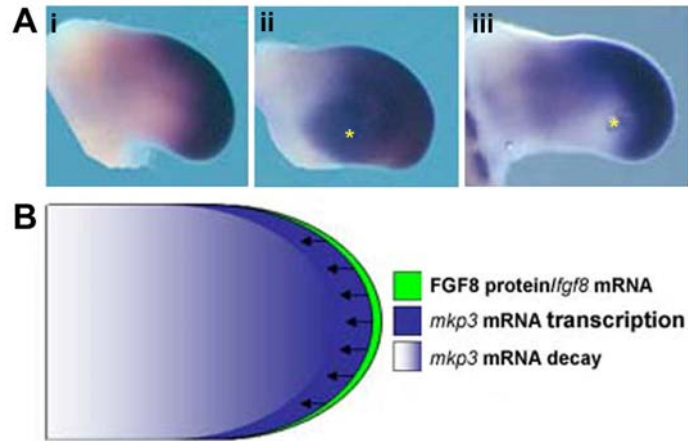


Figure 4







**Thinking clockwise**

Raquel P. Andrade, Susana Pascoal, Isabel Palmeirim

*Brain Research Reviews* 49: 114 – 119 (2005)



Review

# Thinking clockwise

Raquel P. Andrade<sup>a</sup>, Susana Pascoal<sup>a</sup>, Isabel Palmeirim<sup>a,b,\*</sup>

<sup>a</sup>*Life and Health Science Research Institute (ICVS), School of Health Sciences, University of Minho, Braga, Portugal*

<sup>b</sup>*Instituto Gulbenkian Ciência, Oeiras, Portugal*

Accepted 28 March 2005

Available online 12 May 2005

## Abstract

Throughout the Animal Kingdom, the time of embryonic development is maintained and strictly controlled. Each step of the process is successful only when it occurs at the right time and place. This raises the question: how is time controlled during embryonic development? Time control is particularly crucial during embryo segmentation processes, where the number of generated segments, as well as the time of formation of each segment, is extraordinarily constant and specific for each species.

Somitogenesis is the process through which the vertebrate presomitic mesoderm is segmented along its anterior–posterior axis into round-shaped masses of epithelial cells, named somites. In the chick embryo, a new pair of somites is formed every 90 min. The discovery that this clock-like precision is dictated by the somitogenesis molecular clock constituted a landmark in the Developmental Biology field. Several genes exhibit cyclic gene expression in the embryo presomitic mesoderm from which the somites arise, presenting a 90 min oscillation period, the time required to form a pair of somites. The combined levels of dynamic gene expression throughout the presomitic mesoderm enable cells to acquire positional information, thus giving them a notion of time.

Anterior–posterior patterning of the vertebrate nervous system also involves partition into discrete territories. This is particularly evident in the hindbrain where overt segmentation occurs. Nevertheless, little is known about the segmentation genes and mechanisms that may be involved. This paper intends to describe the molecular clock associated with vertebrate somitogenesis, suggesting that it may be operating in many other patterning processes.

© 2005 Elsevier B.V. All rights reserved.

*Theme:* Development and regeneration

*Topic:* Pattern formation, compartments, and boundaries

*Keywords:* Embryo segmentation; Somitogenesis; Molecular clock; Positional information

## Contents

1. Introduction . . . . .	115
2. Segmentation of the vertebrate body . . . . .	115
3. The discovery of the segmentation clock . . . . .	115
4. The clock today . . . . .	117
5. A molecular perspective of the “Clock and Wavefront” model . . . . .	117
6. The clock is providing multidimensional positional information . . . . .	117
7. The segmentation clock is operating in other proliferating tissues . . . . .	118

\* Corresponding author. Life and Health Science Research Institute (ICVS), School of Health Sciences, University of Minho, Braga, Portugal. Fax: +351 253604831.

*E-mail address:* [ipalmeirim@ecea.uminho.pt](mailto:ipalmeirim@ecea.uminho.pt) (I. Palmeirim).

8. Concluding remarks . . . . .	118
Acknowledgments . . . . .	119
References . . . . .	119

## 1. Introduction

During development, the final fate of a cell is strictly dependent on the position it occupies in the embryo. Spatial cellular organization is greatly accomplished by subdivision of the embryonic tissue along the anterior–posterior (a–p) axis, generating multiple segments. Cells within each segment then differentiate into positional-specific structures due to the influence of a unique combination of molecular factors. These segmented structures are formed in a strictly timed manner during embryogenesis, as a result of highly regulated and coordinated molecular mechanisms.

A fundamental characteristic of the vertebrate brain is its anterior–posterior patterning achieved by its partition into discrete territories during development, where each domain will give rise to particular embryonic structures (reviewed in [26]). Hindbrain a–p patterning is unique in the nervous system, in that it involves overt morphological segmentation of the neural tube. Distinct boundaries separate 7 clearly demarcated segments known as rhombomeres [23]. Despite the transient nature of this segmented morphology, the molecular and functional characteristics of each segment endure, conferring a fundamental role to neural tissue segmentation (reviewed in [24]).

The main draw-back in hindbrain segmentation studies is the lack of known or candidate segmentation genes. This is not so for another embryonic overt segmentation process – somitogenesis – which has been extensively studied. The discovery that cyclic gene expression lays down the basis of vertebrate body segmentation [29] constituted a milestone in the Developmental Biology field [32]. During the following years, a burst in our scientific knowledge occurred and may prove to be enlightening in the search for the molecular networks involved in the formation of other segmented structures.

## 2. Segmentation of the vertebrate body

During the first stages of chick embryo development, the axial structures (notochord and neural tube) are flanked by paraxial mesoderm, which is progressively subdivided into round epithelial balls of cells named somites. Somites bud-off in an anterior to posterior direction, from the upper part of the unsegmented paraxial mesoderm, also called presomitic mesoderm (PSM). Concomitantly, gastrulation proceeds in the posterior part of the embryo generating new cells that incorporate PSM, ensuring its elongation. Somites are transient embryonic structures that, although morphologically identical, possess differential anterior–posterior positional information which is evidenced by a commitment to

their final fate. Somites give rise to all overt segmented structures of the vertebrate body, such as vertebrae, intervertebral disks, and ribs, to all body skeletal muscles and to the dermis of the dorsal skin. They also impose a segmented pattern to surrounding tissues that otherwise would not be segmented, such as neural crest cells and the peripheral nervous system [34].

Somitogenesis occurs in a very coordinated manner, involving tight spatial and temporal regulation. In the chick embryo, a new pair of somites is formed every 90 min, culminating in a total of 52 somite pairs. The time required to form a pair of somites, as well as the final somite pair number, is constant and characteristic for each species. This fact suggests the existence of an internal clock-like machinery controlling both the rhythm and duration of somitogenesis, in a species-specific manner.

## 3. The discovery of the segmentation clock

A molecular clock linked to vertebrate segmentation and somitogenesis was first proposed by Cooke and Zeeman in 1976, as the theoretical “Clock and Wavefront” model [5]. This model projected the existence of a biochemical oscillator within PSM cells, which would be synchronized with respect to their oscillations. The cells were proposed to oscillate between a permissive and a non-permissive state for somite formation. A wavefront of differentiation was also postulated, extending posteriorly throughout the embryo and conferring cells with the competence to differentiate. When a group of “competent” cells oscillated to a permissive state, a new somite was formed.

The first molecular evidence for an intrinsic clock operating in the avian presomitic cells was obtained in 1997, with the discovery of the dynamic expression pattern of the chick *hairy1* gene. While performing in situ hybridization experiments in order to study the expression of the chick homologue of the *Drosophila* segmentation gene *hairy*, Palmeirim et al. [29] made an unexpected observation: in embryos with the same somite number, i.e., that did not differ by more than 90 min in their development, a great variety of *hairy1* expression patterns in the PSM was obtained (Fig. 1a). This experiment showed that *hairy1* was expressed in a highly dynamic manner in the chick PSM. To characterize this dynamic behavior, the authors employed several experimental embryology techniques. In a first approach, embryos were cut in two halves, along the a–p axis, and, while one half was immediately fixed, the other was further incubated for varying periods of time. Subsequently, both halves were hybridized with the *hairy1* probe. The comparison of the expression patterns between both control and experimental

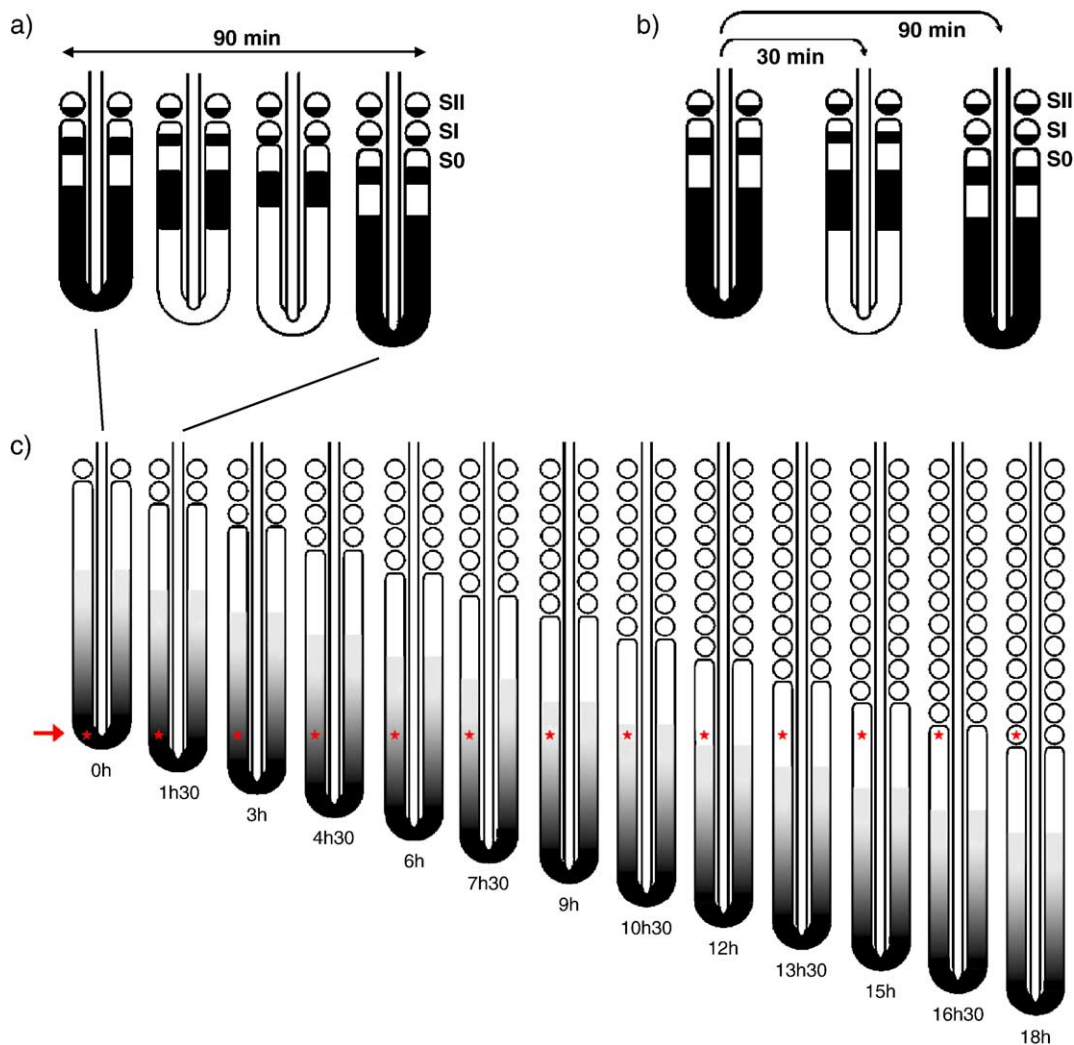


Fig. 1. Schematic representation of the dynamic and cyclic nature of *hairy1* expression and of the posterior to anterior gradient of *FGF8/Wnt3a* expression. The posterior region of chick embryos with 15 to 20 somite pairs is illustrated. S0: somite in formation; SI: newly formed somite; SII: previously formed somite. (a) Variability of *hairy1* gene expression during the formation of a new somite pair. (b) Experimental demonstration of the dynamic and cyclic *hairy1* pattern of expression. Embryos were cut in two halves, along the a–p axis and one half was immediately fixed. When the other half was further incubated for 30 min, *hairy1* expression pattern was completely altered, while incubating the experimental half for 90 min resulted in the initial expression pattern and the formation of a new somite pair. (c) Gradient of *FGF8/Wnt3a* gene expression, arising from the embryo tail bud and diminishing anteriorly in the PSM. When a cell (red star) leaves the gastrulation site in the PSM, it has high levels of *FGF8/Wnt3a* expression that diminish gradually along time. Since the PSM contains 12 prospective somites, the cell undergoes 12 cycles of *hairy1* expression until it is incorporated into a somite.

halves clearly showed that *hairy1* expression varied within the PSM cells and that 30 min of incubation was sufficient to completely change the *hairy1* expression pattern (Fig. 1b). In contrast, the same expression pattern was obtained when the experimental half was incubated for 90 min (Fig. 1b). The authors concluded that *hairy1* was cyclically expressed with a periodicity of 90 min, corresponding to the time of formation of one pair of somites.

Further studies showed that *hairy1* dynamic expression is an intrinsic property of the PSM, not depending on any surrounding tissue or on a signal arising from the gastrulation site [29]. In a first analysis, *hairy1* expression pattern appeared like a caudal–rostral wave along the PSM (Fig. 1a). Nevertheless, this only corresponded to a “kine-

matic” wave since it is not perturbed in isolated pieces of PSM, suggesting that each cell oscillates independently from its neighboring cells. The wave-like appearance arises from the fact that neighboring cells are slightly out-of-phase with respect to their autonomous oscillations.

The evidences available to date suggest that each cell in the PSM undergoes a pre-determined number of *hairy1* oscillations, from the time it emerges from the primitive streak to the time when it is incorporated into a somite. At any given time, the cell has the information of the relative position it occupies at the axial level of the PSM (Fig. 1c), which is given by the number of cycles of gene expression it has already undergone. Thus, the molecular clock may be translating time into positional information along the a–p axis of the embryo PSM.

#### 4. The clock today

Seven years have passed and other genes have been found to have the same type of gene expression oscillation in the chick embryo PSM: *hairy2*, a gene that encodes a transcription factor closely related to *hairy1* [20]; *lunatic fringe*, encoding a secreted protein [1,25] and the transcription factor *hey2* [22]. Similar cycling genes expressed during somitogenesis have been found in other vertebrates: *lunatic fringe* (*Lfng*) [1,11], *hes1* [20], *hey2* [22], *hes7* [3,4], and *nkd1* [18] in mouse; *her1* [16,31], *delta C* [19], and *her7* [28] in zebrafish; *esr9* and *esr10* in xenopus [21]; *her7* in medaka [10].

The majority of the cycling genes found in vertebrates are intimately related to the Notch signaling pathway [reviewed in [13,30]]. The Wnt pathway, however, was recently implicated in the segmentation clock. *Axin2*, a negative regulator of Wnt3a signaling, exhibits an oscillatory expression pattern in the mouse PSM [2]. *Axin2* oscillations persist in Notch pathway mutants, whereas *axin2* and *lunatic fringe* oscillations are disrupted in *wnt3a* mutants, indicating that Wnt signaling could act upstream of the Notch signaling pathway [2].

Negative feedback regulation has been identified for the mouse *hes1* and *hes7* genes. Studies at the protein level demonstrated that these gene products presented oscillations with the same periodicity found for their mRNAs. Furthermore, they inhibited their own promoters creating negative feedback loops [reviewed in [13,30]]. An additional negative feedback regulation has been described for the *lunatic fringe* gene in chick [7]. Lunatic fringe protein oscillates in PSM cells, periodically inhibiting Notch signaling, and consequently down-regulates *lunatic fringe* expression. These negative feedback loops may represent important elements in the segmentation clock mechanism. Using mathematical modeling, Monk showed that oscillatory gene expression results mainly from transcriptional delays and that the oscillation period is determined by the delay in transcription and by both protein and mRNA half-lives [27]. Accordingly, Hes7 protein instability was recently shown to be vital for the segmentation clock [15].

#### 5. A molecular perspective of the “Clock and Wavefront” model

In the context of the “Clock and Wavefront” model, the genes with an oscillatory expression pattern could be part of the core machinery or merely an output of the postulated biochemical oscillator underlying somitogenesis. The scientific community continues to pursue new players that could be involved, as well as putative interactions among them, in an attempt to characterize the molecular clock mechanism.

The “Clock and Wavefront” model also postulates the existence of a wavefront of cell differentiation that extends posteriorly throughout the embryo [5]. In 2001, Dubrulle et

al. showed that there is a gradient of *FGF8* transcripts arising from the embryo tail bud and diminishing towards the uppermost part of the PSM tissue [8]. The observed graded distribution of *FGF8* mRNA was shown to result from progressive mRNA decay rather than from different transcription levels [9]. More recently, *Wnt3a* was shown to present a PSM expression pattern similar to that of *FGF8*. *Wnt3a* is proposed to act upstream of *FGF8* and may operate together with or via the *FGF8* gradient [2]. A PSM cell positioned near the tail bud bears high FGF/Wnt signaling levels, which maintain cells in an undifferentiated state (Fig. 1c). Cellular levels of FGF/Wnt gradually diminish along time, allowing the cell to activate its differentiation program as it achieves the appropriate threshold of FGF/Wnt activity (Fig. 1c). Thus, the anterior limit of *FGF8/Wnt3a* gradient is proposed to establish the prospective somitic boundary location [2,8].

Contrasting with the expression patterns described above, the *Raldh2* gene, encoding retinoic acid (RA)-synthesizing enzyme, is expressed in the more rostral part of PSM and in the somites [33]. Diez del Corral et al. have shown that FGF and RA pathways are mutually inhibitory and promote opposing effects in the PSM tissue. These maintain the necessary balance between naive/proliferative and differentiating PSM cells [6], exerting a strict control on somite boundary positioning.

#### 6. The clock is providing multidimensional positional information

Some years ago, work was performed in our laboratory in order to determine if the segmentation clock was already operating in the prospective PSM territory. The expression patterns of the clock molecular components *hairy1*, *hairy2*, and *lunatic fringe* were analyzed in chick embryos, and we found that the cyclic genes presented a very dynamic expression in this territory [12]. The expression patterns observed in the prospective PSM tissue resembled a “wave” of cyclic gene expression, similar to the one described in the PSM (Fig. 2). By performing detailed fate map studies, we showed that different regions of the prospective PSM territory give rise to distinct PSM compartments: cells located anteriorly give rise to medial PSM cells (PM-PSM domain), while more posterior cells develop into lateral PSM domain (PL-PSM). These observations implied that, simultaneous to the a–p gene expression “wave” that occurs in the PSM, another “wave” of expression is in progress in the most posterior part of the embryo, traveling along the future medial–lateral PSM axis [12]. Accordingly, an asynchrony in cyclic gene expression can be observed between the medial and lateral portions of the PSM, which is evidenced by the appearance of cross-stripes (Fig. 2). Our work showed that the molecular clock associated to vertebrate embryo segmentation is providing cellular positional information in at least two dimensions:



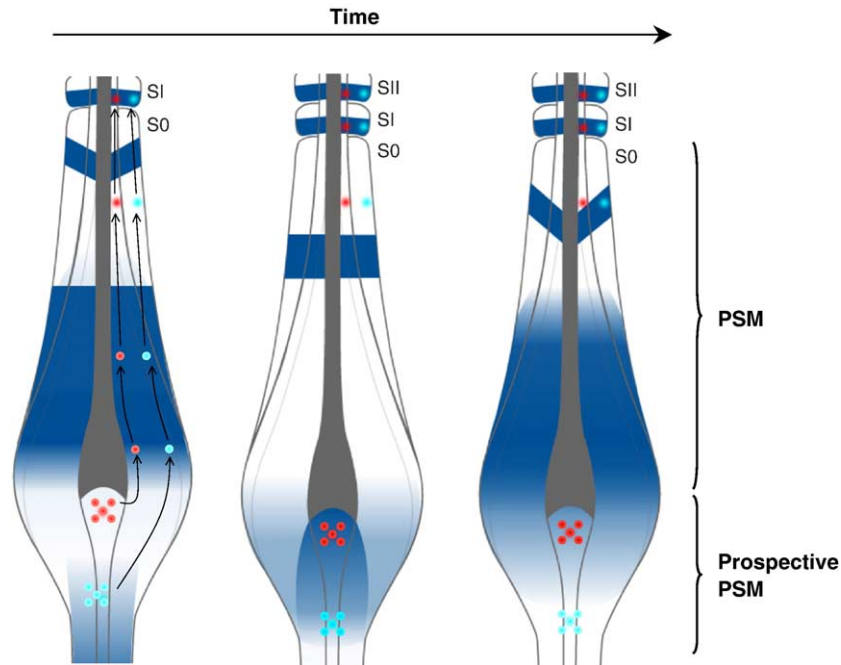


Fig. 2. Schematic representation of *hairy1* dynamic expression observed along the time of formation of one somite pair. Dynamic gene expression occurs in both the PSM and its prospective territory. Lateral PSM cells originate from PL-PSM (light blue), and medial PSM cells originate from PM-PSM (red). Arrows in the first panel show the positions occupied by these cells along time, until they are incorporated into a somite. An asynchrony in cyclic gene expression is observed both in the prospective and the PSM medial and lateral territories. This medial–lateral asynchrony is evidenced in the PSM by the appearance of cross-stripes. S0: somite in formation; SI: newly formed somite; SII: previously formed somite.

along both anterior–posterior and medial–lateral PSM axis [12].

### 7. The segmentation clock is operating in other proliferating tissues

Until now, all the studies regarding cyclic gene expression during development have focused exclusively on the somitogenesis process, which clearly occurs according to a strict temporal control. However, time control is surely present during all embryonic processes and may even be considered a fourth developmental dimension. This leads us to postulate that the molecular clock may not be an exclusive property of the PSM cells but could also be operating in other developing tissues. This hypothesis is supported by the finding of Hirata and colleagues who reported that the administration of a single serum shock could induce cyclic production of both *Hes1* mRNA and protein in several cell lines, such as myoblasts, fibroblasts, neuroblastoma, and teratocarcinoma cells [14]. The observed oscillations occurred with a 2 h time period, corresponding to the periodicity of cyclic gene expression observed in the mouse embryo PSM.

Our group has studied *hairy2* expression during chick limb bud development and observed that this gene is expressed from limb bud initiation until digit formation. We have had very exciting results, showing that *hairy2* is expressed in a very dynamic manner in the proliferative cells of the growing limb bud (progress zone). This and

other new findings from ongoing work in our laboratory suggest that the molecular clock may be operating during proximal–distal limb outgrowth and differentiation (unpublished data). Proliferating cells may record the number of *hairy2* oscillations, specifying their position along the proximal–distal limb axis. These results support our initial hypothesis that the molecular clock is not an exclusive property of PSM tissue rather a more general way to count time during vertebrate development, providing positional information to different types of cells. Taking this into account and considering that Wnt and Notch signaling pathways participate in virtually all developmental processes, great insights could result from the reanalysis of gene expression patterns in numerous other systems.

### 8. Concluding remarks

We wish to congratulate Dr. Rosa Magda Alvarado-Mallart on this occasion, recognizing her undeniable contribution to the Developmental Neurobiology field. It is a great honor to contribute to this special issue in her tribute.

Chick-quail grafting experiments have greatly contributed to our current knowledge of the cellular origin of many embryonic tissues and of the genetic regulatory cascades underlying these events. The chick embryo has, in fact, proved to be an extraordinary experimental model, namely, in the study of both vertebrate body segmentation and central nervous system development.

Somites constitute the most overtly segmented structures of the body plan, and hindbrain rhombomeres also result from an overt segmentation process. The molecular mechanisms associated with each process may have much more in common than might be expected. Could there be a clock-like mechanism underlying vertebrate nervous system development, as has been previously suggested [17]? Throughout history, Science has greatly benefited from the crossing over of the knowledge acquired in different systems. We hope this paper may bring new perspectives in forthcoming studies in the Developmental Neurosciences field.

## Acknowledgments

We would like to thank Vanessa Zuzarte Luís for the critical reading of the manuscript. The work was funded by Fundação para a Ciência e Tecnologia/FEDER (POCTI/BCI/42040/2001). R.P.A. (grant no. SFRH/BPD/9432/2002) and S.P. (grant n° SFRH/BD/8657/2002) were supported by the Fundação para a Ciência e Tecnologia, Portugal.

## References

- [1] A. Aulehla, R.L. Johnson, Dynamic expression of lunatic fringe suggests a link between notch signaling and an autonomous cellular oscillator driving somite segmentation, *Dev. Biol.* 207 (1999) 49–61.
- [2] A. Aulehla, C. Wehrle, B. Brand-Saberi, R. Kemler, A. Gossler, B. Kanzler, B.G. Herrmann, Wnt3a plays a major role in the segmentation clock controlling somitogenesis, *Dev. Cell* 4 (2003) 395–406.
- [3] Y. Bessho, R. Sakata, S. Komatsu, K. Shiota, S. Yamada, R. Kageyama, Dynamic expression and essential functions of Hes7 in somite segmentation, *Genes Dev.* 15 (2001) 2642–2647.
- [4] Y. Bessho, H. Hirata, Y. Masamizu, R. Kageyama, Periodic repression by the bHLH factor Hes7 is an essential mechanism for the somite segmentation clock, *Genes Dev.* 17 (2003) 1451–1456.
- [5] J. Cooke, E.C. Zeeman, A clock and wavefront model for control of the number of repeated structures during animal morphogenesis, *J. Theor. Biol.* 58 (1976) 455–476.
- [6] R. Diez del Corral, I. Olivera-Martinez, A. Goriely, E. Gale, M. Maden, K. Storey, Opposing FGF and retinoid pathways control ventral neural pattern, neuronal differentiation, and segmentation during body axis extension, *Neuron* 40 (2003) 65–79.
- [7] J.K. Dale, M. Maroto, M.L. Dequeant, P. Malapert, M. McGrew, O. Pourquie, Periodic notch inhibition by lunatic fringe underlies the chick segmentation clock, *Nature* 421 (2003) 275–278.
- [8] J. Dubrulle, O. Pourquie, Coupling segmentation to axis formation, *Development* 131 (2004) 5783–5793.
- [9] J. Dubrulle, M.J. McGrew, O. Pourquie, FGF signaling controls somite boundary position and regulates segmentation clock control of spatiotemporal Hox gene activation, *Cell* 106 (2001) 219–232.
- [10] H. Elmasri, D. Liedtke, G. Lucking, J.N. Völff, M. Gessler, C. Winkler, *her7* and *hey1*, but not *lunatic fringe* show dynamic expression during somitogenesis in medaka (*Oryzias latipes*), *Gene Expression Patterns* 4 (2004) 553–559.
- [11] H. Forsberg, F. Crozet, N.A. Brown, Waves of mouse Lunatic fringe expression, in four-hour cycles at two-hour intervals, precede somite boundary formation, *Curr. Biol.* 8 (1998) 1027–1030.
- [12] C. Freitas, S. Rodrigues, J.B. Charrier, M.A. Teillet, I. Palmeirim, Evidence for medial/lateral specification and positional information within the presomitic mesoderm, *Development* 128 (2001) 5139–5147.
- [13] C. Freitas, S. Rodrigues, L. Saúde, I. Palmeirim, Running after the clock, *Int. J. Dev. Biol.* (in press).
- [14] H. Hirata, S. Yoshiura, T. Ohtsuka, Y. Bessho, T. Harada, K. Yoshikawa, R. Kageyama, Oscillatory expression of the bHLH factor Hes1 regulated by a negative feedback loop, *Science* 298 (2002) 840–843.
- [15] H. Hirata, Y. Bessho, H. Kokubu, Y. Masamizu, S. Yamada, J. Lewis, R. Kageyama, Instability of Hes7 protein is crucial for the somite segmentation clock, *Nat. Genet.* 36 (2004) 750–754.
- [16] S.A. Holley, R. Geisler, C. Nusslein-Volhard, Control of *her1* expression during zebrafish somitogenesis by a delta-dependent oscillator and an independent wave-front activity, *Genes Dev.* 14 (2000) 1678–1690.
- [17] M. Hollyday, Neurogenesis in the vertebrate neural tube, *Int. J. Dev. Neurosci.* 19 (2001) 161–173.
- [18] A. Ishikawa, S. Kitajima, Y. Takahashi, H. Kokubo, J. Kanno, T. Inoue, Y. Saga, Mouse Nkd1, a Wnt antagonist, exhibits oscillatory gene expression in the PSM under the control of Notch signaling, *Mech. Dev.* 121 (2004) 1443–1453.
- [19] Y.J. Jiang, B.L. Aerne, L. Smithers, C. Haddon, D. Ish-Horowicz, J. Lewis, Notch signalling and the synchronization of the somite segmentation clock, *Nature* 408 (2000) 475–479.
- [20] C. Jouve, I. Palmeirim, D. Henrique, J. Beckers, A. Gossler, D. Ish-Horowicz, O. Pourquie, Notch signalling is required for cyclic expression of the hairy-like gene HES1 in the presomitic mesoderm, *Development* 127 (2000) 1421–1429.
- [21] Y. Li, U. Fenger, C. Niehrs, N. Pollet, Cyclic expression of *esr9* gene in *Xenopus* presomitic mesoderm, *Differentiation* 71 (2003) 83–89.
- [22] C. Leimeister, K. Dale, A. Fischer, B. Klamt, M. Hrabe de Angelis, F. Radtke, M.J. McGrew, O. Pourquie, M. Gessler, Oscillating expression of *c-Hey2* in the presomitic mesoderm suggests that the segmentation clock may use combinatorial signaling through multiple interacting bHLH factors, *Dev. Biol.* 227 (2000) 91–103.
- [23] A. Lumsden, Segmentation and compartment in the early avian hindbrain, *Mech. Dev.* 121 (2004) 1081–1088.
- [24] A. Lumsden, R. Keynes, Segmental patterns of neuronal development in the chick hindbrain, *Nature* 337 (1989) 424–428.
- [25] M.J. McGrew, J.K. Dale, S. Fraboulet, O. Pourquie, The lunatic fringe gene is a target of the molecular clock linked to somite segmentation in avian embryos, *Curr. Biol.* 8 (1998) 979–982.
- [26] K.R. Melton, A. Iulianella, P.A. Trainor, Gene expression and regulation of hindbrain and spinal cord development, *Front. Biosci.* 9 (2004) 117–138.
- [27] N.A. Monk, Oscillatory expression of *Hes1*, *p53*, and *NF-kappaB* driven by transcriptional time delays, *Curr. Biol.* 13 (2003) 1409–1413.
- [28] A.C. Oates, R.K. Ho, Hairy/E (spl)-related (Her) genes are central components of the segmentation oscillator and display redundancy with the Delta/Notch signaling pathway in the formation of anterior segmental boundaries in the zebrafish, *Development* 129 (2002) 2929–2946.
- [29] I. Palmeirim, D. Henrique, D. Ish-Horowicz, O. Pourquie, Avian hairy gene expression identifies a molecular clock linked to vertebrate segmentation and somitogenesis, *Cell* 91 (1997) 639–648.
- [30] P.C. Rida, N. Le Minh, Y.J. Jiang, A Notch feeling of somite segmentation and beyond, *Dev. Biol.* 265 (2004) 2–22.
- [31] A. Sawada, A. Fritz, Y.J. Jiang, A. Yamamoto, K. Yamasu, A. Kuroiwa, Y. Saga, H. Takeda, Zebrafish *Mesp* family genes, *mesp-a* and *mesp-b* are segmentally expressed in the presomitic mesoderm, and *Mesp-b* confers the anterior identity to the developing somites, *Development* 127 (2000) 1691–1702.
- [32] M. Skipper, Time for segmentation, nature milestones development, *Milestone* 24 (2004) S18.
- [33] E.C. Swindell, C. Thaller, S. Sockanathan, M. Petkovich, T.M. Jessell, G. Eichele, Complementary domains of retinoic acid production and degradation in the early chick embryo, *Dev. Biol.* 216 (1999) 282–296.
- [34] M.A. Teillet, C. Kalcheim, N.M. Le Douarin, Formation of the dorsal root ganglia in the avian embryo: segmental origin and migratory behavior of neural crest progenitor cells, *Dev. Biol.* 120 (1987) 329–347.





**Desenvolvimento embrionário dos membros dos vertebrados e suas  
malformações congénitas**

Susana Pascoal e Isabel Palmeirim

*Acta Pediátrica Portuguesa, in press*



**Desenvolvimento embrionário dos membros dos vertebrados e suas malformações congénitas**

**Vertebrate limb bud embryonic development and linked congenital malformations**

**Desenvolvimento do membro de vertebrados**

Susana Pascoal e Isabel Palmeirim

Instituto de Investigação em Ciências da Vida e Saúde/ Escola de Ciências da Saúde, Universidade do Minho, Campus de Gualtar, 4710-057 Braga, Portugal

Os autores contribuíram com igual prestação para este manuscrito.

**Agradecimentos:**

Agradecemos a Rute Moura, Raquel Andrade e a Lucília Goreti Pinto pelos comentários produtivos feitos após a leitura do artigo. Susana Pascoal (SFRH/BD/8657/2002) foi financiada pela Fundação para a Ciência e Tecnologia (FCT).

Resumo: 114 palavras

Abstract: 118 palavras

Texto: 1907 palavras

Isabel Palmeirim, MD. PhD

Instituto de Investigação em Ciências da Vida e Saúde (ICVS)

Escola de Ciências da Saúde

Universidade do Minho

4710-057 Braga

Portugal

Phone: 253 604 865

Email: [ipalmeirim@ecsaude.uminho.pt](mailto:ipalmeirim@ecsaude.uminho.pt)

## **Resumo**

O embrião de galinha é um dos modelos de eleição para o estudo do desenvolvimento do membro dos vertebrados, devido à facilidade de acesso ao membro do embrião sem comprometer a sobrevivência do mesmo e à sua semelhança com o membro do embrião humano. O estudo do desenvolvimento do embrião de galinha tem permitido grandes avanços na determinação das *vias* de migração celulares e das interações entre células que determinam a correcta formação do membro. A analogia entre o embrião de galinha e o humano tem permitido a extrapolação entre as descobertas realizadas e a medicina, trazendo novos conhecimentos que contribuem para uma melhor compreensão das anomalias congénitas que se observam em membros humanos.

**Palavras-chave:** Embrião de galinha, vertebrados, desenvolvimento do membro, anomalias no desenvolvimento do membro humano

## **Abstract**

The chicken embryo is an excellent model organism for studying vertebrate limb development, due to the ease of manipulating the developing limb *in vivo* and because of the similarities between the human and chicken embryos. Classical chicken embryology has provided fate maps and has elucidated the cell-cell interactions that specify limb patterning. More recently, the role of an increasing number of genes in limb bud development has been uncovered. These genes belong to signaling pathways that work together for perfect limb bud development. The study of limb bud development in chicken is applicable to other vertebrates, as to human, and there are growing links with clinical medicine that bring new inputs in the knowledge of human limb anomalies.

**Key-words:** chicken embryo, vertebrate, limb bud development, human limb anomalies

## **Introdução**

Há milhões de anos atrás, os vertebrados existentes na Terra foram obrigados a sair do meio aquático. Para tal, desenvolveram progressivamente membros que lhes permitiram andar, correr e voar, aumentando assim a sua capacidade de sobrevivência. Desde então, e apesar das mudanças adaptativas ocorridas ao longo dos anos subsequentes, o esqueleto dos membros dos tetrápodes tem-se mantido surpreendentemente conservado.

O embrião de galinha é um excelente modelo para estudar o desenvolvimento do membro dos vertebrados devido à sua fácil obtenção, fácil manipulação *in vivo*, e à sua extraordinária semelhança com o embrião humano. Tal como o membro humano, o membro da galinha é constituído por úmero, rádio e cúbito, metacarpos e falanges (Figura 1B). Os membros não são necessários para a sobrevivência embrionária, sendo por isso passíveis de manipulação cirúrgica experimental (remoção, adição ou transplantes de tecidos) para definir interacções celulares e moleculares que controlem a sua padronização (definição dos seus eixos e segmentos) e o desenvolvimento harmonioso do seu esqueleto, músculos, tendões, vasos, etc. Para o correcto desenvolvimento dos membros é necessário que ocorra: (1) comunicação entre células de tecidos adjacentes, para que se dê a iniciação da formação do membro, (2) formação de centros sinalizadores, responsáveis pelo estabelecimento dos eixos do membro, (3) intensa proliferação celular, indispensável ao crescimento do membro e (4) morte celular programada e localizada, necessária para esculpir o membro e lhe atribuir a forma correcta.

## **Iniciação da formação do botão do membro e sua especificação**

O desenvolvimento do membro inicia-se com a proliferação de células da mesoderme da placa lateral e migração de células da mesoderme somítica, que se acumulam sob o tecido epidérmico (Figura 1A). Estas células multiplicam-se até criar uma protuberância (botão do membro) que vai proliferar para formar o membro<sup>1</sup>. Os músculos, tendões, nervos e vasos do membro derivam de células que migram dos sómitos, enquanto que outros tecidos como a cartilagem, osso e pêlos ou penas derivam da mesoderme da placa lateral.

Os estadios iniciais do botão do membro estão sob a regulação das células da mesoderme intermédia, onde é produzida a molécula *Fibroblast Growth Factor 8* (FGF8). A implantação cirúrgica *in ovo* de uma esfera embebida em FGF8 no flanco de um embrião leva à formação de um membro ectópico, o que significa que esta molécula consegue por si só induzir a formação de um membro <sup>1</sup>.

Na galinha, os membros superiores (asas) formam-se ao nível dos sómitos 15 a 20 do tronco do embrião, enquanto que os membros inferiores (patas) formam-se ao nível dos sómitos 25 a 30 (Figura 2). Nos estadios de iniciação do membro, FGF8 é expresso na mesoderme intermédia apenas ao nível destes sómitos, definindo desta forma o local de formação dos membros. Existem vários genes candidatos à determinação da identidade do membro (asa ou pata): o *Pitx1*, cujos transcritos só são detectados no botão da pata e não no botão da asa da galinha; e dois membros da família de genes T-box, *Tbx4* e *Tbx5*, que são especificamente expressos nos botões da pata e da asa da galinha, respectivamente (Figura 2) <sup>2</sup>. Se se induzir a formação de um membro ectópico, ao implantar uma esfera embebida em FGF no tronco do embrião, entre a asa e a pata, o tipo de membro formado vai depender da proteína Tbx que é expressa. Se houver expressão das duas proteínas Tbx no membro ectópico, obtém-se um membro que contém no seu esqueleto estruturas da asa e da pata (Figura 2).

### **Padronização dos membros nos vertebrados**

No membro dos vertebrados podem identificar-se três eixos: (a) o eixo proximo-distal (p-d), que vai do ombro (proximal) à ponta dos dedos (distal); (b) o eixo anterior-posterior (a-p), que na mão humana corresponde à linha que vai do polegar (anterior) ao quinto dedo (posterior) e (c) o eixo dorso-ventral (d-v), sendo dorsal as costas da mão e ventral a palma (Figura 3 A). A determinação destes três eixos resulta da acção de três regiões do botão do membro que apresentam actividade organizadora: (a) a crista ectodérmica apical (AER), que controla o crescimento do membro no eixo p-d <sup>3</sup>; (b) a zona de actividade polarizadora (ZPA), que controla a organização do eixo a-p <sup>4</sup> e (c) a ectoderme do membro, que é a responsável pela organização do eixo d-v <sup>5</sup> (Figura 3B).

#### - Definição do eixo p-d do membro

À medida que o botão do membro se desenvolve, as células mesodérmicas induzem a ectoderme envolvente a formar uma estrutura chamada crista ectodérmica apical (AER) <sup>6</sup>. Esta crista percorre a margem distal do membro e define a fronteira entre a ectoderme dorsal e ventral (Figura 3B). Imediatamente abaixo da AER, encontra-se um conjunto de células indiferenciadas que compõem a chamada zona de progresso (PZ) <sup>7</sup> (Figura 3B). A AER é um dos centros organizadores do membro e a sua remoção cirúrgica pára o crescimento p-d do botão do membro. Quando se remove a AER e esta é substituída por uma esfera embebida em FGF8, o membro desenvolve-se normalmente. Estes resultados sugerem que é o Fgf8 produzido pelas células da AER que mantêm o crescimento p-d do membro. Quando a AER é removida em estadios precoces do desenvolvimento do membro, as células da PZ deixam de proliferar e o membro fica truncado, formando-se apenas o úmero. Quando a AER é removida em estadios em que o membro se encontra mais desenvolvido, formam-se mais algumas estruturas (rádio, cúbito, metacarpo). Os resultados desta experiência são explicados pela teoria da Zona de Progresso. Esta teoria suporta a ideia de que as células vão alterando o seu destino durante o tempo que estão na PZ. Desta forma, as células que abandonam a PZ mais cedo vão formar as estruturas ósseas mais proximais (úmero), enquanto que as células que sofrem um maior número de divisões celulares e deixam a PZ em último lugar, dão origem aos elementos mais distais do membro (falanges). Segundo esta teoria, o número, tipo e posição dos ossos é determinado pelo tempo que as células passam na zona de progresso <sup>7</sup> (Figura 4).

#### - Definição do eixo a-p do membro

Em 1968, observou-se que transplantar células da região mais posterior do mesênquima do membro para a região anterior de um membro hospedeiro dava origem a um membro cujos dígitos se encontravam duplicados em imagem espelho. Tendo em conta que o padrão normal dos dígitos da galinha é dígito2- dígito3- dígito4 (2-3-4), este padrão alterava-se para (4-3-2-2-3-4) (Figura 5). Estes dígitos adicionais não derivam das células transplantadas mas do embrião hospedeiro e este efeito é tanto mais marcado quanto maior o número de células transplantadas. Estes resultados sugerem que as células desta

região posterior do mesênquima, agora denominada “zona de actividade polarizadora” (ZPA), produzem uma substância que difunde em gradiente e que é responsável pela organização do eixo a-p do botão do membro <sup>4</sup>.

A natureza molecular do sinal produzido pela ZPA foi estabelecida em 1990 através da identificação de um gene denominado *Sonic Hedgehog (shh)* <sup>8</sup>. Shh é uma molécula produzida apenas na ZPA, que difunde e actua como um morfogénio: as células que recebem uma concentração elevada de Shh formam o dígito mais posterior (dígito 4), enquanto que as células mais afastadas desta região recebem uma concentração menor de Shh e formam o dígito mais anterior (dígito 2) <sup>8</sup>.

#### - Definição do eixo d-v do membro

O mesênquima contém toda a informação necessária para a padronização d-v do membro transferindo-a posteriormente para a ectoderme envolvente <sup>9</sup>. Quando se roda a ectoderme 180° relativamente ao mesênquima, as estruturas mesênquimatosas (esqueleto e músculo) tornam-se invertidas, de acordo com a nova polaridade da ectoderme <sup>10</sup>.

O factor de transcrição *Lmx1b* é expresso no mesênquima dorsal do membro atribuindo a essas células um carácter dorsal. À medida que o membro se vai desenvolvendo, *Wnt7a*, que é expresso na ectoderme dorsal do botão do membro, induz a expressão de *Lmx1b* no mesênquima subjacente, atribuindo a essas células um carácter dorsal. Na ausência de *Wnt7a*, o padrão dorsal das estruturas distais não se estabelece e os membros que se formam são bi-ventrais. A expressão de *Wnt7a* é restrita à ectoderme dorsal porque o factor de transcrição *Engrailed1 (En1)* reprime-a na ectoderme ventral, local onde é expresso. Em membros onde a função de *En1* foi anulada, o *Wnt7a* passa a estar expresso por toda a ectoderme, formando-se estruturas distais com um carácter bi-dorsal <sup>11</sup>.



### **Morte celular programada na formação do membro**

A morte celular apresenta um papel importante na modelação do membro, ocorrendo em quatro regiões específicas, a zona necrótica interior, anterior, posterior e interdigital. O rádio e o cúbito são separados entre si pela zona necrótica interior, enquanto que a zona necrótica anterior e posterior conferem a forma ao membro. Estudos sobre a zona necrótica interdigital são realizados nos membros inferiores do pato e da galinha que diferem na ocorrência de morte celular entre os dígitos, envolvendo a formação ou não, de membranas interdigitais. Saunders e colegas<sup>12</sup> demonstraram que na galinha, as células situadas entre a cartilagem dos dígitos estão destinadas a morrer, mesmo quando transplantadas para outra região do embrião ou colocadas em cultura. Este comportamento só é alterado quando estas células são transplantadas para o membro de um pato. O gene BMP4 é expresso nos espaços interdigitais do membro da galinha e é o responsável pela indução de morte celular na zona interdigital. Este gene não se expressa no membro inferior do pato, explicando a presença de membranas interdigitais<sup>13</sup>.

### **Conexões com o membro humano**

Nos últimos anos têm vindo a aumentar as descobertas no campo da biologia do desenvolvimento com aplicação em medicina. Descobriu-se que mutações nos receptores dos FGFs são responsáveis pela acondroplasia e outras anomalias dos dígitos como a síndrome de Apert que é caracterizada por sindactilia nos membros superiores e inferiores<sup>14</sup>. A activação do receptor FGFR3 é a principal causa de vários graus de nanismo<sup>15</sup>. Mutações no FGFR2 são responsáveis por várias síndromes em humanos, como é o caso da síndrome de Pfeiffer e de Jackson-Weiss, que apresentam anomalias severas ao nível dos membros inferiores<sup>16, 17</sup>. Mutações no gene *Hoxd13* e no gene *Gli* estão associadas à polisindactilia humana e à cefalopolisindactilia de Greg<sup>18, 19</sup>. Estes genes são também cruciais no desenvolvimento do membro da galinha. Os genes *Tbx* estão implicados na síndrome Holt-Oram (*Tbx5*) caracterizada por malformações nos membros superiores, como fusões nos ossos do carpo, e na síndrome cúbito-mamário (*Tbx3*), associada à haploinsuficiência de *Tbx3* onde as estruturas posteriores, incluindo os dígitos, não se formam. O mesmo se observa nas experiências de sobre-expressão para estes genes realizadas em galinha<sup>20</sup>. A lista

de genes responsáveis pelos defeitos dos membros em pacientes humanos é cada vez maior, o que dá origem a uma necessidade crescente em compreender como é que mutações específicas de um gene levam a fenótipos tão precisos.

### **Conclusão**

O trabalho experimental em embriões de galinha tem contribuído para o conhecimento do desenvolvimento do membro dos vertebrados. Devido à sua semelhança com o embrião humano, o embrião de galinha tem sido cada vez mais usado no estudo das interações celulares e moleculares que regulam o seu desenvolvimento, sendo possível extrapolar as descobertas realizadas nesta área para os humanos. Experiências realizadas no membro de embrião de galinha têm permitido descobrir quais os genes essenciais à sua formação, à padronização do seu esqueleto, e à modelação da sua forma. Desta forma, podemos actualmente compreender fenótipos como a sindactilia, a polidactilia e outros observados em inúmeras síndromes genéticas humanas.

### **Bibliografia**

1. Crossley PH, Minowada G, MacArthur CA, Martin GR. Roles for FGF8 in the induction, initiation, and maintenance of chick limb development. *Cell*. 1996; 84:127-36.
2. Rodriguez-Esteban C, Tsukui T, Yonei S, Magallon J, Tamura K, Izpisua Belmonte JC. The T-box genes Tbx4 and Tbx5 regulate limb outgrowth and identity. *Nature*. 1999; 398:814-18.
3. Saunders JW Jr. The proximo-distal sequence of origin of the parts of the chick wing and the role of the ectoderm. *J Exp Zool*. 1948; 108:363-04.
4. Saunders JW Jr, Gasseling MT. Ectodermal-mesodermal interactions in the origin of limb symmetry. In: R. Fleischmajer e R. E. Billingham (eds.), *Epithelial-Mesenchymal Interactions*. Williams & Wilkins, Baltimore, pp.78-97.

5. MacCabe JA, Errick J, Saunders JW Jr. Ectodermal control of the dorsoventral axis in the leg bud of the chick embryo. *Dev Biol.* 1974; 39:69-82.
6. Saunders JW Jr, Reuss C. Inductive and axial properties of prospective wing-bud mesoderm in the chick embryo. *Dev Biol.* 1974; 38:41-50.
7. Summerbell D, Lewis JH, Wolpert L. Positional information in chick limb morphogenesis. *Nature.* 1973; 244:492-6.
8. Riddle RD, Johnson RL, Laufer E, Tabin C. Sonic hedgehog mediates the polarizing activity of the ZPA. *Cell.* 1993; 75:1401-16.
9. Geduspan JS, MacCabe JA. Transfer of dorsoventral information from mesoderm to ectoderm at the onset of limb development. *Anat Rec.* 1989; 224:79-87.
10. MacCabe JA, Errick J, Saunders JW Jr. Ectodermal control of the dorsoventral axis in the leg bud of the chick embryo. *Dev Biol.* 1974; 39:69-82.
11. Chen H, Johnson RL. Interactions between dorsal-ventral patterning genes *lmx1b*, *engrailed-1* and *wnt-7a* in the vertebrate limb. *Int J Dev Biol.* 2002; 46:937-41.
12. Saunders JW Jr, Gasseling MT. Cellular death in morphogenesis of the avian wing. *Dev Biol.* 1962; 5:147-78.
13. Zou H, Niswander L. Requirement for BMP signaling in interdigital apoptosis and scale formation. *Science.* 1996; 272:738-41.
14. Wilkie AO. Why study human limb malformations? *J Anat.* 2003; 202:27-35.
15. Naski MC, Wang Q, Xu J, Ornitz DM. Graded activation of fibroblast growth factor receptor 3 by mutations causing achondroplasia and thanatophoric dysplasia. *Nat Genet.* 1996; 13:233-7.
16. Jabs EW, Li X, Scott AF, Meyers G, Chen W, Eccles M, *et al.* Jackson-Weiss and Crouzon syndromes are allelic with mutations in fibroblast growth factor receptor 2. *Nat Genet.* 1994; 8:275-9.
17. Rutland P, Pulleyn LJ, Reardon W, Baraitser M, Hayward R, Jones B, *et al.* Identical mutations in the *FGFR2* gene cause both Pfeiffer and Crouzon syndrome phenotypes. *Nat Genet.* 1995; 9:173-6.

18. Muragaki Y, Mundlos S, Upton J, Olsen BR. Altered growth and branching patterns in synpolydactyly caused by mutations in HOXD13. *Science*. 1996; 272:548-51.
19. Hui CC, Joyner AL. A mouse model of greig cephalopolysyndactyly syndrome: the extra-toesJ mutation contains an intragenic deletion of the Gli3 gene. *Nat Genet*. 1993; 3:241-6.
20. Suzuki T, Takeuchi J, Koshiba-Takeuchi K, Ogura T. Tbx Genes Specify Posterior Digit Identity through Shh and BMP Signaling. *Dev Cell*. 2004; 6:43-53.

### Legendas

Figura 1 – Fotografia de um embrião de galinha e das estruturas que constituem o seu membro superior.

(A) Imagem dorsal de um embrião de galinha com dois dias de incubação e corte transversal do mesmo ao nível do local de formação do membro superior (sómito 15 a 20). (B) Estruturas esqueléticas que constituem o membro superior de galinha (úmero, cúbito, rádio, metacarpos e falanges).

Figura 2 – Esquema ilustrativo da iniciação da formação do membro dos vertebrados. O membro superior (asa) forma-se no tronco do embrião entre o sómito 15 a 20, enquanto o membro inferior (pata) forma-se entre o sómito 25 a 30. A expressão de FGF8 encontra-se ao nível destes sómitos (barra a cinza). Os genes Tbx5 (cinza escuro) e Tbx4 (cinza claro) são especificamente expressos na asa e pata da galinha, respectivamente. Estes são uns dos genes candidatos à determinação da identidade do membro. Se se colocar uma esfera embebida em FGF8 (esfera) no tronco do embrião entre os sómitos 20 a 25, forma-se um membro ectópico. Se houver expressão de ambos os Tbx nesse membro, o esqueleto formado vai apresentar características de asa e de pata.

Figura 3 – Representação dos três eixos do botão do membro e das suas respectivas regiões organizadoras,

(A) Esquema dos três eixos ao longo dos quais se desenvolve o membro dos vertebrados. (B)

Representação das três regiões com capacidade organizadora responsáveis pelo desenvolvimento do membro dos vertebrados.

Figura 4 – Esquema do modelo da zona de progresso, onde a especificação das estruturas que formam o membro é progressiva ao longo do eixo p-d.

Figura 5 – Reorganização do membro dos vertebrados após transplante da ZPA para a parte anterior do membro. Remoção da ZPA de um membro dador (A) e sua respectiva colocação na parte anterior de um membro hospedeiro (B). Após alguns dias de incubação pode-se observar a reorganização do membro (C) que após o seu desenvolvimento apresenta estruturas ósseas duplicadas em imagem em espelho (D).

Figura 1

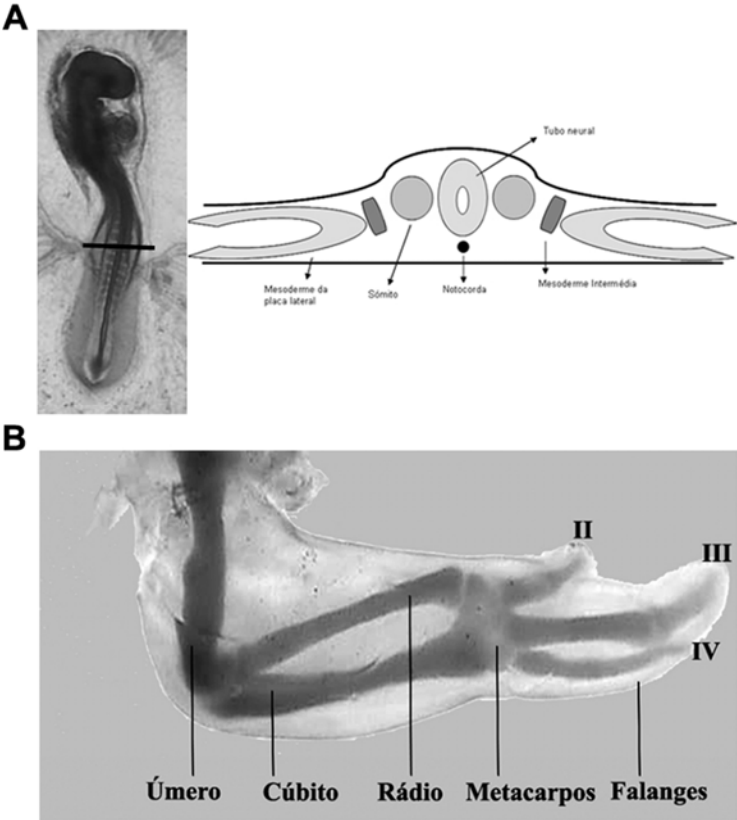


Figura 2

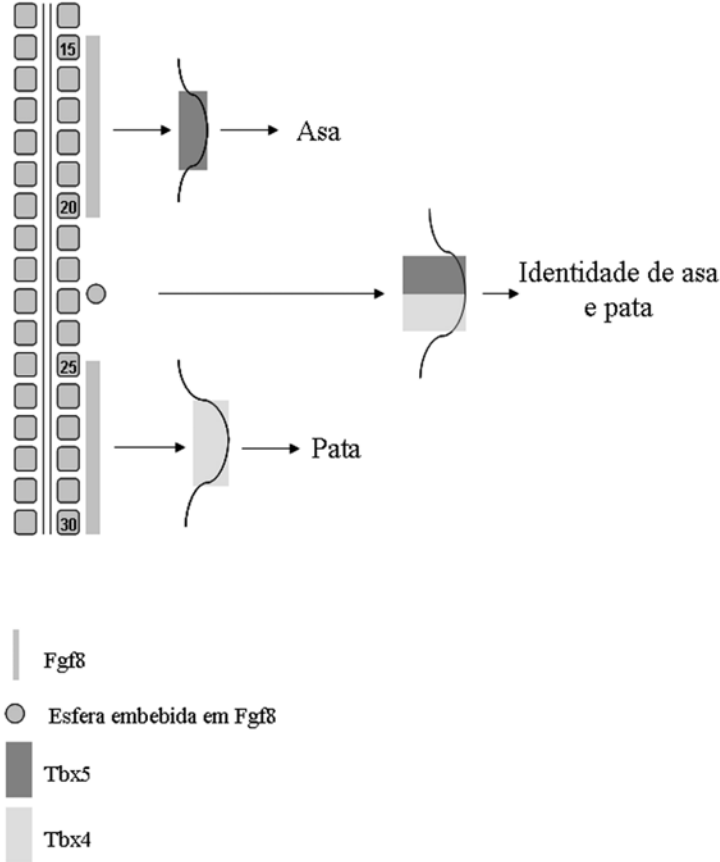


Figura 3

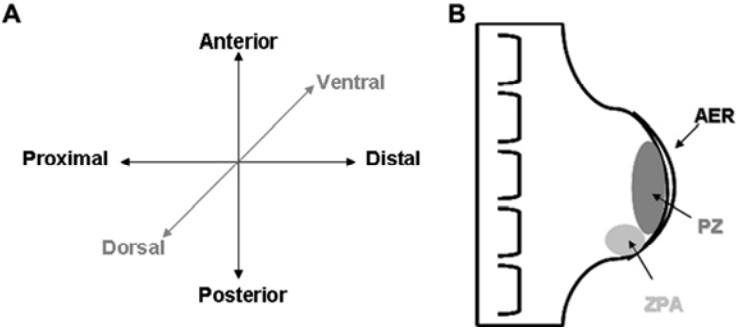


Figura 4

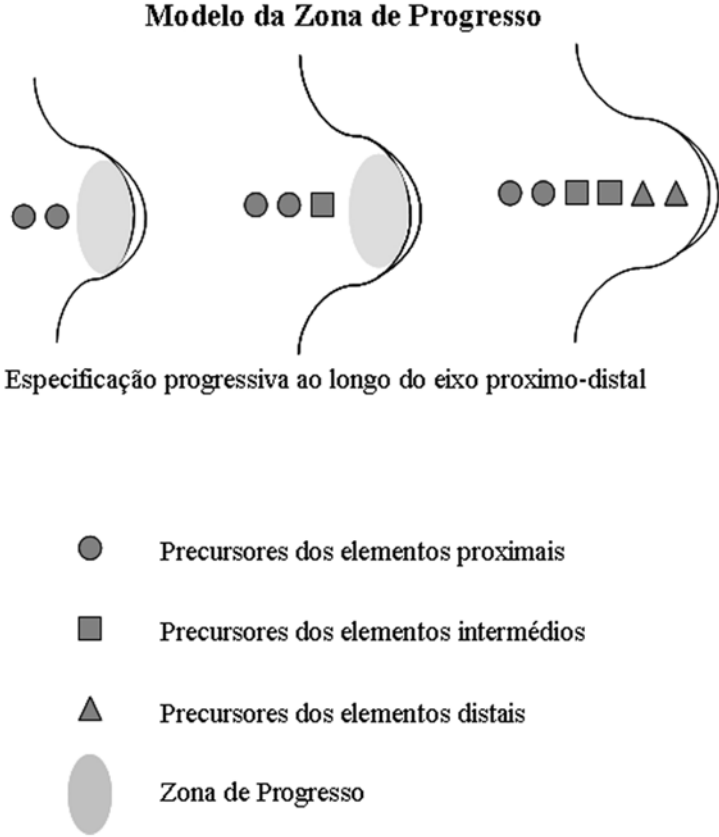
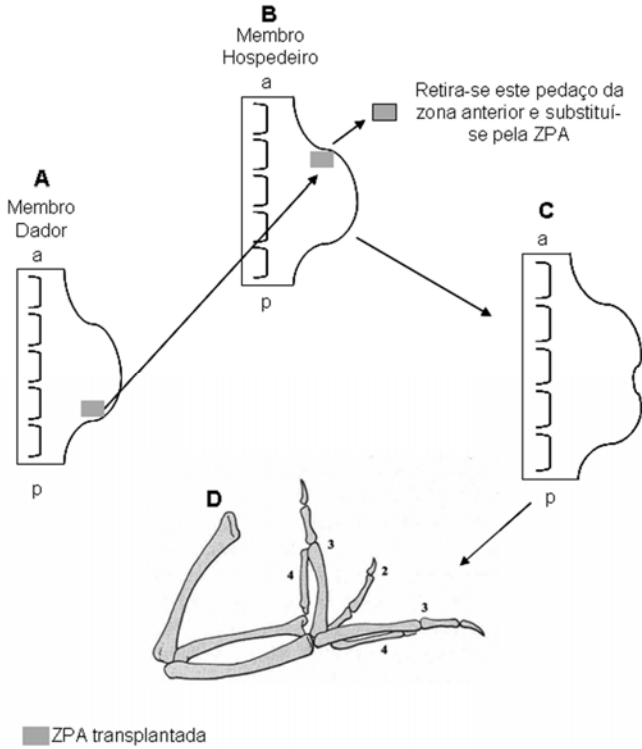




Figura 5





---

## ***CHAPTER VII***

### ***References***



Agarwal, P., Wylie, J. N., Galceran, J., Arkhitko, O., Li, C., Deng, C., Grosschedl, R. and Bruneau, B. G. (2003). *Tbx5* is essential for forelimb bud initiation following patterning of the limb field in the mouse embryo. *Development* 130, 623-33.

Ahn, D. G., Kourakis, M. J., Rohde, L. A., Silver, L. M. and Ho, R. K. (2002). T-box gene *tbx5* is essential for formation of the pectoral limb bud. *Nature* 417, 754-8.

Ahn, K., Mishina, Y., Hanks, M. C., Behringer, R. R. and Crenshaw, E. B., III. (2001). BMPR-IA signaling is required for the formation of the apical ectodermal ridge and dorsal-ventral patterning of the limb. *Development* 128, 4449-61.

Ahn, S. and Joyner, A. L. (2004). Dynamic changes in the response of cells to positive hedgehog signaling during mouse limb patterning. *Cell* 118, 505-16.

Anderson, R., Landry, M. and Muneoka, K. (1993). Maintenance of ZPA signaling in cultured mouse limb bud cells. *Development* 117, 1421-33.

Anderson, R., Landry, M., Reginelli, A., Taylor, G., Achkar, C., Gudas, L. and Muneoka, K. (1994). Conversion of anterior limb bud cells to ZPA signaling cells *in vitro* and *in vivo*. *Dev. Biol.* 164, 241-57.

Andrade, R. P., Pascoal, S. and Palmeirim, I. (2005). Thinking clockwise. *Brain Research Reviews* 49, 114-19.

Aulehla, A. and Johnson, R. L. (1999). Dynamic expression of lunatic fringe suggests a link between notch signalling and an autonomous cellular oscillator driving somite segmentation. *Dev. Biol.* 207, 49-61.

Aulehla, A., Wehrle, C., Brand-Saberi, B., Kemler, R., Gossler, A., Kanzler, B. and Herrmann, B. G. (2003). *Wnt3a* plays a major role in the segmentation clock controlling somitogenesis. *Dev. Cell* 4, 395-406.

## *References*

---

Bessho, Y., Hirata, H., Masamizu, Y. and Kageyama, R. (2003). Periodic repression by the bHLH factor Hes7 is an essential mechanism for the somite segmentation clock. *Genes Dev.* 17, 1451-56.

Bessho, Y., Sakata, R., Komatsu, S., Shiota, K., Yamada, S. and Kageyama, R. (2001). Dynamic expression and essential functions of Hes7 in somite segmentation. *Genes Dev.* 15, 2642-47.

Boulet, A. M., Moon, A. M., Arenkiel, B. R. and Capecchi, M. R. (2004). The roles of Fgf4 and Fgf8 in limb bud initiation and outgrowth. *Dev. Biol.* 273, 361-72.

Bryant, S. V. and Gardiner, D. M. (1992). Retinoic acid, local cell-cell interactions, and pattern formation in vertebrate limbs. *Dev. Biol.* 152, 1-25.

Burke, A. C. (2000). Hox genes and the global patterning of the somitic mesoderm. *Curr. Top Dev. Biol.* 47, 155-81.

Burke, A. C., Nelson, C. E., Morgan, B. A. and Tabin, C. (1995). Hox genes and the evolution of vertebrate axial morphology. *Development* 121, 333-46.

Capdevila, J., Tsukui, T., Rodriguez Esteban, C., Zappavigna, V. and Izpisua Belmonte, J. C. (1999). Control of vertebrate limb outgrowth by the proximal factor Meis2 and distal antagonism of BMPs by Gremlin. *Mol. Cell* 4, 839-49.

Carapuco, M., Novoa, A., Bobola, N. and Mallo, M. (2005). Hox genes specify vertebral types in the presomitic mesoderm. *Genes Dev.* 19, 2116-21.

Cecconi, F., Proetzel, G., Alvarez-Bolado, G., Jay, D. and Gruss, P. (1997). Expression of Meis2, a Knotted-related murine homeobox gene, indicates a role in the differentiation of the forebrain and the somitic mesoderm. *Dev. Dyn.* 210, 184-90.

Charite, J., de Graaff, W., Shen, S. and Deschamps, J. (1994). Ectopic expression of Hoxb-8 causes duplication of the ZPA in the forelimb and homeotic transformation of axial structures. *Cell* 78, 589-601.

Charite, J., McFadden, D. G. and Olson, E. N. (2000). The bHLH transcription factor dHAND controls Sonic hedgehog expression and establishment of the zone of polarizing activity during limb development. *Development* 127, 2461-70.

Chen, H., Lun, Y., Ovchinnikov, D., Kokubo, H., Oberg, K. C., Pepicelli, C. V., Gan, L., Lee, B. and Johnson, R. L. (1998). Limb and kidney defects in Lmx1b mutant mice suggest an involvement of LMX1B in human nail patella syndrome. *Nat. Genet.* 19, 51-5.

Chen, H. and Johnson, R. L. (1999). Dorsoventral patterning of the vertebrate limb: a process governed by multiple events. *Cell Tissue Res.* 296, 67-73.

Chevallier, A., Kieny, M. and Mauger, A. (1977). Limb-somite relationship: origin of the limb musculature. *J. Embryol. Exp. Morphol.* 41, 245-58.

Chiang, C., Litingtung, Y., Harris, M. P., Simandl, B. K., Li, Y., Beachy, P. A. and Fallon, J. F. (2001). Manifestation of the limb prepattern: limb development in the absence of sonic hedgehog function. *Dev. Biol.* 236, 421-35.

Chiang, C., Litingtung, Y., Lee, E., Young, K. E., Corden, J. L., Westphal, H. and Beachy, P. A. (1996). Cyclopia and defective axial patterning in mice lacking Sonic hedgehog gene function. *Nature* 383, 407-13.

Christ, B., Jacob, H. J. and Jacob, M. (1977). Experimental analysis of the origin of the wing musculature in avian embryos. *Anat. Embryol. (Berl)* 150, 171-86.

Christ, B., Schmidt, C., Huang, R., Wilting, J. and Brand-Saberi, B. (1998). Segmentation of the vertebrate body. *Anat. Embryol. (Berl)* 197, 1-8.

## *References*

---

Cohn, M. J., Izpisua-Belmonte, J. C., Abud, H., Heath, J. K. and Tickle, C. (1995). Fibroblast growth factors induce additional limb development from the flank of chick embryos. *Cell* 80, 739-46.

Cooke, J. and Zeeman, E. C. (1976). A clock and wavefront model for control of the number of repeated structures during animal morphogenesis. *J. Theor. Biol.* 58, 455-76.

Cordes, R., Schuster-Gossler, K., Serth, K. and Gossler, A. (2004). Specification of vertebral identity is coupled to Notch signalling and the segmentation clock. *Development* 131, 1221-33.

Corson, L. B., Yamanaka, Y., Lai, K. M. and Rossant, J. (2003). Spatial and temporal patterns of ERK signaling during mouse embryogenesis. *Development* 130, 4527-37.

Crossley, P. H., Minowada, G., MacArthur, C. A. and Martin, G. R. (1996). Roles for FGF8 in the induction, initiation, and maintenance of chick limb development. *Cell* 84, 127-36.

Crowe, R., Zikherman, J. and Niswander, L. (1999). Delta-1 negatively regulates the transition from prehypertrophic to hypertrophic chondrocytes during cartilage formation. *Development* 126, 987-98.

Dahn, R. D. and Fallon, J. F. (2000). Interdigital regulation of digit identity and homeotic transformation by modulated BMP signaling. *Science* 289, 438-41.

Dale, J. K., Malapert, P., Chal, J., Vilhais-Neto, G., Maroto, M., Johnson, T., Jayasinghe, S., Trainor, P., Herrmann, B. and Pourquie, O. (2006). Oscillations of the snail genes in the presomitic mesoderm coordinate segmental patterning and morphogenesis in vertebrate somitogenesis. *Dev. Cell* 10, 355-66.

Dale, J. K., Maroto, M., Dequeant, M. L., Malapert, P., McGrew, M. and Pourquie, O. (2003). Periodic notch inhibition by lunatic fringe underlies the chick segmentation clock. *Nature* 421, 275-78.



Davis, A. P., Witte, D. P., Hsieh-Li, H. M., Potter, S. S. and Capecchi, M. R. (1995). Absence of radius and ulna in mice lacking *hoxa-11* and *hoxd-11*. *Nature* 375, 791-5.

Delfini, M. C., Dubrulle, J., Malapert, P., Chal, J. and Pourquie, O. (2005). Control of the segmentation process by graded MAPK/ERK activation in the chick embryo. *Proc. Natl. Acad. Sci U.S.A* 102, 11343-8.

Deschamps, J. and van Nes, J. (2005). Developmental regulation of the Hox genes during axial morphogenesis in the mouse. *Development* 132, 2931-42.

Diez, d. C., Olivera-Martinez, I., Goriely, A., Gale, E., Maden, M. and Storey, K. (2003). Opposing FGF and retinoid pathways control ventral neural pattern, neuronal differentiation, and segmentation during body axis extension. *Neuron* 40, 65-79.

Dolle, P., Izpisua-Belmonte, J. C., Falkenstein, H., Renucci, A. and Duboule, D. (1989). Coordinate expression of the murine *Hox-5* complex homeobox-containing genes during limb pattern formation. *Nature* 342, 767-72.

Dubrulle, J., McGrew, M. J. and Pourquie, O. (2001). FGF signaling controls somite boundary position and regulates segmentation clock control of spatiotemporal Hox gene activation. *Cell* 106, 219-32.

Dubrulle, J. and Pourquie, O. (2004). *fgf8* mRNA decay establishes a gradient that couples axial elongation to patterning in the vertebrate embryo. *Nature* 427, 419-22.

Dudley, A. T., Ros, M. A. and Tabin, C. J. (2002). A re-examination of proximodistal patterning during vertebrate limb development. *Nature* 418, 539-44.

Eblaghie, M. C., Lunn, J. S., Dickinson, R. J., Munsterberg, A. E., Sanz-Ezquerro, J. J., Farrell, E. R., Mathers, J., Keyse, S. M., Storey, K. and Tickle, C. (2003). Negative feedback regulation of FGF signaling levels by Pyst1/MKP3 in chick embryos. *Curr. Biol.* 13, 1009-18.

## References

---

Elmasri, H., Liedtke, D., Lucking, G., Volff, J. N., Gessler, M. and Winkler, C. (2004). *her7* and *hey1*, but not *lunatic fringe* show dynamic expression during somitogenesis in medaka (*Oryzias latipes*). *Gene Expr. Patterns* 4, 553-9.

Fallon, J. F., Lopez, A., Ros, M. A., Savage, M. P., Olwin, B. B. and Simandl, B. K. (1994). FGF-2: apical ectodermal ridge growth signal for chick limb development. *Science* 264, 104-7.

Fernandez-Teran, M., Piedra, M. E., Kathiriya, I. S., Srivastava, D., Rodriguez-Rey, J. C. and Ros, M. A. (2000). Role of dHAND in the anterior-posterior polarization of the limb bud: implications for the Sonic hedgehog pathway. *Development* 127, 2133-42.

Fisher, D. A., Kivimae, S., Hoshino, J., Suriben, R., Martin, P. M., Baxter, N. and Cheyette, B. N. (2006). Three Dact gene family members are expressed during embryonic development and in the adult brains of mice. *Dev. Dyn.* 235, 2620-30.

Forsberg, H., Crozet, F. and Brown, N. A. (1998). Waves of mouse Lunatic fringe expression, in four-hour cycles at two-hour intervals, precede somite boundary formation. *Curr. Biol.* 8, 1027-30.

Francis, J. C., Radtke, F. and Logan, M. P. (2005). Notch1 signals through Jagged2 to regulate apoptosis in the apical ectodermal ridge of the developing limb bud. *Dev. Dyn.* 234, 1006-15.

Francis-West, P. H., Abdelfattah, A., Chen, P., Allen, C., Parish, J., Ladher, R., Allen, S., MacPherson, S., Luyten, F. P. and Archer, C. W. (1999). Mechanisms of GDF-5 action during skeletal development. *Development* 126, 1305-15.

Freitas, C., Rodrigues, S., Charrier, J. B., Teillet, M. A. and Palmeirim, I. (2001). Evidence for medial/lateral specification and positional information within the presomitic mesoderm. *Development* 128, 5139-47.

Freitas, C., Rodrigues, S., Saude, L. and Palmeirim, I. (2005). Running after the clock. *Int. J. Dev. Biol.* 49, 317-24.

Garrity, D. M., Childs, S. and Fishman, M. C. (2002). The heartstrings mutation in zebrafish causes heart/fin Tbx5 deficiency syndrome. *Development* 129, 4635-45.

Gaunt, S. J., Sharpe, P.T., and Duboule, D. (1988). Spatially restricted domains of homeo-gene transcripts in mouse embryos: relation to a segmented body plan. *Development* 104, 169–79.

Geduspan, J. S. and Solursh, M. (1992). A growth-promoting influence from the mesonephros during limb outgrowth. *Dev. Biol.* 151, 242-50.

Gibson-Brown, J. J., Agulnik, S. I., Silver, L. M., Niswander, L. and Papaioannou, V. E. (1998). Involvement of T-box genes Tbx2-Tbx5 in vertebrate limb specification and development. *Development* 125, 2499-509.

Graham, A., Papalopulu, N. and Krumlauf, R. (1989). The murine and *Drosophila* homeobox gene complexes have common features of organization and expression. *Cell* 57, 367-78.

Groom, L. A., Sneddon, A. A., Alessi, D. R., Dowd, S. and Keyse, S. M. (1996). Differential regulation of the MAP, SAP and RK/p38 kinases by Pyst1, a novel cytosolic dual-specificity phosphatase. *Embo J.* 15, 3621-32.

Hamburger, V. and Hamilton, H. L. (1951). A series of normal stages in the development of the chick embryo. *Dev. Dyn.* 195, 231-72.

Harfe, B. D., Scherz, P. J., Nissim, S., Tian, H., McMahon, A. P. and Tabin, C. J. (2004). Evidence for an expansion-based temporal Shh gradient in specifying vertebrate digit identities. *Cell* 118, 517-28.

## *References*

---

Henrique, D., Adam, J., Myat, A., Chitnis, A., Lewis, J. and Ish-Horowicz, D. (1995). Expression of a Delta homologue in prospective neurons in the chick. *Nature* 375, 787-90.

Hinchliffe. (1977). The Chronodogenic Pattern in Chick limb morphogenesis: a problem of development and evolution. In *The Third Symposium of the British Society for Developmental Biology* (eds Ede D, Hinchcliffe JR, Balls M), Cambridge University Press, 293-310.

Hirata, H., Bessho, Y., Kokubu, H., Masamizu, Y., Yamada, S., Lewis, J. and Kageyama, R. (2004). Instability of Hes7 protein is crucial for the somite segmentation clock. *Nat. Genet.* 36, 750-4.

Hirata, H., Yoshiura, S., Ohtsuka, T., Bessho, Y., Harada, T., Yoshikawa, K. and Kageyama, R. (2002). Oscillatory expression of the bHLH factor Hes1 regulated by a negative feedback loop. *Science* 298, 840-43.

Holley, S. A., Geisler, R. and Nusslein-Volhard, C. (2000). Control of her1 expression during zebrafish somitogenesis by a delta-dependent oscillator and an independent wave-front activity. *Genes Dev.* 14, 1678-90.

Hooper, J. E. a. S., M. P. (2005). Communicating with hedgehogs. *Nature Rev. Mol. Cell Biol.*, 306-17.

Huppert, S. S., Ilagan, M. X., De Strooper, B. and Kopan, R. (2005). Analysis of Notch Function in Presomitic Mesoderm Suggests a gamma-Secretase-Independent Role for Presenilins in Somite Differentiation. *Dev. Cell* 8, 677-88.

Hurle, J. M. and Ganan, Y. (1986). Interdigital tissue chondrogenesis induced by surgical removal of the ectoderm in the embryonic chick leg bud. *J. Embryol. Exp. Morphol.* 94, 231-44.

Iimura, T. P., Olivier. (2006). Collinear activation of Hoxb genes during gastrulation is linked to mesoderm cell ingression. *Nature*, 1-4.

Irving, C. and Mason, I. (2000). Signalling by FGF8 from the isthmus patterns anterior hindbrain and establishes the anterior limit of Hox gene expression. *Development* 127, 177-86.

Isaac, A., Rodriguez-Esteban, C., Ryan, A., Altabef, M., Tsukui, T., Patel, K., Tickle, C. and Izpisua-Belmonte, J. C. (1998). Tbx genes and limb identity in chick embryo development. *Development* 125, 1867-75.

Ishikawa, A., Kitajima, S., Takahashi, Y., Kokubo, H., Kanno, J., Inoue, T. and Saga, Y. (2004). Mouse Nkd1, a Wnt antagonist, exhibits oscillatory gene expression in the PSM under the control of Notch signalling. *Mech. Dev.* 121, 1443-53.

Javerzat, S., Auguste, P. and Bikfalvi, A. (2002). The role of fibroblast growth factors in vascular development. *Trends Mol. Med.* 8, 483-9.

Jiang, R., Lan, Y., Chapman, H. D., Shawber, C., Norton, C. R., Serreze, D. V., Weinmaster, G. and Gridley, T. (1998). Defects in limb, craniofacial, and thymic development in Jagged2 mutant mice. *Genes Dev.* 12, 1046-57.

Jiang, Y. J., Aerne, B. L., Smithers, L., Haddon, C., Ish-Horowicz, D. and Lewis, J. (2000). Notch signalling and the synchronization of the somite segmentation clock. *Nature* 408, 475-79.

Jouve, C., Palmeirim, I., Henrique, D., Beckers, J., Gossler, A., Ish-Horowicz, D. and Pourquie, O. (2000). Notch signalling is required for cyclic expression of the hairy-like gene HES1 in the presomitic mesoderm. *Development* 127, 1421-29.

Kawakami, Y., Capdevila, J., Buscher, D., Itoh, T., Rodriguez Esteban, C. and Izpisua Belmonte, J. C. (2001). WNT signals control FGF-dependent limb initiation and AER induction in the chick embryo. *Cell* 104, 891-900.

## References

---

Kawakami, Y., Rodriguez-Leon, J., Koth, C. M., Buscher, D., Itoh, T., Raya, A., Ng, J. K., Esteban, C. R., Takahashi, S., Henrique, D. *et al.* (2003). MKP3 mediates the cellular response to FGF8 signalling in the vertebrate limb. *Nat. Cell Biol.* 5, 513-9.

Kawakami, Y., Wada, N., Nishimatsu, S. I., Ishikawa, T., Noji, S. and Nohno, T. (1999). Involvement of Wnt-5a in chondrogenic pattern formation in the chick limb bud. *Dev. Growth Differ.* 41, 29-40.

Kengaku, M., Capdevila, J., Rodriguez-Esteban, C., De La, P. J., Johnson, R. L., Belmonte, J. C. and Tabin, C. J. (1998). Distinct WNT pathways regulating AER formation and dorsoventral polarity in the chick limb bud. *Science* 280, 1274-77.

Kerszberg, M. and Wolpert, L. (2000). A clock and trail model for somite formation, specialization and polarization. *J. Theor. Biol.* 205, 505-10.

Kessel, M. and Gruss, P. (1991). Homeotic transformations of murine vertebrae and concomitant alteration of Hox codes induced by retinoic acid. *Cell* 67, 89-104.

Kmita, M. and Duboule, D. (2003). Organizing axes in time and space; 25 years of colinear tinkering. *Science* 301, 331-3.

Kmita, M., Tarchini, B., Zakany, J., Logan, M., Tabin, C. J. and Duboule, D. (2005). Early developmental arrest of mammalian limbs lacking HoxA/HoxD gene function. *Nature* 435, 1113-6.

Knezevic, V., De Santo, R., Schughart, K., Huffstadt, U., Chiang, C., Mahon, K. A. and Mackem, S. (1997). Hoxd-12 differentially affects preaxial and postaxial chondrogenic branches in the limb and regulates Sonic hedgehog in a positive feedback loop. *Development* 124, 4523-36.

Kraus, P., Fraidenaich, D. and Loomis, C. A. (2001). Some distal limb structures develop in mice lacking Sonic hedgehog signalling. *Mech. Dev.* 100, 45-58.

Laufer, E., Nelson, C. E., Johnson, R. L., Morgan, B. A. and Tabin, C. (1994). Sonic hedgehog and Fgf-4 act through a signaling cascade and feedback loop to integrate growth and patterning of the developing limb bud. *Cell* 79, 993-1003.

Leimeister, C., Dale, K., Fischer, A., Klamt, B., Hrabe, d. A., Radtke, F., McGrew, M. J., Pourquie, O. and Gessler, M. (2000). Oscillating expression of c-Hey2 in the presomitic mesoderm suggests that the segmentation clock may use combinatorial signaling through multiple interacting bHLH factors. *Dev. Biol.* 227, 91-103.

Lewandoski, M., Sun, X. and Martin, G. R. (2000). Fgf8 signalling from the AER is essential for normal limb development. *Nat. Genet.* 26, 460-3.

Lewis, E. B. (1978). A gene complex controlling segmentation in *Drosophila*. *Nature* 276, 565-70.

Li, S., Anderson, R., Reginelli, A. D. and Muneoka, K. (1996). FGF-2 influences cell movements and gene expression during limb development. *J. Exp. Zool.* 274, 234-47.

Li, S. and Muneoka, K. (1999). Cell migration and chick limb development: chemotactic action of FGF-4 and the AER. *Dev. Biol.* 211, 335-47.

Li, Y., Fenger, U., Niehrs, C. and Pollet, N. (2003). Cyclic expression of *esr9* gene in *Xenopus* presomitic mesoderm. *Differentiation* 71, 83-9.

Litingtung, Y., Dahn, R. D., Li, Y., Fallon, J. F. and Chiang, C. (2002). Shh and Gli3 are dispensable for limb skeleton formation but regulate digit number and identity. *Nature* 418, 979-83.

Logan, M., Simon, H. G. and Tabin, C. (1998). Differential regulation of T-box and homeobox transcription factors suggests roles in controlling chick limb-type identity. *Development* 125, 2825-35.

## References

---

Logan, M. and Tabin, C. J. (1999). Role of Pitx1 upstream of Tbx4 in specification of hindlimb identity. *Science* 283, 1736-9.

Loomis, C. A., Harris, E., Michaud, J., Wurst, W., Hanks, M. and Joyner, A. L. (1996). The mouse Engrailed-1 gene and ventral limb patterning. *Nature* 382, 360-3.

Lu, H. C., Revelli, J. P., Goering, L., Thaller, C. and Eichele, G. (1997). Retinoid signaling is required for the establishment of a ZPA and for the expression of Hoxb-8, a mediator of ZPA formation. *Development* 124, 1643-51.

MacCabe, J. A., Errick, J. and Saunders, J. W., Jr. (1974). Ectodermal control of the dorsoventral axis in the leg bud of the chick embryo. *Dev. Biol.* 39, 69-82.

Maden, M. (1982). Vitamin A and pattern formation in the regenerating limb. *Nature* 295, 672-5.

Mahmood, R., Bresnick, J., Hornbruch, A., Mahony, C., Morton, N., Colquhoun, K., Martin, P., Lumsden, A., Dickson, C. and Mason, I. (1995). A role for FGF-8 in the initiation and maintenance of vertebrate limb bud outgrowth. *Curr. Biol.* 5, 797-806.

Marcil, A., Dumontier, E., Chamberland, M., Camper, S. A. and Drouin, J. (2003). Pitx1 and Pitx2 are required for development of hindlimb buds. *Development* 130, 45-55.

Martin, G. R. (1998). The roles of FGFs in the early development of vertebrate limbs. *Genes Dev.* 12, 1571-86.

McGinnis, W. and Krumlauf, R. (1992). Homeobox genes and axial patterning. *Cell* 68, 283-302.

McGlinn, E., van Bueren, K. L., Fiorenza, S., Mo, R., Poh, A. M., Forrest, A., Soares, M. B., Bonaldo Mde, F., Grimmond, S., Hui, C. C. *et al.* (2005). Pax9 and Jagged1 act downstream of Gli3 in vertebrate limb development. *Mech. Dev.* 122, 1218-33.



McGrew, M. J. and Pourquie, O. (1998). Somitogenesis: segmenting a vertebrate. *Curr. Opin. Genet. Dev.* 8, 487-93.

Medina-Martinez, O., Bradley, A. and Ramirez-Solis, R. (2000). A large targeted deletion of Hoxb1-Hoxb9 produces a series of single-segment anterior homeotic transformations. *Dev. Biol.* 222, 71-83.

Mercader, N., Leonardo, E., Azpiazu, N., Serrano, A., Morata, G., Martinez, C. and Torres, M. (1999). Conserved regulation of proximodistal limb axis development by Meis1/Hth. *Nature* 402, 425-9.

Mercader, N., Leonardo, E., Piedra, M. E., Martinez, A. C., Ros, M. A. and Torres, M. (2000). Opposing RA and FGF signals control proximodistal vertebrate limb development through regulation of Meis genes. *Development* 127, 3961-70.

Minguillon, C., Del Buono, J. and Logan, M. P. (2005). Tbx5 and Tbx4 are not sufficient to determine limb-specific morphologies but have common roles in initiating limb outgrowth. *Dev. Cell* 8, 75-84.

Molven, A., Wright, C. V., Bremiller, R., De Robertis, E. M. and Kimmel, C. B. (1990). Expression of a homeobox gene product in normal and mutant zebrafish embryos: evolution of the tetrapod body plan. *Development* 109, 279-88.

Monk, N. A. (2003). Oscillatory expression of Hes1, p53, and NF-kappaB driven by transcriptional time delays. *Curr. Biol.* 13, 1409-13.

Moon, A. M., Boulet, A. M. and Capecchi, M. R. (2000). Normal limb development in conditional mutants of Fgf4. *Development* 127, 989-96.

Moon, A. M. and Capecchi, M. R. (2000). Fgf8 is required for outgrowth and patterning of the limbs. *Nat. Genet.* 26, 455-9.

## References

---

Moskow, J. J., Bullrich, F., Huebner, K., Daar, I. O. and Buchberg, A. M. (1995). Meis1, a PBX1-related homeobox gene involved in myeloid leukemia in BXH-2 mice. *Mol. Cell Biol.* 15, 5434-43.

Mourey, R. J., Vega, Q. C., Campbell, J. S., Wenderoth, M. P., Hauschka, S. D., Krebs, E. G. and Dixon, J. E. (1996). A novel cytoplasmic dual specificity protein tyrosine phosphatase implicated in muscle and neuronal differentiation. *J. Biol. Chem.* 271, 3795-802.

Muda, M., Boschert, U., Dickinson, R., Martinou, J. C., Martinou, I., Camps, M., Schlegel, W. and Arkininstall, S. (1996). MKP-3, a novel cytosolic protein-tyrosine phosphatase that exemplifies a new class of mitogen-activated protein kinase phosphatase. *J. Biol. Chem.* 271, 4319-26.

Nakamura, T., Jenkins, N. A. and Copeland, N. G. (1996). Identification of a new family of Pbx-related homeobox genes. *Oncogene* 13, 2235-42.

Nelson, C. E., Morgan, B. A., Burke, A. C., Laufer, E., DiMambro, E., Murtaugh, L. C., Gonzales, E., Tessarollo, L., Parada, L. F. and Tabin, C. (1996). Analysis of Hox gene expression in the chick limb bud. *Development* 122, 1449-66.

Ng, J. K., Kawakami, Y., Buscher, D., Raya, A., Itoh, T., Koth, C. M., Rodriguez Esteban, C., Rodriguez-Leon, J., Garrity, D. M., Fishman, M. C. *et al.* (2002). The limb identity gene Tbx5 promotes limb initiation by interacting with Wnt2b and Fgf10. *Development* 129, 5161-70.

Niswander, L. (2002). Interplay between the molecular signals that control vertebrate limb development. *Int. J. Dev. Biol.* 46, 877-81.

Niswander, L., Jeffrey, S., Martin, G. R. and Tickle, C. (1994). A positive feedback loop coordinates growth and patterning in the vertebrate limb. *Nature* 371, 609-12.

Niswander, L., Tickle, C., Vogel, A., Booth, I. and Martin, G. R. (1993). FGF-4 replaces the apical ectodermal ridge and directs outgrowth and patterning of the limb. *Cell* 75, 579-87.

Nogueira-Silva, C., Santos, M., Baptista, M. J., Moura, R. S. and Correia-Pinto, J. (2006). IL-6 is constitutively expressed during lung morphogenesis and enhances fetal lung explant branching. *Pediatr. Res.* 60, 530-6.

Oates, A. C. and Ho, R. K. (2002). Hairy/E(spl)-related (Her) genes are central components of the segmentation oscillator and display redundancy with the Delta/Notch signaling pathway in the formation of anterior segmental boundaries in the zebrafish. *Development* 129, 2929-46.

Ohuchi, H., Nakagawa, T., Yamamoto, A., Araga, A., Ohata, T., Ishimaru, Y., Yoshioka, H., Kuwana, T., Nohno, T., Yamasaki, M. *et al.* (1997). The mesenchymal factor, FGF10, initiates and maintains the outgrowth of the chick limb bud through interaction with FGF8, an apical ectodermal factor. *Development* 124, 2235-44.

Ohuchi, H., Takeuchi, J., Yoshioka, H., Ishimaru, Y., Ogura, K., Takahashi, N., Ogura, T. and Noji, S. (1998). Correlation of wing-leg identity in ectopic FGF-induced chimeric limbs with the differential expression of chick Tbx5 and Tbx4. *Development* 125, 51-60.

Oliver, G., Wright, C. V., Hardwicke, J. and De Robertis, E. M. (1988). A gradient of homeodomain protein in developing forelimbs of *Xenopus* and mouse embryos. *Cell* 55, 1017-24.

Oulad-Abdelghani, M., Chazaud, C., Bouillet, P., Sapin, V., Chambon, P. and Dolle, P. (1997). Meis2, a novel mouse Pbx-related homeobox gene induced by retinoic acid during differentiation of P19 embryonal carcinoma cells. *Dev. Dyn.* 210, 173-83.

## *References*

---

Palmeirim, I., Henrique, D., Ish-Horowicz, D. and Pourquie, O. (1997). Avian hairy gene expression identifies a molecular clock linked to vertebrate segmentation and somitogenesis. *Cell* 91, 639-48.

Pan, Y., Liu, Z., Shen, J. and Kopan, R. (2005). Notch1 and 2 cooperate in limb ectoderm to receive an early Jagged2 signal regulating interdigital apoptosis. *Dev. Biol.* 286, 472-82.

Parr, B. A. and McMahon, A. P. (1995). Dorsalizing signal Wnt-7a required for normal polarity of D-V and A-P axes of mouse limb. *Nature* 374, 350-53.

Pizette, S., Abate-Shen, C. and Niswander, L. (2001). BMP controls proximodistal outgrowth, via induction of the apical ectodermal ridge, and dorsoventral patterning in the vertebrate limb. *Development* 128, 4463-74.

Pizette, S. and Niswander, L. (1999). BMPs negatively regulate structure and function of the limb apical ectodermal ridge. *Development* 126, 883-94.

Pourquie, O. (2001). Vertebrate somitogenesis. *Annu. Rev. Cell Dev. Biol.* 17, 311-350.

Pourquie, O., Fan, C. M., Coltey, M., Hirsinger, E., Watanabe, Y., Breant, C., Francis-West, P., Brickell, P., Tessier-Lavigne, M. and Le Douarin, N. M. (1996). Lateral and axial signals involved in avian somite patterning: a role for BMP4. *Cell* 84, 461-71.

Rallis, C., Bruneau, B. G., Del Buono, J., Seidman, C. E., Seidman, J. G., Nissim, S., Tabin, C. J. and Logan, M. P. (2003). Tbx5 is required for forelimb bud formation and continued outgrowth. *Development* 130, 2741-51.

Rida, P. C., Le Minh, N. and Jiang, Y. J. (2004). A Notch feeling of somite segmentation and beyond. *Dev. Biol.* 265, 2-22.

Riddle, R. D., Johnson, R. L., Laufer, E. and Tabin, C. (1993). Sonic hedgehog mediates the polarizing activity of the ZPA. *Cell* 75, 1401-16.

Rodriguez-Esteban, C., Tsukui, T., Yonei, S., Magallon, J., Tamura, K. and Izpisua Belmonte, J. C. (1999). The T-box genes *Tbx4* and *Tbx5* regulate limb outgrowth and identity. *Nature* 398, 814-18.

Ros, M. A., Dahn, R. D., Fernandez-Teran, M., Rashka, K., Caruccio, N. C., Hasso, S. M., Bitgood, J. J., Lancman, J. J. and Fallon, J. F. (2003). The chick oligozeugodactyly (*ozd*) mutant lacks sonic hedgehog function in the limb. *Development* 130, 527-37.

Rubin, L. and Saunders, J.W.J. (1972). Ectodermal-mesodermal interactions in the growth of limb buds in chick embryo: constancy and temporal limits of the ectodermal induction. *Dev. Biol.* 28, 94-112.

Saga, Y. and Takeda, H. (2001). The making of the somite: molecular events in vertebrate segmentation. *Nat. Rev. Genet.* 2, 835-45.

Saito, D., Yonei-Tamura, S., Kano, K., Ide, H. and Tamura, K. (2002). Specification and determination of limb identity: evidence for inhibitory regulation of *Tbx* gene expression. *Development* 129, 211-20.

Saito, D., Yonei-Tamura, S., Takahashi, Y. and Tamura, K. (2006). Level-specific role of paraxial mesoderm in regulation of *Tbx5/Tbx4* expression and limb initiation. *Dev. Biol.* 292, 79-89.

Sanz-Ezquerro, J. J. and Tickle, C. (2000). Autoregulation of *Shh* expression and *Shh* induction of cell death suggest a mechanism for modulating polarising activity during chick limb development. *Development* 127, 4811-23.

Sanz-Ezquerro, J. J. and Tickle, C. (2003). *Fgf* signaling controls the number of phalanges and tip formation in developing digits. *Curr. Biol.* 13, 1830-6.

Saunders, J. (1948). The proximo-distal sequence of the origin of the parts of the chick wing and the role of the ectoderm. *J. Exp. Zool.* 108, 363-403.

## References

---

Saunders, J. a. F., J. (1966). Cell death in morphogenesis. New York: Locke, M., (Ed.), Major Problems of Developmental Biology, Academic Press, 289-314.

Saunders, J. W., Jr, Cairns, J. M. and Gasseling, M. T. (1957). The role of the apical ectodermal ridge of ectoderm in the differentiation of the morphological structure and inductive specificity of limb parts in the chick. *J. Morph.* 101, 57-88.

Saunders, J. W., Jr, Gasseling, M. T. and Cairns, J. M. (1959). The differentiation of prospective thigh mesoderm grafted beneath the apical ectodermal ridge of the wing bud in the chick embryo. *Dev. Biol.* 1, 281-301.

Saunders, J. W., Jr and Gasseling, M. T. (1968). Epithelial-Mesenchymal Interactions (eds Fleischmajer, R. and Billingham, R. E.), Williams and Wilkins, Baltimore, 78-97.

Sawada, A., Fritz, A., Jiang, Y. J., Yamamoto, A., Yamasu, K., Kuroiwa, A., Saga, Y. and Takeda, H. (2000). Zebrafish Mesp family genes, *mesp-a* and *mesp-b* are segmentally expressed in the presomitic mesoderm, and *Mesp-b* confers the anterior identity to the developing somites. *Development* 127, 1691-702.

Schneider, A., Mijalski, T., Schlange, T., Dai, W., Overbeek, P., Arnold, H. H. and Brand, T. (1999). The homeobox gene *NKX3.2* is a target of left-right signalling and is expressed on opposite sides in chick and mouse embryos. *Curr. Biol.* 9, 911-14.

Searls, R. L. and Janners, M. Y. (1971). The initiation of limb bud outgrowth in the embryonic chick. *Dev. Biol.* 24, 198-213.

Shimada, N., Ishii, T., Imada, T., Takaba, K., Sasaki, Y., Maruyama-Takahashi, K., Maekawa-Tokuda, Y., Kusaka, H., Akinaga, S., Tanaka, A. *et al.* (2005). A neutralizing anti-fibroblast growth factor 8 monoclonal antibody shows potent antitumor activity against androgen-dependent mouse mammary tumors in vivo. *Clin. Cancer Res.* 11, 3897-904.

Sidow, A., Bulotsky, M. S., Kerrebrock, A. W., Bronson, R. T., Daly, M. J., Reeve, M. P., Hawkins, T. L., Birren, B. W., Jaenisch, R. and Lander, E. S. (1997). *Serrate2* is disrupted in the mouse limb-development mutant syndactylism. *Nature* 389, 722-25.

Smith, A., Price, C., Cullen, M., Muda, M., King, A., Ozanne, B., Arkininstall, S. and Ashworth, A. (1997). Chromosomal localization of three human dual specificity phosphatase genes (*DUSP4*, *DUSP6*, and *DUSP7*). *Genomics* 42, 524-27.

Spitz, F., Gonzalez, F. and Duboule, D. (2003). A global control region defines a chromosomal regulatory landscape containing the *HoxD* cluster. *Cell* 113, 405-17.

Stephens, T. D., Beier, R. L., Bringham, D. C., Hiatt, S. R., Prestridge, M., Pugmire, D. E. and Willis, H. J. (1989). Limbness in the early chick embryo lateral plate. *Dev. Biol.* 133, 1-7.

Stephens, T. D. and McNulty, T. R. (1981). Evidence for a metameric pattern in the development of the chick humerus. *J. Embryol. Exp. Morphol.* 61, 191-205.

Storm, E. E. and Kingsley, D. M. (1996). Joint patterning defects caused by single and double mutations in members of the bone morphogenetic protein (BMP) family. *Development* 122, 3969-79.

Strahle, U., Blader, P., Adam, J. and Ingham, P. W. (1994). A simple and efficient procedure for non-isotopic in situ hybridization to sectioned material. *Trends Genet.* 10, 75-6.

Stratford, T., Horton, C. and Maden, M. (1996). Retinoic acid is required for the initiation of outgrowth in the chick limb bud. *Curr. Biol.* 6, 1124-33.

Strecker, T. R. and Stephens, T. D. (1983). Peripheral nerves do not play a trophic role in limb skeletal morphogenesis. *Teratology* 27, 159-67.

## *References*

---

Suemori, H. and Noguchi, S. (2000). Hox C cluster genes are dispensable for overall body plan of mouse embryonic development. *Dev. Biol.* 220, 333-42.

Summerbell, D. (1974). A quantitative analysis of the effect of excision of the AER from the chick limb-bud. *J. Embryol. Exp. Morphol.* 32, 651-60.

Summerbell, D., Lewis, J. H. and Wolpert, L. (1973). Positional information in chick limb morphogenesis. *Nature* 244, 492-6.

Sun, X., Lewandoski, M., Meyers, E. N., Liu, Y. H., Maxson, R. E., Jr. and Martin, G. R. (2000). Conditional inactivation of *Fgf4* reveals complexity of signalling during limb bud development. *Nat. Genet.* 25, 83-6.

Sun, X., Mariani, F. V. and Martin, G. R. (2002). Functions of FGF signalling from the apical ectodermal ridge in limb development. *Nature* 418, 501-8.

Suriben, R., Fisher, D. A. and Cheyette, B. N. (2006). *Dact1* presomitic mesoderm expression oscillates in phase with *Axin2* in the somitogenesis clock of mice. *Dev. Dyn.* 235, 3177-83.

Swindell, E. C., Thaller, C., Sockanathan, S., Petkovich, M., Jessell, T. M. and Eichele, G. (1999). Complementary domains of retinoic acid production and degradation in the early chick embryo. *Dev. Biol.* 216, 282-96.

Szeto, D. P., Rodriguez-Esteban, C., Ryan, A. K., O'Connell, S. M., Liu, F., Kioussi, C., Gleiberman, A. S., Izpisua-Belmonte, J. C. and Rosenfeld, M. G. (1999). Role of the Bicoid-related homeodomain factor *Pitx1* in specifying hindlimb morphogenesis and pituitary development. *Genes Dev.* 13, 484-94.

Takeuchi, J. K., Koshiba-Takeuchi, K., Matsumoto, K., Vogel-Hopker, A., Naitoh-Matsuo, M., Ogura, K., Takahashi, N., Yasuda, K. and Ogura, T. (1999). *Tbx5* and *Tbx4* genes determine the wing/leg identity of limb buds. *Nature* 398, 810-4.



Takeuchi, J. K., Koshiha-Takeuchi, K., Suzuki, T., Kamimura, M., Ogura, K. and Ogura, T. (2003). Tbx5 and Tbx4 trigger limb initiation through activation of the Wnt/Fgf signaling cascade. *Development* 130, 2729-39.

Tamura, K., Yokouchi, Y., Kuroiwa, A. and Ide, H. (1997). Retinoic acid changes the proximodistal developmental competence and affinity of distal cells in the developing chick limb bud. *Dev. Biol.* 188, 224-34.

Tanaka, A., Furuya, A., Yamasaki, M., Hanai, N., Kuriki, K., Kamiakito, T., Kobayashi, Y., Yoshida, H., Koike, M. and Fukayama, M. (1998). High frequency of fibroblast growth factor (FGF) 8 expression in clinical prostate cancers and breast tissues, immunohistochemically demonstrated by a newly established neutralizing monoclonal antibody against FGF 8. *Cancer Res.* 58, 2053-6.

Tarchini, B. and Duboule, D. (2006). Control of Hoxd genes' collinearity during early limb development. *Dev. Cell* 10, 93-103.

te Welscher P, F.-T. M., Ros MA, Zeller R. (2002). Mutual genetic antagonism involving GLI3 and dHAND prepatterns the vertebrate limb bud mesenchyme prior to SHH signaling. *Genes Dev.* 16, 421-6.

te Welscher P, Z. A., Kuijper S, Drenth T, Goedemans HJ, Meijlink F, Zeller R. . (2002). Progression of vertebrate limb development through SHH-mediated counteraction of GLI3. *Science* 298, 827-30.

Tickle, C. (2003). Patterning systems--from one end of the limb to the other. *Dev. Cell.* 4, 449-58.

Tickle, C., Alberts, B., Wolpert, L. and Lee, J. (1982). Local application of retinoic acid to the limb bud mimics the action of the polarizing region. *Nature* 296, 564-6.

Tickle, C., Shellswell, G., Crawley, A. and Wolpert, L. (1976). Positional signalling by mouse limb polarising region in the chick wing bud. *Nature* 259, 396-7.

## References

---

Tickle, C., Summerbell, D. and Wolpert, L. (1975). Positional signalling and specification of digits in chick limb morphogenesis. *Nature* 254, 199-202.

Tickle, C. and Wolpert, L. (2002). The progress zone -- alive or dead? *Nat. Cell Biol.* 4, E216-7.

Vargesson, N., Clarke, J. D., Vincent, K., Coles, C., Wolpert, L. and Tickle, C. (1997). Cell fate in the chick limb bud and relationship to gene expression. *Development* 124, 1909-18.

Vargesson, N., Patel, K., Lewis, J. and Tickle, C. (1998). Expression patterns of Notch1, Serrate1, Serrate2 and Delta1 in tissues of the developing chick limb. *Mech. Dev.* 77, 197-9.

Vasiliauskas, D., Laufer, E. and Stern, C. D. (2003). A role for hairy1 in regulating chick limb bud growth. *Dev. Biol.* 262, 94-106.

Vasiliauskas, D. and Stern, C. D. (2001). Patterning the embryonic axis: FGF signaling and how vertebrate embryos measure time. *Cell* 106, 133-6.

Vogel, A., Rodriguez, C. and Izpisua-Belmonte, J. C. (1996). Involvement of FGF-8 in initiation, outgrowth and patterning of the vertebrate limb. *Development* 122, 1737-50.

Vogel, A. and Tickle, C. (1993). FGF-4 maintains polarizing activity of posterior limb bud cells *in vivo* and *in vitro*. *Development* 119, 199-206.

Wellik, D. M. and Capecchi, M. R. (2003). Hox10 and Hox11 genes are required to globally pattern the mammalian skeleton. *Science* 301, 363-7.

Wolpert, L. (1969). Positional information and the spatial pattern of cellular differentiation. *J. Theor. Biol.* 25, 1-47.

Wolpert, L., Lewis, J. and Summerbell, D. (1975). Morphogenesis of the vertebrate limb. *Ciba Found Symp.* 0, 95-130.

Wolpert, L., Tickle, C. and Sampford, M. (1979). The effect of cell killing by x-irradiation on pattern formation in the chick limb. *J. Embryol. Exp. Morphol.* 50, 175-93.

Yang, Y., Drossopoulou, G., Chuang, P. T., Duprez, D., Marti, E., Bumcrot, D., Vargesson, N., Clarke, J., Niswander, L., McMahon, A. *et al.* (1997). Relationship between dose, distance and time in Sonic Hedgehog-mediated regulation of anteroposterior polarity in the chick limb. *Development* 124, 4393-404.

Yang, Y. and Niswander, L. (1995). Interaction between the signalling molecules WNT7a and SHH during vertebrate limb development: dorsal signals regulate anteroposterior patterning. *Cell* 80, 939-47.

Yelon, D., Ticho, B., Halpern, M. E., Ruvinsky, I., Ho, R. K., Silver, L. M. and Stainier, D. Y. (2000). The bHLH transcription factor *hand2* plays parallel roles in zebrafish heart and pectoral fin development. *Development* 127, 2573-82.

Zakany, J., Kmita, M., Alarcon, P., de la Pompa, J. L. and Duboule, D. (2001). Localized and transient transcription of Hox genes suggests a link between patterning and the segmentation clock. *Cell* 106, 207-17.

Zakany, J., Kmita, M. and Duboule, D. (2004). A dual role for Hox genes in limb anterior-posterior asymmetry. *Science* 304, 1669-72.

Zou, H. and Niswander, L. (1996). Requirement for BMP signaling in interdigital apoptosis and scale formation. *Science* 272, 738-41.

Zuniga, A., Haramis, A. P., McMahon, A. P. and Zeller, R. (1999). Signal relay by BMP antagonism controls the SHH/FGF4 feedback loop in vertebrate limb buds. *Nature* 401, 598-602.

